Journal of Great Lakes Research 44 (2018) 693–704

Contents lists available at ScienceDirect

Journal of Great Lakes Research

journal homepage: www.elsevier.com/locate/jglr

Accumulation rates, focusing factors, and chronologies from depth profiles of ^{210}Pb and ^{137}Cs in sediments of the Laurentian Great Lakes

Margaret Corcoran [a,1], Mahmoud I. Sherif [b], Colin Smalley [a,2], An Li [c], Karl J. Rockne [d], John P. Giesy [e], Neil C. Sturchio [b,*]

[a] Department of Earth and Environmental Sciences, University of Illinois, Chicago, IL, USA
[b] Department of Geological Sciences, University of Delaware, Newark, DE, USA
[c] School of Public Health, University of Illinois at Chicago, Chicago, IL, USA
[d] Department of Civil and Materials Engineering, University of Illinois at Chicago, Chicago, IL, USA
[e] Department of Veterinary Biomedical Sciences and Toxicology Centre, University of Saskatchewan, Saskatoon, Saskatchewan, Canada

ARTICLE INFO

Article history:
Received 31 January 2018
Accepted 25 May 2018
Available online 7 June 2018

Communicated by Alexander Y. Karatayev

Keywords:
Great Lakes
Sediments
Radionuclides
Sedimentation rates
Dating
^{210}Pb
^{137}Cs

ABSTRACT

Sediment cores from 41 sites were collected from the Laurentian Great Lakes during 2010–2014, sectioned into 0.5–2.0 cm intervals, and the activities of ^{210}Pb, ^{137}Cs, and ^{226}Ra were measured in the upper 25 to 40 cm of the sediment column by gamma spectrometry. Sediment mass accumulation rates (dry mass) calculated from ^{210}Pb profiles range from 0.006 ± 0.001 to 0.59 ± 0.06 g cm^{-2} yr^{-1} and are similar to those reported in previous Great Lakes sediment studies. Sediment mass accumulation rates decreased with increasing water depth. ^{210}Pb-based models in cores exhibiting favorable characteristics (i.e., those having the highest unsupported-^{210}Pb activity at the sediment-water interface, exponential decrease of unsupported-^{210}Pb with increasing depth in sediment cores, and a clear peak in ^{137}Cs activity at some depth below the sediment-water interface) give calendar date profiles that are largely concordant with the maximum ^{137}Cs peak activity at 1963. Sediment focusing factors derived from unsupported-^{210}Pb inventories range from 0.09 to >5.34, and are well correlated with those derived from ^{137}Cs inventories that range from 0.07 to 4.04, demonstrating the ubiquitous occurrence of horizontal sediment transport processes within the lakes. This more recent survey provides a Great Lakes-wide chronological framework for comparing the depositional histories and inventories of a wide variety of persistent, bioaccumulative and toxic pollutants that have been measured in the same sediment cores. This information will be useful for resolving scientific and practical issues pertaining to the environmental quality and management of contaminated sediments in the Laurentian Great Lakes ecosystem.

Introduction

Sediments in large lakes are repositories of environmental change and can provide chronological records of loadings for various substances that enter the lakes from atmospheric deposition and riverine input (Astle et al., 1987; Carroll et al., 1999; Colman et al., 2002; Johnson, 1984; Tylmann et al., 2016). For the Laurentian Great Lakes of North America, such records are of particular interest when studying pollutant loadings over the past ~150 years, as this period includes the maximum human population growth and industrial activity in the region. Population and industrial activity are heterogeneously distributed in the region, with major population centers in southwestern Lake Michigan (Chicago-Milwaukee), western Lake Erie (Detroit-Toledo), and western Lake Ontario (Toronto-Hamilton).

Watersheds of the Laurentian Great Lakes were sculpted by repeated glaciations of bedrock and sediment, which deposited glacial moraines at the limits of the oscillating ice sheet, along with other glacial landforms in the southern portions of the lakes and surrounding landscapes (Soller and Garrity, 2018). The lake shores consist of a mixture of bedrock cliffs, bluffs cut into glacial sediments, lacustrine plains and beach ridges, and sandy beaches with large dunes (Chrzastowski and Thompson, 1994; Johnston et al., 2012; Johnston et al., 2014; Karrow and Calkin, 1985; Kincare and Larson, 2009; Larson and Schaetzl, 2001; Loope and Arbogast, 2000). Sources of sediment to the lakes include aerosol input, riverine input, bluff erosion and lake bottom erosion, as well as biogenic particulates including silica, carbonates, and organic matter formed within the lakes (Eadie et al., 2008). Variations in bathymetry, water currents, and sediment supplies generally result in inhomogeneous sedimentation patterns within the Great Lakes (Bell and Eadie, 1983; Cahill, 1981; Eadie et al., 1990; Eadie et al.,

* Corresponding author.
E-mail address: sturchio@udel.edu (N.C. Sturchio).
[1] Present address: CSRA, Inc., Chicago, Illinois, USA.
[2] Present address: U.S. Army Corps of Engineers, Kansas City, Missouri, USA.

https://doi.org/10.1016/j.jglr.2018.05.013
0380-1330/

2008; Edgington and Robbins, 1990; Plattner et al., 2006; Waples et al., 2005). Some locations within the lakes might have nearly continuous deposition, whereas others are almost completely non-depositional. Post-depositional events that can alter the chronological record include sediment disturbances caused by large storms, sediment slumps, wind- and thermally-driven currents, bioturbation, and anthropogenic activity such as dredging (Hermanson and Christensen, 1991; Robbins, 1978; Robbins, 1982; Robbins et al., 1978; White and Miller, 2008).

For determining rates of sediment mass accumulation in lakes, previous studies have employed methods based on measurements of ^{210}Pb, a radioactive decay product in the ^{238}U decay chain having a half-life ($t_{½}$) of 22.2 years (Goldberg, 1963; Krishnaswami et al., 1971; Robbins, 1978; Appleby and Oldfield, 1978). Determination of recent (<150 y) sediment mass accumulation rates commonly involves simple models that are based on either of two fundamental assumptions about accumulation of ^{210}Pb in sediments: (1) the constant initial concentration (CIC) model, which assumes that the initial ^{210}Pb concentration in the deposited sediment is a constant, regardless of changes in the sediment accumulation rate; and (2) the constant rate of supply (CRS) model, which assumes that the flux of ^{210}Pb to the accumulating sediment is constant when averaged over a timescale of 100–200 years (Robbins and Edgington, 1975). Assumptions and limitations of ^{210}Pb-based sedimentation models are discussed elsewhere (Robbins and Herche, 1993; Smith, 2001; Kirchner, 2011; Mackenzie et al., 2011). The sediment focusing factor (FF) measures sediment redistribution caused by horizontal movement of sediment particles on the lake bottom due to wind- and thermally-induced water currents, downslope creep, and other causes (Edgington and Robbins, 1990). It is an important parameter for calculating the fluxes of direct deposition of pollutants from the water column to sediment at specified locations. It is generally assumed that the pollutants of interest are sorbed to sediment particles in a way that is analogous to the sorption of ^{210}Pb and ^{137}Cs.

This work is part of the Great Lakes Sediment Surveillance Program (GLSSP), which examined depositional histories and inventories of persistent, bioaccumulative and toxic pollutants in sediments. The radionuclide profiles measured in this work provided sediment mass accumulation rates and focusing factors to allow reconstruction of the temporal trends of pollutants deposited and sequestered in the Laurentian Great Lakes sediments. Companion papers in this issue (Bonina et al., 2018, this issue; Li et al., 2018, this issue) and a number of papers published elsewhere (e.g., Codling et al., 2014, 2018a, 2018b; Guo et al., 2017; Peng et al., 2016) have used the data from this study to establish depositional histories of anthropogenic pollutants, and to distinguish natural from anthropogenic sources of halogenated organics. The principal objectives of this paper are to report the data of measured activities for radionuclides, to examine the spatial patterns of sediment mass accumulation rates and focusing factors, and to explore synoptic relationships of the key measured and derived variables. The data set presented here provides a new baseline for future studies of sedimentation in the Laurentian Great Lakes.

Methods

Sample collection and preparation

A total of 41 sediment cores were collected in 2010–2014 from the five Laurentian Great Lakes aboard the EPA research vessel *R.V. Lake Guardian*. Coring locations (Fig. 1) were selected from open-lake stations used for regular EPA water-quality monitoring surveys, at sites considered likely to have experienced continuous sediment accumulation based on available information from previous studies. A box-corer and an Ekman-corer were used initially during sampling on Lake Michigan in 2010. The collecting area of the box-corer was 30 cm × 30 cm, with a maximum depth of 90 cm. Four polycarbonate core tubes (10 cm o.d., 9.5 cm i.d. and 59.6 cm long) were carefully inserted into the sediment collected in the box. The tubes were capped on top, and a polyethylene puck with two o-ring seals was inserted into the bottom opening of each tube. The tubes were pulled upwards from the bottom with a custom-made L-shaped metal puller. During sampling of Lakes Michigan, Superior, Huron, Erie, and Ontario in 2011–2014, a multicorer MC400 (Ocean Instrument, San Diego, CA) was used to collect four subcores in each deployment. The individual core tubes were

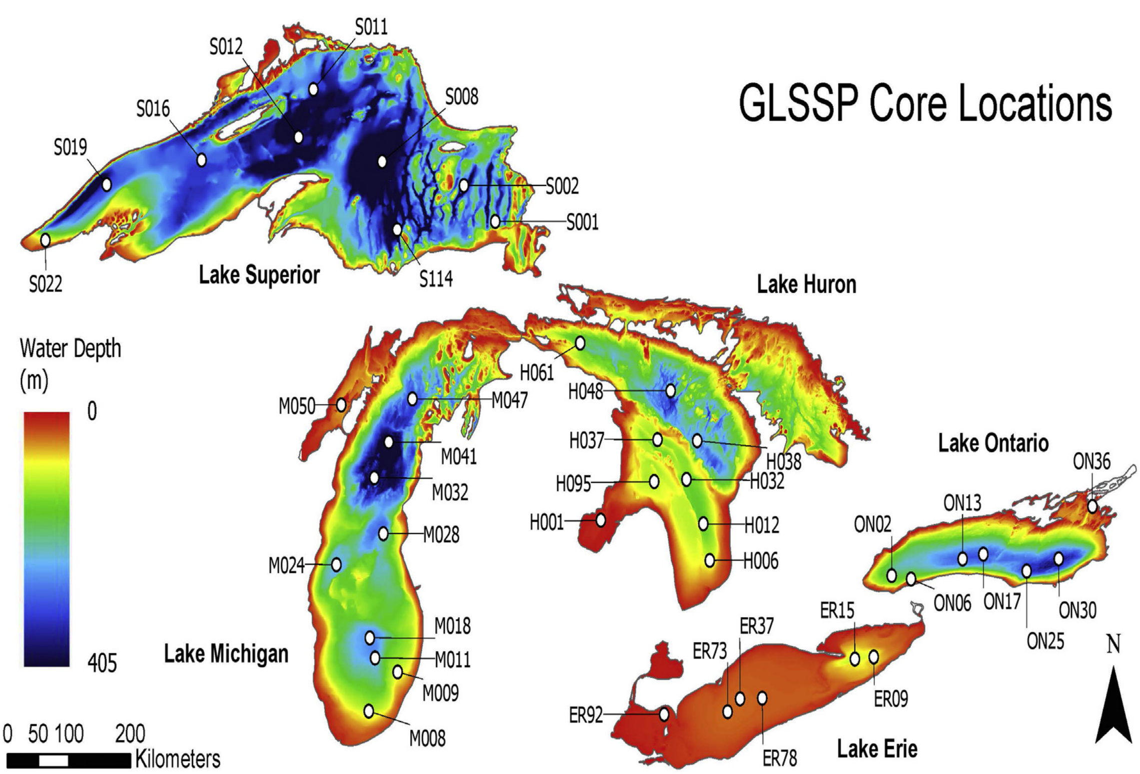

Fig. 1. Core locations and bathymetry of the Great Lakes (NOAA, 2018).

made of the same material and had the same dimension as used in 2010 with the box-corer. At each site, the corer was deployed at least twice, resulting in at least eight subcores. Care was taken to maintain the vertical position of the cores and avoid any disturbance of the sediment in the coring tubes. Accidentally disturbed cores were discarded.

As soon as the corer was brought to deck, the GLSSP team leader on duty visually inspected the cores and a decision was made on whether to accept the retrieved cores, using the following criteria: (i) for sites in depositional zones, the difference in sediment depth from the same site was <5 cm, and the visual appearance was similar among cores. Exceptions could be made for sites on slopes, near lake inlets/outlets, or with benthic animals (e.g. mussels); (ii) the depth of overlying water (the distance from top of the tubes to the sediment-water interface) was no <12 cm, in order to ensure proper handling during core sectioning; and (iii) no sign of sediment disturbance, thus the sediment-water interface was clear with no significant suspension of sediment particles in the overlaying water.

At each coring site, five to seven cores at each location were accepted, extruded, and sectioned in the General Laboratory of the ship, using hydraulic extruders. Due to the beveled upper opening of the polycarbonate tubes, a specially designed extension tube ("collar") was secured on the top of the tube to prevent the widening of core segment when it came up to surface. To minimize the "smearing" effect that could cause lower chronological resolution (Chant and Cornett, 1991), a stainless-steel trimmer was used to trim off a 2-mm rind of sediment that touched the coring tube. This was done for all core segments except the top layers that were generally too watery to cut. Cutting was performed using stainless-steel scrapers, and sample material was transferred carefully into Pyrex mixing bowls, without losing sediment particles or water.

Sectioning schemes were designed considering the targeted chronological resolution (≤5 yr), length of core sufficient to reach sediments deposited back to at least 1900 CE, mass of each section sufficient for various laboratory analyses, and feasibility of handling. Same-depth sections from all of the subcores from a single site were homogenized in

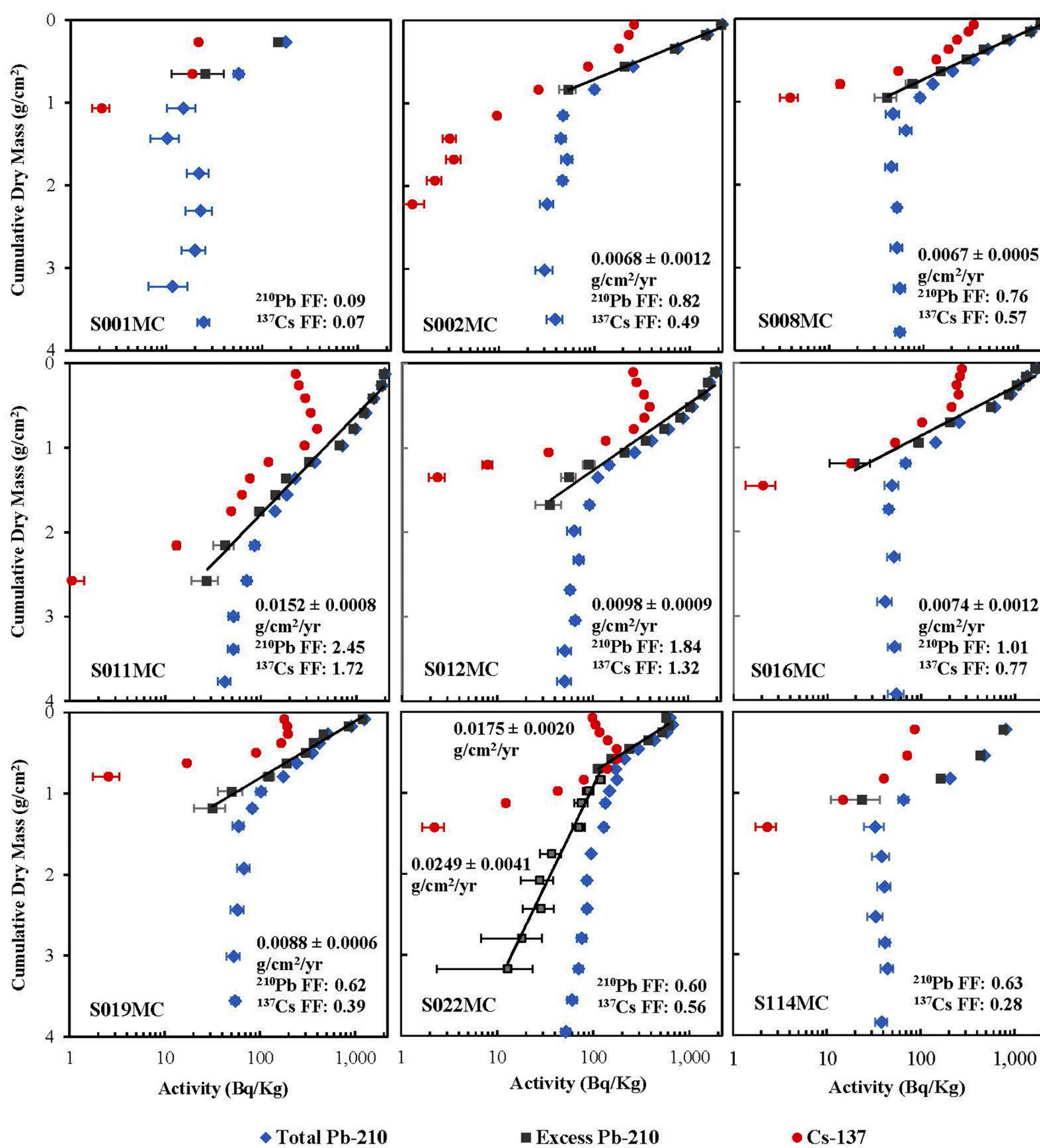

Fig. 2. Cumulative dry mass (g cm^{-2}) vs. log activities of ^{137}Cs, total-^{210}Pb, and unsupported-^{210}Pb in Lake Superior sediment cores. Also shown are values of apparent mean sediment mass accumulation rates (g cm^{-2} yr^{-1}) as determined from the best-fit CRS or CIC models, and values of FF_{Pb} and FF_{Cs}.

Pyrex bowls with stainless steel spoons, and distributed into six containers for analysis in different laboratories. Dry bulk density was calculated from weight loss of a known mass and volume of wet, homogenized sediment after heating at 105 °C for 48 h as described by Buckley et al. (2004). Water contents of core-top sediments ranged from 66 to 95 wt%, and increased to 40 to 81 wt% at the maximum core depths (25 to 50 cm). Sample aliquots used for radionuclide analyses were frozen shipboard, and later freeze-dried and pulverized using a mortar and pestle. Samples were then placed into pre-weighed polypropylene vials of two types: 1.0 cm diameter, 4 cm length (first three measured cores only) and 1.5 cm diameter, 5.7 cm length, polypropylene "Omni-vials" (all other cores) and lightly packed by tapping.

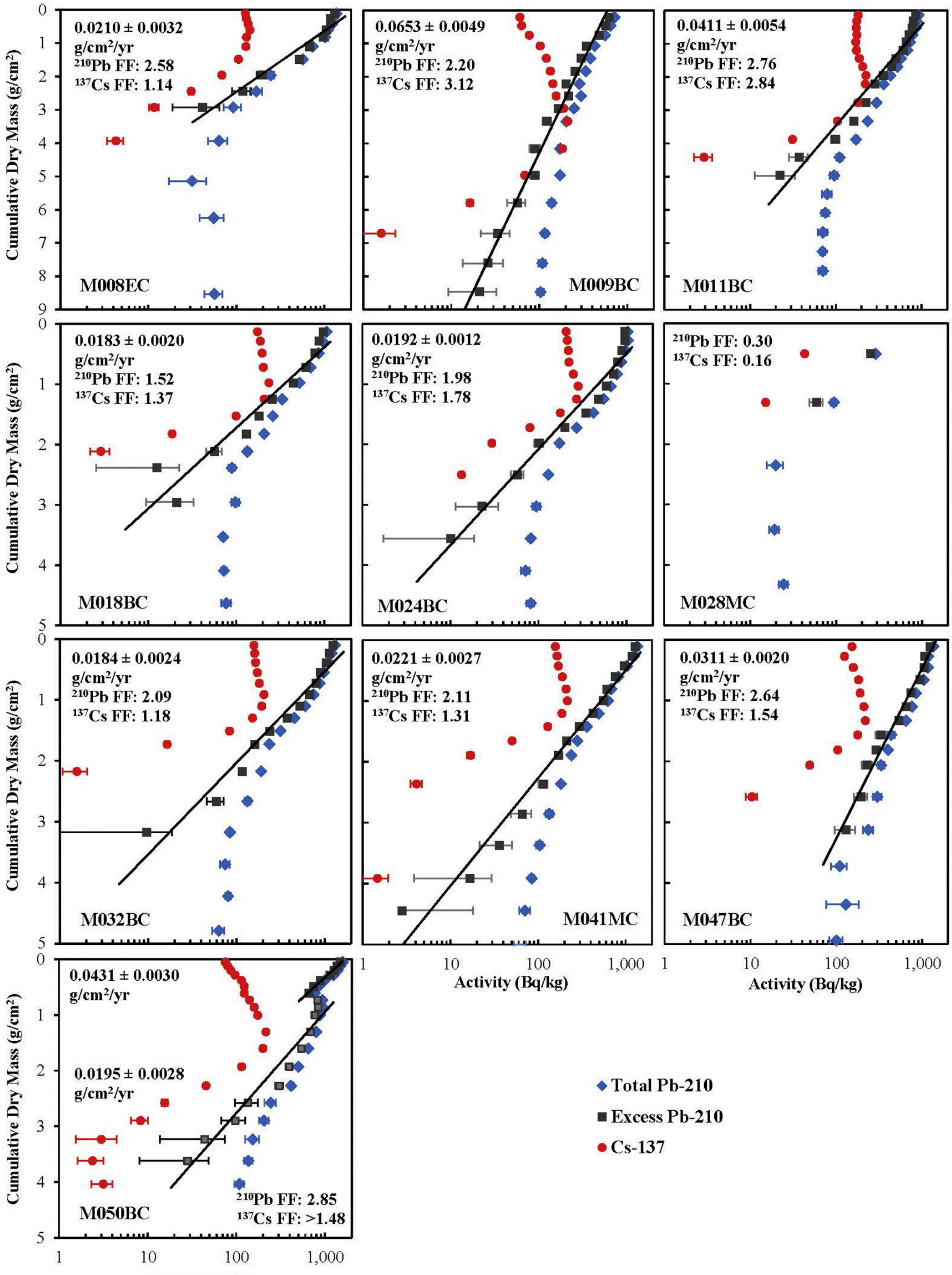

Fig. 3. Cumulative dry mass (g cm^{-2}) vs. log activities of ^{137}Cs, total-^{210}Pb, and unsupported-^{210}Pb in Lake Michigan sediment cores. Also shown are values of apparent mean sediment mass accumulation rates (g cm^{-2} yr^{-1}) as determined from the best-fit CRS or CIC models, and values of FF_{Pb} and FF_{Cs}.

Heights and weights of samples in each vial were measured prior to quantification of radionuclide activities by use of gamma spectrometry. As part of sampling quality control, additional corer deployments were made at two convenient locations where time was available for more sampling (ER15 and ON30). The same-depth segments from the four individual sub-cores from these deployments were not combined, but individually packed, characterized, and dated, in order to assess the difference among the sub-cores in a single multi-corer deployment. The results for each of the sub-cores were compared with the composite samples from these two stations, to evaluate whether combining sub-cores caused any sampling bias or loss of temporal resolution.

Quantification of radionuclides

Three high-purity Ge gamma spectrometers (2 Model GWL-170-15-LB-AWT with 15-mm well diameter, and 1 model GWL-170-10-LB-AWT with 10 mm well diameter, EG&G Ortec, Ametek, Inc.) were used to measure gamma emissions. Radionuclide photopeaks quantified in this study were ^{210}Pb (46.5 keV), ^{137}Cs (661.6 keV) and ^{226}Ra (186.2 keV). Gamma spectrometers were calibrated using efficiency equations based on measurements of certified radionuclide standards, including DL-1A (Reference Uranium-Thorium Ore, Canada Centre for Mineral and Energy Technology, Ontario, Canada) for ^{210}Pb and other U- and Th-series radionuclides, and NIST 4357 (Standard Reference Material 4357, National Institute of Standards and Technology, Gaithersburg, Maryland, USA) for ^{137}Cs, adjusted for decay from the date of certification. Specific activities and one sigma counting errors were calculated using standard counting techniques (Mook, 2001) and are reported in becquerels per kilogram dry mass (Bq/kg). Reported activities were corrected for detector background and decay from time of sampling to the starting time of the gamma spectrometry measurement. Limits of quantification for radionuclides were defined as three times the standard deviation of the background under the peak used for the activity quantification, and values less than the limit of quantification are not reported.

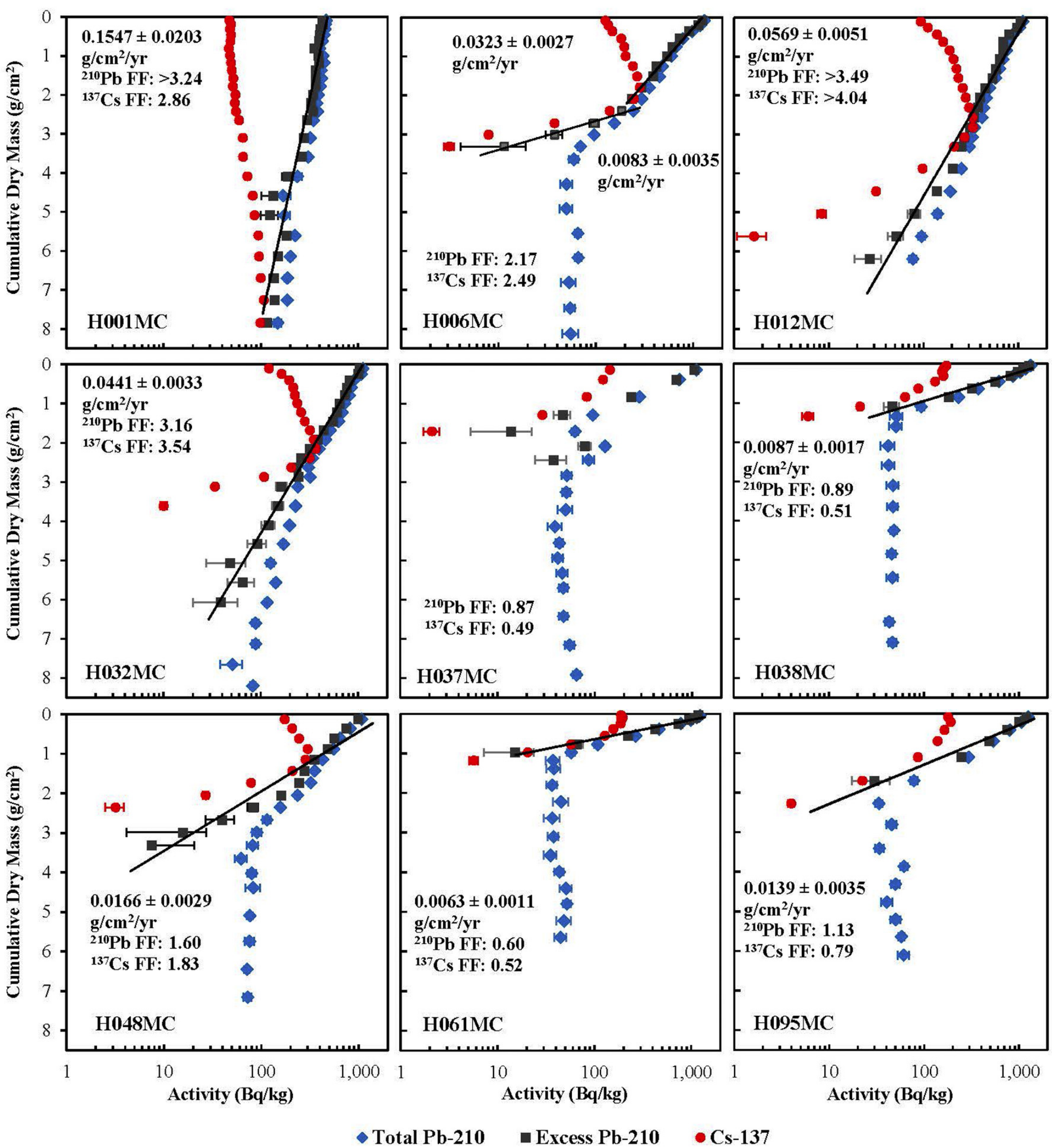

Fig. 4. Cumulative dry mass (g cm^{-2}) vs. log activities of ^{137}Cs, total-^{210}Pb, and unsupported-^{210}Pb in Lake Huron sediment cores. Also shown are values of apparent mean sediment mass accumulation rates (g cm^{-2} yr^{-1}) as determined from the best-fit CRS or CIC models, and values of FF_{Pb} and FF_{Cs}.

Calculation of sediment mass accumulation rate, focusing factor, and calendar year of deposition

The approach was to apply simple ^{210}Pb models uniformly to all sediment cores to obtain net apparent mean sediment mass accumulation rates, and to validate these models using the anthropogenic radionuclide ^{137}Cs ($t_{½} = 30.08$ years) as an independent constraint on sediment age at the 1963 horizon that marks the global maximum deposition of ^{137}Cs from above-ground nuclear weapons tests. Independent validation of ^{210}Pb model ages is critical for accurate assignment of calendar year dates to specific sediment horizons (Kirchner, 2011; Robbins and Edgington, 1975; Smith, 2001).

According to the CIC and CRS models, site-specific sediment mass accumulation rates were derived from the slopes of least-squares linear regressions of $\ln C_0/C_z$ and $\ln A_0/A_z$, respectively, versus cumulative sediment dry mass. CIC variables C_0 and C_z are the ^{210}Pb activity, and the CRS variables A_0 and A_z are the cumulative ^{210}Pb activity, in the sediment surface segment (subscript 0) and below a particular depth z, respectively. The sediment mass accumulation rate was then estimated from the slope of the linear regression (Eq. (1)).

$$\text{Sediment mass accumulation rate } (\text{g cm}^{-2}\text{ yr}^{-1}) = \text{Slope} \times \gamma \quad (1)$$

where $\lambda = (\ln 2) / \text{half life of } ^{210}Pb = 0.693 / 22.26\text{ yr} = 0.3114\text{ yr}^{-1}$ is the radioactive decay constant of ^{210}Pb.

Both the CIC and CRS models were used in this study. Supported ^{210}Pb values (for cores reaching the depth where unsupported-^{210}Pb activity was undetectable) were calculated as the mean value (±standard deviation) of total-^{210}Pb activity for the deepest 4 to 10 sections of the core, where activities of total-^{210}Pb were approximately constant with depth. Unsupported-^{210}Pb was then obtained for each core section by subtracting this value for supported-^{210}Pb activity from the measured value of total-^{210}Pb. Most cores gave statistically better results using CRS models, and showed good agreement between the depth of the ^{137}Cs peak (~1963) and the corresponding deposition year calculated from the CRS (or CIC) model by use of ^{210}Pb. Although most cores reached a depth where unsupported-^{210}Pb activity was less than the limit of quantification, which is a necessary condition for application of the CRS model, there were a number of exceptions at locations where coring depth did not reach this depth. These exceptions were in Lake Huron (H001 and H012), Lake Erie (ER09, ER15, ER37, and ER73), and Lake Ontario (ON06). At these locations of relatively rapid sedimentation, core depths did not reach the ^{137}Cs peak nor did unsupported-^{210}Pb reach undetectable levels, so the mean ^{226}Ra activity in the core was used as a proxy for supported ^{210}Pb. This was justified by the relatively constant values of ^{226}Ra activity with depth in each of these cores, but bears the caveat that ^{222}Rn mobility within the sediments might have caused some ^{210}Pb—^{226}Ra disequilibrium as observed by Thomson et al. (1975) and Robbins et al. (1978).

The focusing factor obtained from the unsupported-^{210}Pb (FF_{Pb}) inventory at each sampling location was calculated as the ratio of the cumulative unsupported-^{210}Pb activity to that expected from the regional atmospheric input, which was reported as 15.5 pCi cm^{-2} (= 0.573 Bq cm^{-2}) for the Great Lakes region (Simcik et al., 1996; Urban et al., 1990). The focusing factor obtained from the ^{137}Cs (FF_{Cs}) inventory was similarly calculated using the atmospheric input values of ^{137}Cs from Robbins (1985). In cores that were not sufficiently deep to reach zero unsupported-^{210}Pb activity or zero ^{137}Cs activity, owing to relatively high sedimentation rates, FF_{Pb} and FF_{Cs} values are reported as lower limits. We realize that the ^{210}Pb deposition flux to the lake depends on precipitation amounts and therefore at a given location these might vary substantially on an annual basis (Baskaran and Naidu, 1995).

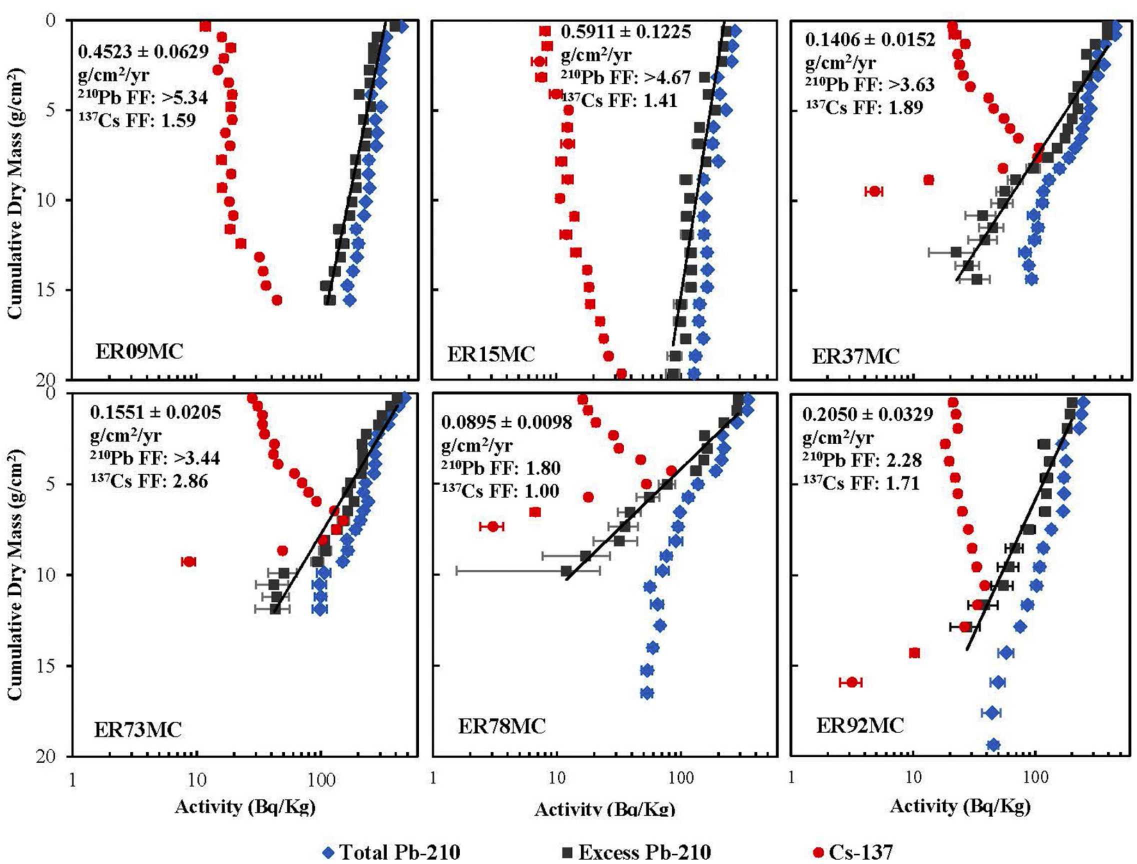

Fig. 5. Cumulative dry mass (g cm^{-2}) vs. log activities of ^{137}Cs, total-^{210}Pb, and unsupported-^{210}Pb in Lake Erie sediment cores. Also shown are values of apparent mean sediment mass accumulation rates (g cm^{-2} yr^{-1}) as determined from the best-fit CRS or CIC models, and values of FF_{Pb} and FF_{Cs}.

Thus, we consider the FF values to represent approximations that depend on the specific value assumed for the annual ^{210}Pb deposition flux.

The calendar date of deposition and its error calculated for each core section is based on the 95% upper and lower confidence limits of the slope the corresponding CRS or CIC regression. The 95% confidence limits for the slope are calculated (Eqs. (2) and (3)) (Sokal and Rohlf, 1981):

$$L95 = (\text{slope}) - t_{(0.05,df)} * se \tag{2}$$

$$U95 = (\text{slope}) + t_{(0.05,df)} * se \tag{3}$$

where, L95 and U95 = Lower and Upper 95% confidence limits, respectively, on slope; df = degrees of freedom for the t-test, calculated as (n − 2); n = number of sections used in the regression; $t_{(0.05,df)}$ = t-distribution for the 95% confidence limit and the specific df; and se = standard error of the slope.

Results and discussion

Profiles of radionuclides in the sediment cores collected during this study from Lakes Superior, Michigan, Huron, Erie, and Ontario are portrayed in Figs. 2-6, respectively. A summary of the results of this study, including selected dating models, sedimentation mass accumulation rates with errors, and sediment focusing factors from both ^{210}Pb and ^{137}Cs inventories is given in Table 1. Complete analytical data for all core profiles, including dry bulk densities, radionuclide activities (^{137}Cs, ^{226}Ra, total ^{210}Pb, unsupported-^{210}Pb), and calculated calendar date profiles, are included with the Electronic Supplementary Material (ESM, Table S1). Data for comparisons of composite cores with individual subcores from ER15 and ON30 are also included with the ESM (Figs. S1 and S2). Additional figures provided in ESM include CRS and CIC regression plots and calendar date profile plots (Figs. S3–S12).

^{210}Pb activities

The highest measured activity of ^{210}Pb for each site was observed in the top section of each core, at the sediment-water interface (with one

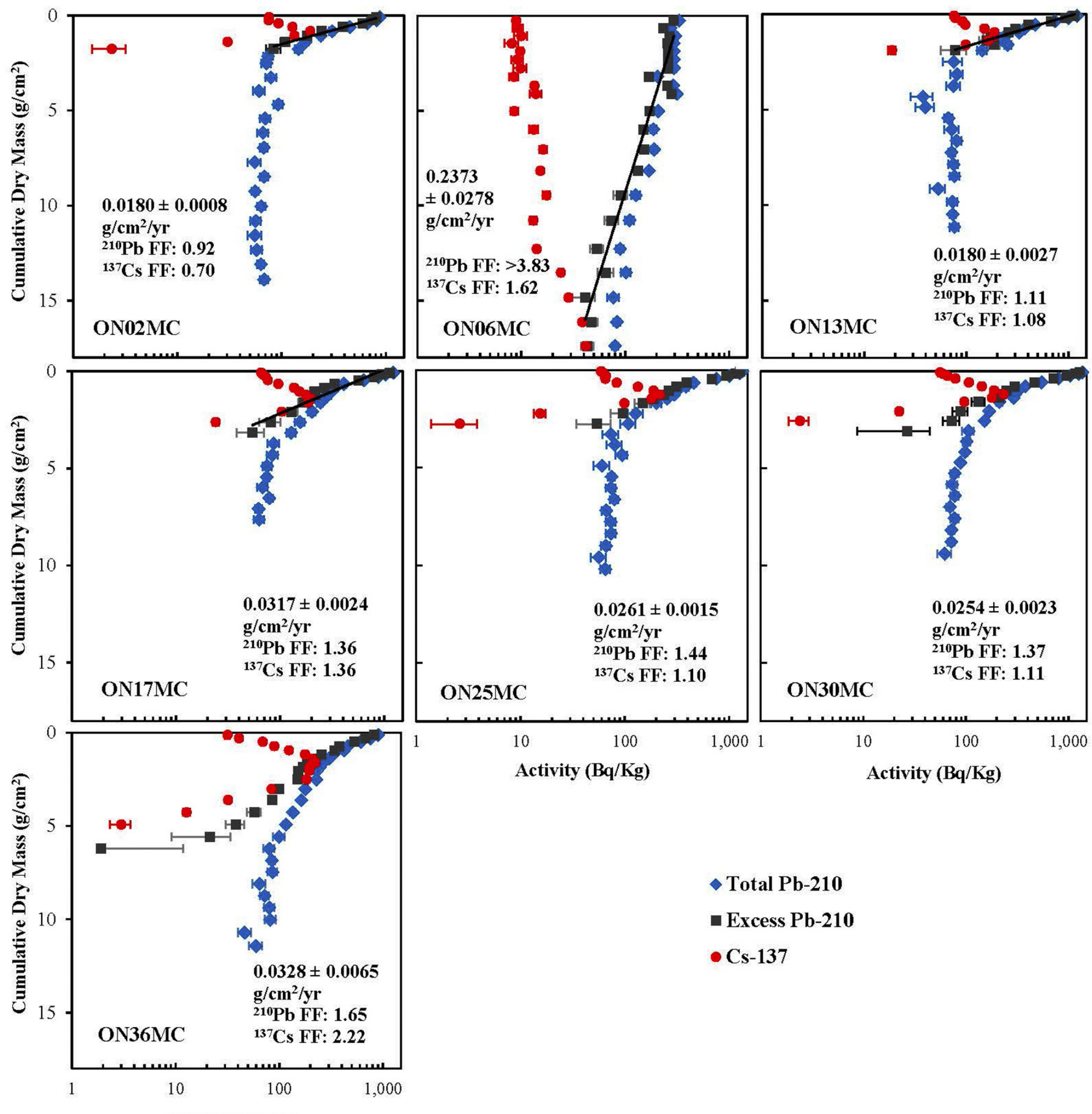

Fig. 6. Cumulative dry mass (g cm^{-2}) vs. log activities of ^{137}Cs, total-^{210}Pb, and unsupported-^{210}Pb in Lake Ontario sediment cores. Also shown are values of apparent mean sediment mass accumulation rates (g cm^{-2} yr^{-1}) as determined from the best-fit CRS or CIC models, and values of FF_{Pb} and FF_{Cs}.

exception, S022). The range of unsupported-^{210}Pb activities in the top sections of the sediment cores was from 146 to 2150 Bq/kg. Unsupported-^{210}Pb activity generally decreased exponentially with depth to reach an undetectable level (~10 to 20 Bq/kg) which occurred within the sampled depth range of most cores, except those having relatively high (>0.15 g cm^{-2} yr^{-1}) sediment mass accumulation rate (H001, ER09, ER15, and ON06) (Figs. 2-6). For most cores, the results were sufficient to allow determination of sediment mass accumulation rates by use of unsupported-^{210}Pb profiles. In contrast to the relatively large range of unsupported-^{210}Pb activities observed in the top sections of cores (146 to 2150 Bq/kg), the supported-^{210}Pb activities based on a summary of those derived by use of the ^{210}Pb dating models had a relatively small range of mean ± standard deviation, at 47.7 ± 8.1 Bq/kg ($n = 9$) in Lake Superior, 74.8 ± 22.3 Bq/kg ($n = 10$) in Lake Michigan, 54.7 ± 13.1 Bq/kg (n = 9) in Lake Huron, 50.5 ± 6.3 Bq/kg ($n = 6$) in Lake Erie, and 67.4 ± 14.7 Bq/kg ($n = 7$) in Lake Ontario.

^{137}Cs activities

Profiles of ^{137}Cs activity in most cores had well-defined maxima, with relatively high activities occurring from the surface to the depth of the peak activity, followed by a steep decrease in activity with depth (Figs. 2-6). The depth of the ^{137}Cs peak (where present) gave a 1963 reference horizon for validation of calendar dates obtained from ^{210}Pb model regressions. Several cores from locations having relatively high sedimentation rates exhibited gradually increasing activities of ^{137}Cs activity as a function of depth, but exhibited no clear maxima (H001, ER09, ER15, and ON06), which indicated that the 1963 reference horizon might not have been reached at total core depth. In other cores from Lake Superior (S001, S002, S008, S016, S114) and Lake Huron (H037, H038), the highest ^{137}Cs activities were found in the top sections. These cores also had relatively low values of FF_{Cs} (ranging from 0.07 to 0.77) and FF_{Pb} (ranging from 0.09 to 1.01), indicating net loss of deposited sediment by horizontal sediment transport processes (Edgington and Robbins, 1990).

To use ^{137}Cs profiles to validate calendar dates predicted by models based on ^{210}Pb requires confidence that the peak ^{137}Cs activity has remained at a fixed horizon within the core. High ^{137}Cs activities in surficial sediments as well as broadened ^{137}Cs peaks at depth have been widely reported, which may indicate considerable ^{137}Cs mobility by horizontal transport of sediments, biological mixing, and pore-scale vertical migration (Abril and Gharbi, 2012; Davis et al., 1984; Guinasso and Schink, 1975; Klaminder et al., 2012; Robbins, 1986; Robbins et al., 1977). Some models predict that the ^{137}Cs peak could move downward within the sediment column (Crusius et al., 2004; Crusius and Kenna, 2007; Robbins, 1986; Robbins and Edgington, 1975; Smith et al.,

Table 1
Core locations, depths, sediment mass accumulation rates and focusing factors.

Core	Lat	Long	Water Depth, m	Model	MAR, g cm^{-2}y^{-1} [a]	^{210}Pb FF	^{137}Cs FF
S001MC	46.9930	−85.1612	95	na	na	0.09	0.07
S002MC	47.3603	−85.6208	154	CRS	0.007 ± 0.001	0.82	0.49
S008MC	47.6058	−86.8177	301	CRS	0.007 ± 0.001	0.76	0.57
S011MC	48.3438	−87.8250	230	CRS	0.015 ± 0.001	2.45	1.72
S012MC	47.8553	−88.0418	238	CRS	0.010 ± 0.001	1.84	1.32
S016MC	47.6212	−89.4633	180	CRS	0.007 ± 0.001	1.01	0.77
S019MC	47.3703	−90.8535	188	CRS	0.009 ± 0.001	0.62	0.39
S022MC (0–3.5 cm)	46.8002	−91.7508	54	CRS	0.017 ± 0.002	0.60	0.56
S022MC (3.5–25 cm)	46.8002	−91.7508	54	CRS	0.025 ± 0.004		
S114MC	46.9095	−86.5980	398	na	na	0.63	0.28
M008EC	41.9842	−87.0142	66	CRS	0.021 ± 0.003	2.58	1.14
M009BC	42.3850	−86.5915	62	CRS	0.065 ± 0.005	2.20	3.12
M011BC	42.5283	−86.9220	164	CIC	0.041 ± 0.005	2.76	2.84
M018BC	42.7338	−86.9995	165	CRS	0.018 ± 0.002	1.52	1.37
M024BC	43.4830	−87.4882	150	CRS	0.019 ± 0.001	1.98	1.78
M028MC	43.8000	−86.8005	133	na	na	0.30	0.16
M032BC	44.3715	−86.9333	257	CRS	0.018 ± 0.002	2.09	1.18
M041MC	44.7367	−86.7213	266	CRS	0.022 ± 0.003	2.11	1.31
M047BC	45.1783	−86.3745	200	CRS	0.031 ± 0.002	2.64	1.54
M050BC (0–7 cm)	45.1165	−87.4165	33	CRS	0.043 ± 0.003	2.85	>1.48
M050BC (7–28 cm)	45.1165	−87.4165	33	CRS	0.020 ± 0.003		
H001MC	43.9374	−83.6142	13	CIC	0.155 ± 0.020	>3.24	>2.86
H006MC (0–10 cm)	43.5265	−82.0185	62	CRS	0.032 ± 0.003	2.17	2.49
H006MC (10–14 cm)	43.5265	−82.0185	62	CRS	0.008 ± 0.003		
H012MC	43.9007	−82.1130	99	CIC	0.057 ± 0.005	>3.49	4.04
H032MC	44.3542	−82.3596	94	CRS	0.044 ± 0.003	3.16	3.54
H037MC	44.7619	−82.7836	76	na	na	0.87	0.49
H038MC	44.7507	−82.2024	166	CRS	0.009 ± 0.002	0.89	0.51
H048MC	45.2614	−82.5912	183	CRS	0.017 ± 0.003	1.60	1.83
H061MC	45.7498	−83.9164	122	CRS	0.006 ± 0.001	0.60	0.52
H095MC	44.3328	−82.8326	70	CRS	0.014 ± 0.003	1.13	0.79
ER09MC	42.5387	−79.6163	51	CIC	0.452 ± 0.063	>5.34	>1.59
ER15MC	42.5171	−79.8930	65	CIC	0.591 ± 0.123	>4.67	>1.41
ER37MC	42.1097	−81.5748	25	CIC	0.141 ± 0.015	>3.63	1.89
ER73MC	41.9778	−81.7571	25	CIC	0.155 ± 0.021	>3.44	2.86
ER78MC	42.1168	−81.2501	24	CIC	0.090 ± 0.010	1.80	1.00
ER92MC	41.9506	−82.6867	12	CIC	0.205 ± 0.033	2.28	1.71
ON02MC	43.3713	−79.3533	101	CRS	0.018 ± 0.001	0.92	0.70
ON06MC	43.3360	−79.0700	69	CIC	0.237 ± 0.028	>3.50	>1.62
ON13MC	43.5414	−78.3143	181	CRS	0.018 ± 0.003	1.11	1.08
ON17MC	43.5902	−78.0111	183	CRS	0.032 ± 0.002	1.36	1.36
ON25MC	43.4180	−77.3762	200	CRS	0.026 ± 0.002	1.44	1.10
ON30MC	43.5429	−76.9066	220	CRS	0.025 ± 0.002	1.37	1.11
ON36MC	44.0780	−76.4125	26	CRS	0.033 ± 0.007	1.65	2.22

na - not applicable.
[a] Errors on mass accumulation rates are 95% confidence limits.

2009). A study of varved sediments from a location in northern Sweden that was sampled multiple times before and after the 1986 Chernobyl accident showed that the location of the ^{137}Cs maximum in the sediment core remained fixed despite apparent diffusive relaxation of the peak (Klaminder et al., 2012). In the present study, there is evidence for diffusive relaxation of the ^{137}Cs peak, because the onset of the horizon for ^{137}Cs predated 1951 in some of the cores (ESM Tables S1–S5). Apparent early appearance of ^{137}Cs in dated sediment profiles has also been observed in other studies, and this phenomenon has been attributed to downward diffusion of ^{137}Cs (Appleby, 2001; Davis et al., 1984) or downward advection of fine particles with sorbed ^{137}Cs (Abril and Gharbi, 2012).

Sediment mass accumulation rates

A comparison of the sediment mass accumulation rates among lakes demonstrated that four of the 41 cores were not suitable for estimating such rates, and these all had low (≤1.0) FF_{Pb} and FF_{Cs} values (Fig. 7). Three of the cores were clearly best-fit by two-slope CRS models (S022, M050, and H006). Rates of sediment mass accumulation in all other cores were satisfactorily fitted by either a one-slope CRS or CIC model. All regressions obtained by use of the CRS model had coefficients of determination (R^2) values ≥0.89, while all regressions for CIC models had R^2 values ≥0.84 (ESM Figs. S3–S7). Profiles of ^{137}Cs activities were used to provide independent validation of the calendar year age profiles obtained from the ^{210}Pb models. The model used to estimate calendar year age profiles was defined as the one that best agreed with the depth associated with the maximum ^{137}Cs activity defined to be ~1963 (Kirchner, 2011; Robbins and Edgington, 1975). Nineteen of the 41 regressions of unsupported-^{210}Pb yielded calendar date profiles that agreed with that determined by the maximum ^{137}Cs activity. The date of deposition determined to be 1963 by use of ^{210}Pb was always near to that predicted to be the 1963 maximum activity observed for ^{137}Cs. If not in the same segment of the core, it was in an immediately adjacent section. Of the 22 cores for which such agreement was not obtained, nine had maximum ^{137}Cs activities at the top of the core as well as relatively low (≤1.0) FF_{Pb} and FF_{Cs} values, and four cores did not appear to have reached the depth of the ^{137}Cs peak at the bottom of the core. In those cores not yielding agreement between ^{137}Cs maxima and ^{210}Pb-based calendar dates of ~1963, most yielded apparently reasonable sediment mass accumulation rates.

Calendar dates and concentrations of persistent organochlorine pollutants such as PCBs were also compared with known histories of industrial production for polychlorinated biphenyls and other legacy pollutants (e.g., Li et al., 2018, this issue). For example, in the core from site M050 in Green Bay, Lake Michigan, the ^{210}Pb activity profile is noticeably discontinuous (Fig. 3). Applications of the 2-slope CRS model, separately to the upper 0–7 cm and below 7 cm core segments, yielded calendar dates of 1920–1937 for the onset of PCB deposition and 1969 for the peak of PCB deposition in the sediment. These timings are in agreement with the history of PCB production and its deposition history for the Lower Fox River, Wisconsin, and Lake Michigan (ATSDR, 2006; Durfee, 1976; Golden et al., 1993).

Sediment mass accumulation rates derived from ^{210}Pb models ranged from 0.007 to 0.065 g cm^{-2} y^{-1} in Lakes Superior, Michigan, Huron and Ontario, except for the outliers from sites H001 (0.155 g cm^{-2} yr^{-}1) and ON06 (0.237 g cm^{-2} yr^{-1}) which are located proximal to the outlets of the Saginaw and Niagara Rivers, respectively. Relatively high sediment mass accumulation rates in Lakes Superior and Michigan were also associated with outlets of the St. Louis River at Duluth, MN at site S022 (0.025 g cm^{-2} yr^{-1}) and the Fox River at Green Bay, WI at site M050 (0.043 g cm^{-2} yr^{-1}), as well as a region of sediment accumulation in southeastern Lake Michigan offshore near the outlet of the St. Joseph River at site M009 (0.065 g cm^{-2} yr^{-1}). The high sedimentation rates near the outlets of the St. Louis and St. Joseph Rivers are largely fed by erosion of lake bluffs in Wisconsin, which is the largest source of sediment to both Lakes Superior and Michigan (Edgington and Robbins, 1990; Kemp et al., 1978). Lake Erie has much higher sediment mass accumulation rates (ranging from 0.090 to 0.591 g cm^{-2} yr^{-1}) than the other lakes, especially in its Eastern Basin. Relatively high sediment mass accumulation rates in Green Bay and in the basins of Lake Erie may be partly due to enhanced preservation of sedimentary organic matter under conditions of persistent hypoxia in these locations (Paytan et al., 2017).

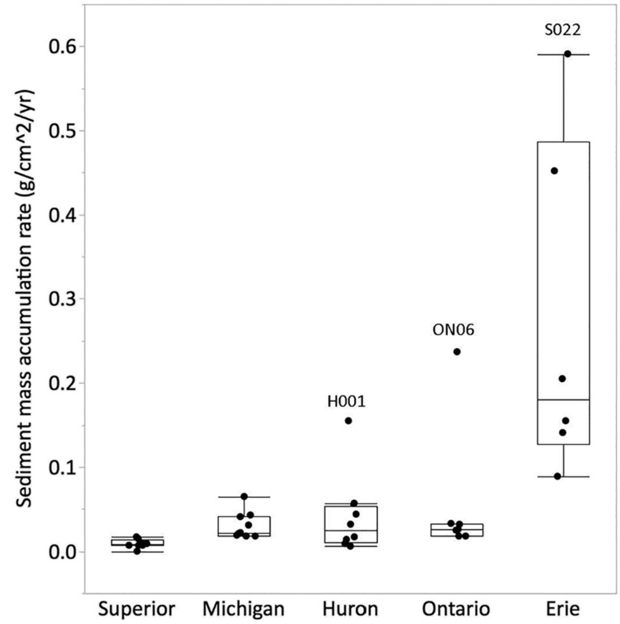

Fig. 7. Lake-by-lake comparison of the sediment dry mass accumulation rates (g cm^{-2} yr^{-1}) obtained in this study. Outliers having anomalously high rates are labeled.

Sediment mass accumulation rates in depositional basins of the Laurentian Great Lakes are apparently related to the depth of the water column; a power-law relationship describes this relationship, where log of the rate of sediment mass accumulation is inversely proportional to log of water depth (Fig. 8). A similar relationship occurs between the unsupported-^{210}Pb activity measured in the top section of each sediment core and the sediment mass accumulation rate at the core location (Fig. 9). This is due to the lesser flux of deposition of sediments in deeper portions of the lakes, and thus a concomitantly greater loading of unsupported-^{210}Pb onto available surfaces of particles. Where sediment mass accumulation rate is higher, the unsupported-^{210}Pb is diluted with material having lower specific activity of

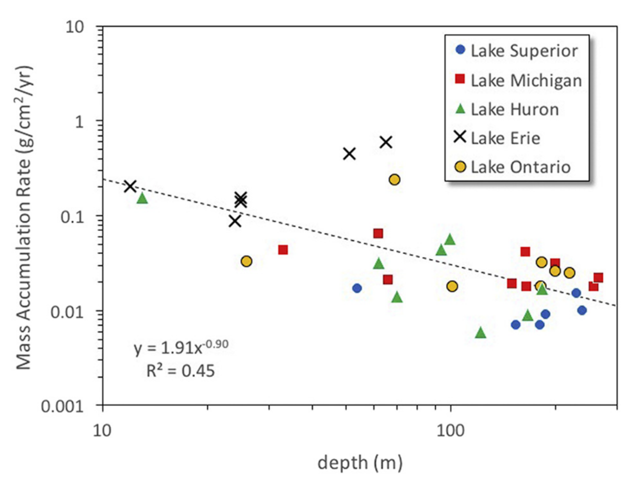

Fig. 8. Sediment dry mass accumulation rates (g cm^{-2} yr^{-1}) vs. water depth (m) for sediment cores measured in this study.

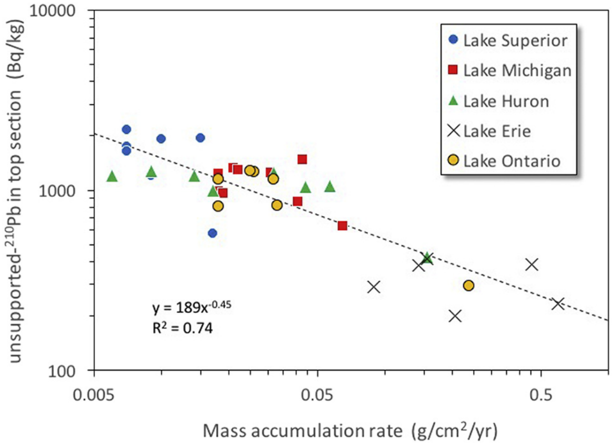

Fig. 9. Unsupported-^{210}Pb activity (Bq/kg) measured in the top section of each sediment core vs. sediment dry mass accumulation rate (g cm^{-2} yr^{-1}).

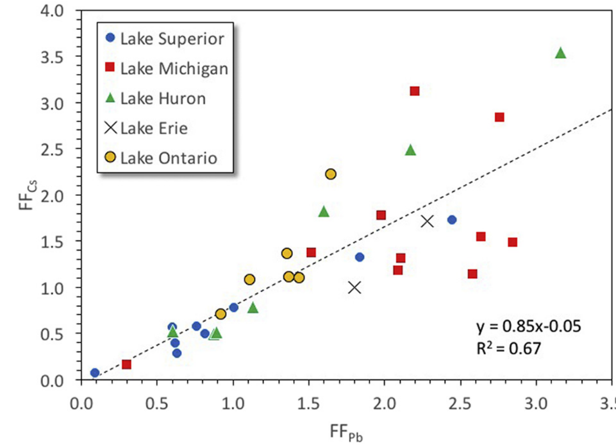

Fig. 10. FF_{Cs} vs. FF_{Pb} values and a least-squares linear regression indicates that the ratio of FF_{Cs}/FF_{Pb} is ~0.82, with values diverging at FF values >1.5.

unsupported-^{210}Pb. For example, sediments eroded from lake bluffs typically have negligible amounts of unsupported-^{210}Pb. The overall trend in sediment mass accumulation rates, from lowest rates in Lake Superior to highest rates in Lake Erie, is roughly consistent with the ratios of lake catchment areas (km^2) to lake surface areas (km^2); these ratios increase in the following order: Superior (1.86), Michigan (2.04), Huron (2.25), Erie (3.04), and Ontario (3.37). Sediment mass accumulation rates determined in this study agree well overall with previously reported rates (Bruland et al., 1975; Robbins and Edgington, 1975; Robbins et al., 1977; Robbins et al., 1978; Evans et al., 1981; Hermanson and Christensen, 1991; Johnson et al., 2012; Klump et al., 1989; O'Beirne et al., 2017).

Some of the measured ^{210}Pb profiles from this study have a steepening-upward slope in the top several cm of the core, including several in Lake Superior and about half of those in Lake Michigan. This may indicate local biological mixing (Crusius et al., 2004; Guinasso and Schink, 1975; Robbins and Edgington, 1975; Robbins, 1978; Robbins et al., 1977, 1979). Most of our ^{210}Pb profiles do not show this effect, including all of the Huron, Erie, and Ontario cores, therefore it was not included in our calculations of sediment mass accumulation rates. Where upward-steepening ^{210}Pb profiles occur, a more accurate assessment of sediment mass accumulation could be obtained by incorporating a diffusion-like mixing term at the sediment-water interface; this describes the near-surface mixing caused by typical feeding patterns of benthic amphipods (Guinasso and Schink, 1975; Robbins et al., 1979). Despite the large-scale ecological changes observed in the Great Lakes since the early 1980's with steep decline of benthic amphipod populations and increase of dreissenid mussels (Thayer et al., 1997; Vanderploeg et al., 2002), as well as more effective sediment load management of croplands (Ouyang et al., 2005), our ^{210}Pb profiles do not appear to indicate substantial changes in sediment mixing or mass accumulation rates in the past three decades since similar studies were published in the 1970's and 1980's (Bruland et al., 1975; Edgington and Robbins, 1990; Evans et al., 1981; Klump et al., 1989; Robbins and Edgington, 1975; Robbins et al., 1977, 1978).

Sediment focusing factors

Focusing factors derived from ^{210}Pb and ^{137}Cs inventories ranged widely from 0.09 to >5.3 for FF_{Pb} and from 0.07 to 4.04 for FF_{Cs}. These results demonstrate the dynamic processes that redistribute sediments within the lakes, such as landslides, wind-generated currents, and thermal overturn. The FF_{Pb} and FF_{Cs} values were well-correlated and a least-squares linear regression indicated that the ratio of FF_{Cs}/FF_{Pb} is ~0.85, with values diverging at FF values >1.5 (Fig. 10). The generally lower value of FF_{Cs} is expected, because ^{137}Cs was not present in the Laurentian Great Lakes system prior to 1951, while unsupported-^{210}Pb was being deposited and focused continuously with sediments over a time period much greater than its 22.3-year half-life. Therefore, even if the focusing behavior of these two radionuclides had been identical since the start of ^{137}Cs deposition in 1951 in a steady-state scenario, about 9% of the ^{210}Pb inventory present in 2011 was already present when ^{137}Cs deposition began, and about 22% was present when the ^{137}Cs peak was deposited in 1963. The divergence of FF_{Pb} and FF_{Cs} at values higher than 1.5 might indicate that subtle differences in geochemical behavior of Cs and Pb are accentuated with more extensive resuspension and redeposition of sediments. Earlier studies in Lake Michigan also noted differences between ^{210}Pb and ^{137}Cs focusing factors, and discussed their significance (Robbins and Edgington, 1975; Edgington and Robbins, 1976; Edgington and Robbins, 1990; Rossmann, 2010).

Atmospheric deposition of radionuclides onto the surface of water is directly related to amounts of precipitation and is thus partly dependent on latitude (Baskaran and Naidu, 1995). Therefore, the assumption of constant region-wide mean depositional fluxes could result in artifacts in focusing factors between sampling sites. In addition, the differences in geochemical behavior of Pb and Cs, as well as the continuous deposition of ^{210}Pb in contrast to the pulse-like deposition of ^{137}Cs that was greatest in 1963, produce contrasting outcomes when subject to the dynamic limnologic processes (including sediment resuspension caused by large storms, sediment slumps, wind- and thermally-driven currents, and bioturbation) that affect transport and deposition of sediments (Edgington and Robbins, 1990). Focusing factors are used for computation of fluxes of deposition of contaminants into sediments. It is generally assumed for this purpose that ^{210}Pb and ^{137}Cs have similar affinities for sorption to particle surfaces as do the hydrophobic pollutant compounds of interest (Eadie and Robbins, 1987). Because, over time, the flux of ^{210}Pb via atmospheric deposition is fairly constant, the value of FF_{Pb} is more suitable than that of FF_{Cs} for use in the normalization of contaminant flux calculations.

Summary and conclusions

Sediment cores were collected during the period of 2010–2014 from 41 locations in all five Laurentian Great Lakes. Gamma spectrometry was used to measure profiles of the activities of ^{210}Pb, ^{137}Cs, and ^{226}Ra in each core. The ^{210}Pb data were applied to estimate apparent net accumulation rates of sediment mass by using the conventional Constant Rate of Supply (CRS) and Constant Initial Concentration (CIC) models for each coring site that yielded an applicable data set. In addition, sediment focusing factors were derived from ^{210}Pb and ^{137}Cs inventories. Sediment mass accumulation rates determined in this study ranged from 0.007 to 0.065 g cm^{-2} yr^{-1} in Lakes Superior, Michigan, Huron and Ontario, with only two outliers having greater rates (~0.2 g cm^{-2} yr^{-1}) near outlets of the Saginaw and Niagara Rivers in Lakes Huron and Ontario, respectively. Greater rates of sediment mass accumulation were observed for Lake Erie than those for the other lakes, ranging from 0.090 to 0.591 g cm^{-2} yr^{-1}. The sediment mass accumulation rates determined in this study were similar to those obtained in previous studies of sediment cores from the same (or nearby) locations (Bruland et al., 1975; Robbins and Edgington, 1975; Robbins et al., 1977; Robbins et al., 1978; Evans et al., 1981; Hermanson and Christensen, 1991; Johnson et al., 2012; Klump et al., 1989; O'Beirne et al., 2017). The sediment mass accumulation rates in depositional basins among the Laurentian Great Lakes are a function of water depth resembling a power-law relationship by which the accumulation rate declines with increasing water depth. Sediment focusing factors derived from ^{210}Pb and ^{137}Cs inventories ranged widely from 0.09 to >5.3 for FF_{Pb} and from 0.07 to 4.04 for FF_{Cs}, reflecting contrasting outcomes for these two radionuclides when subjected to the dynamic sediment redistribution processes within the lakes over time. The FF_{Pb} and FF_{Cs} values are well-correlated and a least-squares linear regression indicates that the ratio of FF_{Cs}/FF_{Pb} is ~0.85, with values diverging at FF values >1.5. Of the cores for which ^{210}Pb and ^{137}Cs profiles exhibited favorable characteristics (i.e., highest ^{210}Pb activity at the sediment-water interface, exponential decrease of unsupported-^{210}Pb with depth, and maximum ^{137}Cs activity at some depth below the sediment-water interface), most yielded good agreement between calendar date profiles calculated from the ^{210}Pb-based sediment mass accumulation rates and the ^{137}Cs activity peak at 1963. The results of this study provide a firm basis for establishing comprehensive pollutant inventories and depositional chronologies of persistent, bioaccumulative and toxic compounds across the Laurentian Great Lakes. Concentrations for thousands of such compounds were measured in the dated core profiles, along with basic physical and chemical characteristics of the sediments (e.g., Bonina et al., 2018, this issue; Codling et al., 2014, 2018a, 2018b; Guo et al., 2017; Li et al., 2018, this issue; Peng et al., 2016). These associated studies have yielded new knowledge and insights into the variety and magnitude of pollutants sequestered in Laurentian Great Lakes sediments, and will comprise an important source of information for resolving scientific and practical issues pertaining to the environmental quality and management of the contaminated sediments of the Laurentian Great Lakes.

Acknowledgements

This research was funded by a Cooperative Agreement from the US EPA Great Lakes Restoration Initiative with Assistance No. GL-00E00538 (EPA Program Officers Todd Nettesheim and Elizabeth Murphy). One of the gamma spectrometers used throughout this study was purchased with funds from the NSF Instrumentation and Facilities grant EAR-0949404. Additional support was provided by the University of Illinois at Chicago (UIC), the University of Delaware (UD), and the Environmental Isotope Geochemistry Laboratory at both UIC (2010-2014) and UD (2014-2017). Prof. Giesy was supported by the Canada Research Chair program, the "High Level Foreign Experts" (#GDT20143200016) program, funded by the State Administration of Foreign Experts Affairs, the P.R. China to Nanjing University and the Einstein Professor Program of the Chinese Academy of Sciences and a Distinguished Visiting Professorship in the School of Biological Sciences of the University of Hong Kong. The authors gratefully acknowledge the assistance provided by the captain and crew of the *R/V Lake Guardian* during sediment sampling, as well as the participation of Jiehong Guo, Solidea Bonina, Andy L. Sandy, Gregory Bourgon, Garry Codling, Kelly Granberg, Rajashankar Kaliappan, Felipe Tendick-Matesanz, Yawei Wang, Valerie Blomgren, Zhuona Li, Prabha Ranasinghe, Anja Vogt, Admasu Wondmagegn, Benjamin Alsip, Lisa Duran, Changmin Long, and Yumin Su.

Appendix A. Supplementary data

Supplementary data to this article can be found online at https://doi.org/10.1016/j.jglr.2018.05.013.

References

Abril, J.-M., Gharbi, F., 2012. Radiometric dating of recent sediments: beyond the boundary conditions. J. Paleolimnol. 48, 449–460.

Appleby, P.G., 2001. Chronostratigraphic techniques in recent sediments. In: Last, W.M., Smol, J.P. (Eds.), Tracking Environmental Change Using Lake Sediments, Volume I: Basin Analysis, Coring, and Chronological Techniques. Kluwer Academic Publishers, Dordrecht, The Netherlands.

Appleby, P.G., Oldfield, 1978. The calculation of lead-210 dates assuming a constant rate of supply of unsupported ^{210}Pb to the sediments. Catena 5, 1–8.

Astle, J.W., Gobas, F.A.P.C., Shiu, W.-Y., MacKay, D., 1987. Lake sediments as historic records of atmospheric contamination by organic chemicals. In: Hites, R.A., Eisenreich, S.J. (Eds.), Sources and Fates of Aquatic Pollutants. American Chemical Society, Washington, DC.

ATSDR (Agency for Toxic Substances and Disease Registry), 2006. PCB contaminated sediment in the Lower Fox River and Green Bay, Northeastern Wisconsin. EPA Facility ID: WI0001954841, March 14, 2006. U.S. Dept. Health Human Services. :p. 25. https://www.atsdr.cdc.gov/hac/pha/foxriver/pcbinfoxriver_greenbaypha031406.pdf.

Baskaran, M., Naidu, A.S., 1995. ^{210}Pb-derived chronology and the fluxes of ^{210}Pb and ^{137}Cs isotopes into continental shelf sediments, East Chukchi Sea, Alaskan Arctic. Geochim. Cosmochim. Acta 59, 4435–4448.

Bell, G., Eadie, B., 1983. Variations in the distribution of suspended particles during an upwelling event in Lake Michigan in 1980. J. Great Lakes Res. 9, 559–567.

Bonina, S.M.C., Codling, G., Corcoran, M.B., Guo, J., Giesy, J.P., Li, A., Sturchio, N.C., Rockne, K.J., 2018. Sedimentation fluxes of nitrogen, organic matter and carbon species in Lake Michigan over the period 1850–2010. J. Great Lakes Res. this issue.

Bruland, K.W., Koide, M., Bowser, C., Maher, L.J., Goldberg, E.D., 1975. Lead-210 and pollen geochronologies on Lake Superior sediments. Quat. Res. 5, 89–98.

Buckley, D.R., Rockne, K.J., Li, A., Mills, W.J., 2004. Soot deposition in the Great Lakes: implications for semi-volatile hydrophobic organic pollutant deposition. Environ. Sci. Technol. 38, 1732–1739.

Cahill, R.A., 1981. Geochemistry of Recent Lake Michigan Sediments. 517. Illinois State Geological Survey Circular, p. 92.

Carroll, J., Williamson, M., Lerche, I., Karabanov, E., Williams, D.F., 1999. Geochronology of Lake Baikal from ^{210}Pb and ^{137}Cs radioisotopes. Appl. Radiat. Isot. 50, 1105–1119.

Chant, L.A., Cornett, R.J., 1991. Smearing of gravity core profiles in soft sediments. Limnol. Oceanogr. 36, 1492–1498.

Chrzastowski, M.J., Thompson, T.A., 1994. Late Wisconsinan and Holocene geologic history of the Illinois-Indiana coast of Lake Michigan. J. Great Lakes Res. 20, 9–26.

Codling, G., Vogt, A., Jones, P.D., Wang, T., Wang, P., Lu, Y.-L., Li, A., Sturchio, N.C., Rockne, K.J., Ji, K., Khim, J.-S., Naile, J., Giesy, J.P., 2014. Historical trends of inorganic and organic fluorine in sediments of Lake Michigan. Chemosphere 114, 203–209.

Codling, G., Hosseini, S., Corcoran, M.B., Bonina, S., Lin, T., Li, A., Sturchio, N.C., Rockne, K.J., Ji, K., Peng, H., Giesy, J.P., 2018a. Current and historical concentrations of poly and perfluorinated compounds in sediments of the northern Great Lakes – Superior, Huron, and Michigan. Environ. Pollut. 236, 373–381.

Codling, G., Sturchio, N.C., Rockne, K.J., Li, A., Ji, K., Peng, H., Tse, T.J., Jones, P.D., Giesy, J.P., 2018b. Spatial and temporal trends in poly- and per-fluorinated compounds in the Laurentian Great Lakes Erie, Ontario and St. Clair. Environ. Pollut. 237, 396–405.

Colman, S.M., Baucom, P.C., Bratton, J.F., Cronin, T.M., Mcgeehin, J.P., Willard, D., Zimmerman, A.R., Vogt, P.R., 2002. Radiocarbon dating, chronologic framework, and changes in accumulation rates of Holocene estuarine sediments from Chesapeake Bay. Quat. Res. 57, 58–70.

Crusius, J., Kenna, T.C., 2007. Ensuring confidence in radionuclide-based sediment chronologies and bioturbation rates. Estuar. Coast. Shelf Sci. 71, 537–544.

Crusius, J., Bothner, M.H., Sommerfield, C.K., 2004. Bioturbation depths, rates and processes in Massachusetts Bay sediments inferred from modeling of ^{210}Pb and $^{239+240}Pu$ profiles. Estuar. Coast. Shelf Sci. 61, 643–655.

Davis, R.P., Hess, C.T., Norton, S.A., Hanson, D.W., Hoaglund, K.D., Anderson, D.S., 1984. ^{137}Cs and ^{210}Pb dating of sediments from soft-water lakes in New England (U.S.A.) and Scandanavia, a failure of ^{137}Cs dating. Chem. Geol. 44, 151–185.

Durfee, R., 1976. Production and usage of PCBs in the United States. Proc. Natl. Conf. on Polychlorinated Biphenyls (Report # EPA-560/6–75-004), Washington, D.C., Office of Toxic Substances, U.S. Environmental Protection Agency, March 1976. pp. 103–107.

Eadie, B., Robbins, J.A., 1987. The role of particulate matter in the movement of contaminants in the Great Lakes. In: Hites, R.A., Eisenreich, S.J. (Eds.), Sources and Fates of Aquatic Pollutants. American Chemical Society, Washington, DC, pp. 319–364.

Eadie, B., Vanderploeg, H.A., Robbins, J.A., Bell, G., 1990. Significance of sediment resuspension and particle settling. In: Tilzer, M.M., Serruya, C. (Eds.), Large Lakes: ecological structure and function. Springer-Verlag, New York, pp. 196–209.

Eadie, B., Robbins, J.A., Klump, J.V., Schwab, D.J., Edgington, D.N., 2008. Winter-spring storms and their influence on sediment resuspension transport and accumulation patterns in southern Lake Michigan. Oceanography 21, 118–135.

Edgington, D.N., Robbins, J.A., 1976. Patterns of deposition of natural and fallout radionuclides in the sediments of Lake Michigan and their relation to limnological processes. In: Nriagu, J.O. (Ed.), Environmental Biogeochemistry. 2. Ann Arbor Science, Ann Arbor, MI, pp. 705–729.

Edgington, D.N., Robbins, J.A., 1990. Time scales of sediment focusing in large lakes as revealed by measurements of fallout ^{137}Cs. In: Tilzer, M.M., Serruya, C. (Eds.), Large Lakes: Ecological Structure and Function. Springer-Verlag, New York, pp. 210–223.

Evans, J.E., Johnson, T.C., Alexander Jr., E.C., Lively, R.S., Eisenreich, S.J., 1981. Sedimentation rates and depositional processes in Lake Superior, (USA, Canada) from lead-210 geochronology. J. Great Lakes Res. 7, 299–310.

Goldberg, E.D., 1963. Geochronology with Pb-210. Proceedings of the Symposium on Radioactive Dating: I.A.E.A., Vienna, pp. 121–131.

Golden, K.A., Wong, C.S., Jeremiason, J.D., Eisenreich, S.J., Sanders, G., Hallgren, J., Swackhamer, D.L., Engstrom, D.R., Long, D.T., 1993. Accumulation and preliminary inventory of organochlorines in Great Lakes sediments. Water Sci. Technol. 29, 19–31.

Guinasso, N.L., Schink, D.R., 1975. Quantitative estimates of biological mixing rates in abyssal sediments. J. Geophys. Res. 80, 3032–3043.

Guo, J., Li, Z., Ranasinghe, P., Bonina, S., Hosseini, S., Corcoran, M.B., Smalley, C., Rockne, K.J., Sturchio, N.C., Giesy, J.P., Li, A., 2017. Spatial and temporal trends of polyhalogenated carbazoles in sediments of upper Great Lakes: insights into their origin. Environ. Sci. Technol. 51, 89–97.

Hermanson, M.H., Christensen, E.R., 1991. Recent sedimentation in Lake Michigan. J. Great Lakes Res. 17, 33–50.

Johnson, T.C., 1984. Sedimentation in large lakes. Annu. Rev. Earth Planet. Sci. 12, 179–204.

Johnson, T.C., Van Alstine, J.D., Rolfhus, K.R., Colman, S.M., Wattrus, N.J., 2012. A high resolution study of spatial and temporal variability of natural and anthropogenic compounds in offshore Lake Superior sediments. J. Great Lakes Res. 38, 673–685.

Johnston, J.W., Argyilan, E.P., Thompson, T.A., Baedke, S.J., Lepper, K., Wilcox, D.A., Forman, S.L., 2012. A sault-outlet-referenced mid-to late-Holocene paleohydrograph for Lake Superior constructed from strandplains of beach ridges. Can. J. Earth Sci. 49, 1263–1279.

Johnston, J.W., Thompson, T.A., Wilcox, D.A., 2014. Paleohydrographic reconstructions from strandplains of beach ridges in the Laurentian Great Lakes. In: Martini, I.P., Wanless, H.R. (Eds.), Sedimentary Coastal Zones from High to Low Latitudes: Similarities and Differences. Geological Society, London, Special Publications. Vol. 388, pp. 213–228.

Karrow, P.F., Calkin, P.E., 1985. The Quaternary Evolution of the Great Lakes. 30. Geological Association of Canada, St John's, Newfoundland (Special Papers).

Kemp, A.L.W., Dell, C.I., Harper, N.S., 1978. Sedimentation rates and sediment budget for Lake Superior. J. Great Lakes Res. 4, 276–287.

Kincare, K., Larson, G.J., 2009. Evolution of the Great Lakes. In: Schaetzel, R., Darden, J., Brandt, D. (Eds.), Michigan Geography and Geology. Pearson, New York, pp. 174–190.

Kirchner, G., 2011. ^{210}Pb as a tool for establishing sediment chronologies: examples of potentials and limitations of conventional dating models. J. Environ. Radioact. 102, 490–494.

Klaminder, J., Appleby, P., Crook, P., Renberg, I., 2012. Post-deposition diffusion of ^{137}Cs in lake sediment: implications for radiocaesium dating. Sedimentology 59, 2259–2267.

Klump, J.V., Paddock, R., Remsen, C.C., Fitzgerald, S., Boraas, M., Anderson, P., 1989. Variations in sediment accumulation rates and the flux of labile organic matter in eastern Lake Superior basins. J. Great Lakes Res. 15, 104–122.

Krishnaswami, S., Lal, D., Martin, J.M., Meybeck, M., 1971. Geochronology of lake sediments. Earth Planet. Sci. Lett. 11, 407–414.

Larson, G., Schaetzl, R., 2001. Origin and evolution of the Great Lakes. J. Great Lakes Res. 27, 518–546.

Li, A., Guo, J., Li, Z., Lin, T., Zhou, S., He, H., Ranansinghe, P., Sturchio, N.C., Rockne, K.J., Giesy, J.P., 2018. Legacy polychlorinated organic pollutants in the sediment of the Great Lakes. J. Great Lakes Res. (this issue).

Loope, W.L., Arbogast, A.F., 2000. Dominance of an ~150-year cycle of sand-supply change in Late Holocene dune-building along the eastern shore of Lake Michigan. Quat. Res. 54, 414–422.

Mackenzie, A.B., Hardie, S.M., Farmer, J.G., Eades, L.J., Pulford, I.D., 2011. Analytical and sampling constraints in Pb-210 dating. Sci. Total Environ. 409, 1298–1304.

Mook, W.G., 2001. Environmental Isotopes in the Hydrological Cycle: Principles and Applications. http://www-naweb.iaea.org/napc/ih/IHS_resources_publication_hydroCycle_en.html IAEA-UNESCO.

NOAA (National Oceanic and Atmospheric Administration), 2018. National Centers for Environmental Information. https://www.ngdc.noaa.gov/mgg/greatlakes/greatlakes.html, Accessed date: 21 May 2018.

O'Beirne, M.D., Werne, J.P., Hecky, R.E., Johnson, T.C., Katsev, S., Reavie, E.D., 2017. Anthropogenic climate change has altered primary productivity in Lake Superior. Nat. Commun. https://doi.org/10.1038/ncomms15713.

Ouyang, D., Bartholic, J., Selegean, J., 2005. Assessing sediment loading from agricultural croplands in the Great Lakes Basin. Journal of American Science 1, 14–21.

Paytan, A., Roberts, K., Watson, S., Peek, S., Chuang, P.C., Defforey, D., Kendall, C., 2017. Intenal loading of phosphate in Lake Erie central basin. J. Great Lakes Res. 36, 50–59.

Peng, Hui, Chen, Chunli, Cantin, Jenna, Saunders, David, Sun, Jianxian, Tang, Song, Codling, Garry, Hecker, Markus, Wiseman, Steve, Jones, Paul, Li, An, Rockne, Karl, Sturchio, Neil, Giesy, John, 2016. Untargeted screening and distribution of organo-bromine compounds in sediments of Lake Michigan. Environ. Sci. Technol. 50, 321–330.

Plattner, S., Mason, D.M., Leshkevich, G.A., Schwab, D.J., Rutherford, E.S., 2006. Classifying and forecasting coastal upwellings in Lake Michigan using satellite derived temperature images and buoy data. J. Great Lakes Res. 32, 63–76.

Robbins, J.A., 1978. Geochemical and geophysical applications of radioactive lead. In: Nriagu, J.O. (Ed.), The Biogeochemistry of Lead in the Environment, Volume 1A. Amsterdam. Elsevier/North Holland Biomedical Press, The Netherlands.

Robbins, J.A., 1982. Stratigraphic and dynamic effects of sediment reworking by Great Lakes zoobenthos. Hydrobiologia 92, 611–622.

Robbins, J.A., 1985. Great Lakes Regional Fallout Source Functions. Great Lakes Environmental Research Laboratory, National Oceanic and Atmospheric Administration, NOAA Technical Memorandum ERL GLERL-56. p. 26.

Robbins, J.A., 1986. A model for particle-selective transport of tracers in sediments with conveyor belt deposit feeders. J. Geophys. Res. 91, 8542–8558.

Robbins, J.A., Edgington, D.N., 1975. Determination of recent sedimentation rates in Lake Michigan using Pb-210 and Cs-137. Geochim. Cosmochim. Acta 39, 285–304.

Robbins, J.A., Herche, L.R., 1993. Models and uncertainty in 21OPb dating of sediments. SIL Proceedings, Verhandlungen Internationalen Vereinigung Theoretische Angewandte Limnol. 25, pp. 217–222.

Robbins, J.A., Krezoski, J.R., Mozley, S.C., 1977. Radioactivity in sediments of the Great Lakes: post-depositional redistribution by deposit-feeding organisms. Earth Planet. Sci. Lett. 36, 325–333.

Robbins, J.A., Edgington, D.N., Kemp, A.L.W., 1978. Comparative ^{210}Pb, ^{137}Cs, and pollen chronologies of sediments from lakes Ontario and Erie. Quat. Res. 10, 256–278.

Robbins, J.A., McCall, P.L., Fisher, J.B., Krezoski, J.R., 1979. Effect of deposit feeders on migration of ^{137}Cs in lake sediments. Earth Planet. Sci. Lett. 42, 277–287.

Rossmann, R., 2010. Protocol to reconstruct historic contaminant loading to large lakes: the Lake Michigan sediment record history. Environ. Sci. Technol. 44, 935–940.

Simcik, M.F., Eisenreich, S.J., Golden, K.A., Liu, S.-P., Lipiatou, E., Swackhamer, D.L., Long, D.T., 1996. Atmospheric loading of polycyclic aromatic hydrocarbons to Lake Michigan as recorded in the sediments. Environ. Sci. Technol. 30, 3039–3046.

Smith, J.N., 2001. Why should we believe ^{210}Pb sediment geochronologies? J. Environ. Radioact. 55, 121–123.

Smith, J.N., Lee, K., Gobeil, C., MacDonald, R.W., 2009. Natural rates of sediment containment of PAH, PCB and metal inventories in Sydney Harbour, Nova Scotia. Sci. Total Environ. 407, 4858–4869.

Sokal, R.R., Rohlf, F.J., 1981. Biometry, the Principles and Practice of Statistics in Biological Research. W. H. Freeman & Company.

Soller, D.R., Garrity, C.P., 2018. Quaternary Sediment Thickness and Bedrock Topography of the Glaciated United States East of the Rocky Mountains: U.S. Geological Survey Scientific Investigations Map 3392, 2 Sheets, Scale 1:5,000,000. https://doi.org/10.3133/sim3392.

Thayer, S.A., Haas, R.C., Hunter, R.D., Kushler, R.H., 1997. Zebra mussel (*Dreissena polymorpha*) effects on sediment, other zoobenthos, and the diet and growth of adult yellow perch (*Perca flavescens*) in pond enclosures. Can. J. Fish. Aquat. Sci. 54, 1903–1915.

Thomson, J., Turekian, K.K., Mccaffrey, J., 1975. The accumulation of metals in and release from sediments of Long Island Sound. Estuarine Research, L. E. Cronin. Academic Press, New York, pp. 28–43.

Tylmann, W., Bonk, A., Goslar, T., Wulf, S., Grosjean, M., 2016. Calibrating ^{210}Pb dating results with varve chronology and independent chronostratigraphic markers: problems and implications. Quat. Geochronol. 32, 1–10.

Urban, N.R., Eisenreich, S.J., Grigal, D.F., Schurr, K.T., 1990. Mobility and diagenesis of Pb and ^{210}Pb in peat. Geochim. Cosmochim. Acta 54, 3329–3346.

Vanderploeg, H.A., Nalepa, T.F., Jude, D.J., Mills, E.L., Holeck, K.T., Liebig, J.R., Grigorovich, I.A., Ojaveer, H., 2002. Dispersal and emerging ecological impacts of Ponto-Caspian species in the Laurentian Great Lakes. Can. J. Fish. Aquat. Sci. 59, 1209–1228.

Waples, J.T., Paddock, R., Jannsen, J., Lovalvo, D., Schulze, B., Kaster, J., Klump, J.V., 2005. High resolution bathymetry and lakebed characterization in the nearshore of Western Lake Michigan. J. Great Lakes Res. 31, 64–74.

White, D.S., Miller, M.F., 2008. Benthic invertebrate activity in lakes: linking present and historical bioturbation patterns. Aquat. Biol. 2, 269–277.

SUPPLEMENTARY INFORMATION

Accumulation rates, focusing factors, and chronologies from depth profiles of ^{210}Pb and ^{137}Cs in sediments of the Laurentian Great Lakes

Margaret Corcoran[a I], Mahmoud Sherif[b], Colin Smalley[a II], An Li[c], Karl J. Rockne[d], John P. Giesy[e], Neil C. Sturchio[b *]

[a] Department of Earth and Environmental Sciences, University of Illinois, Chicago, IL, USA
[b] Department of Geological Sciences, University of Delaware, Newark, DE, USA
[c] School of Public Health, University of Illinois at Chicago, Chicago, IL, USA
[d] Department of Civil and Materials Engineering, University of Illinois at Chicago, Chicago, IL, USA
[e] Department of Veterinary Biomedical Sciences and Toxicology Centre, University of Saskatchewan, Saskatoon, Saskatchewan, Canada

[I] Present address: CSRA, Inc., Chicago, Illinois, USA
[II] Present address: U.S. Army Corps of Engineers, Kansas City, Missouri, USA

* Corresponding author:
Neil C. Sturchio
Department of Geological Sciences
University of Delaware
255 Academy Street/103 Penny Hall
Newark, DE 19716
Phone: 302-831-8706
Email: sturchio@udel.edu

Table S1. Core section depths (cm) ; section thicknesses (cm); dry mass depth (g/cm^2); supported and unsupported-^{210}Pb activities and 1-sigma counting errors (Bq/kg) ; ^{226}Ra activities and 1-sigma counting errors (Bq/kg); ^{137}Cs activities and 1-sigma counting errors (Bq/kg) ; selected ^{210}Pb model and calendar dates with 95%confidence limits.

Table S2. Comparison of data for composite cores from sites ER15 and ON30 with individual subcores from a separate cast at each location.

Figures S1-S2. Comparison of data for composite cores from sites ER15 and ON30 with individual cores from a separate cast.

Figures S3-S7. CRS and CIC plots for cores from all samples Great Lakes sites, 2010-2014. Error bars are 95% confidence intervals as defined in text.

Figures S8-S12. Calendar date profiles for cores from all samples Great Lakes sites, 2010-2014. Error bars are 95% confidence intervals as defined in text.

Table S1.

Sample ID	Depth (cm)	Thick (cm)	Ave Depth (cm)	Dry Mass Depth (g/cm^2)	Total Pb-210 (Bq/Kg)	Total Pb-210 error (Bq/Kg)	Unsup-ported Pb-210 (Bq/Kg)	Unsup-ported Pb-210 error (Bq/Kg)	Ra-226 (Bq/Kg)	Ra-226 error (Bq/Kg)	Cs-137 (Bq/Kg)	Cs-137 error (Bq/Kg)	Selected model (top line) and average date of section (date)	Error in years (95% confidence) (± years)
S001MC													**Not Datable**	
S001MC-01	0-0.5	0.5	0.25	0.27	177	5	146	14	9	2	22	1		
S001MC-02	0.5-1	0.5	0.75	0.65	57	6	26	14	9	3	19	1		
S001MC-03	1-1.5	0.5	1.25	1.07	15	5			12	4	2	0		
S001MC-04	1.5-2	0.5	1.75	1.44	10	3			19	2				
S001MC-05	2-2.5	0.5	2.25	1.86	22	6			17	4				
S001MC-06	2.5-3	0.5	2.75	2.31	23	7			21	4				
S001MC-07	3-3.5	0.5	3.25	2.79	20	6			14	4				
S001MC-08	3.5-4	0.5	3.75	3.23	12	5			19	4				
S001MC-09	4-4.5	0.5	4.25	3.66	25	3			23	3				
S001MC-10	4.5-5	0.5	4.75	4.25	20	3			18	3				
S001MC-11	5-6	1	5.5	5.18	21	5			23	4				
S001MC-12	6-7	1	6.5	6.37	25	3			26	3				
S001MC-13	7-8	1	7.5	7.44	24	5			20	4				
S001MC-14	8-9	1	8.5	8.53	34	6			30	5				
S001MC-15	9-10	1	9.5	9.56	38	4			29	3				
S001MC-16	10-11	1	10.5	10.58	39	6			27	4				
S001MC-17	11-12	1	11.5	11.71	39	3			33	2				
S001MC-18	12-13	1	12.5	12.85	46	6			33	3				
S001MC-19	13-14	1	13.5	13.92	43	4			32	3				
S001MC-20	14-15	1	14.5	15.06	47	5			35	4				
S001MC-21	15-17	2	16	17.44	38	5			38	4				
S001MC-22	17-19	2	18	19.66	39	6			34	5				
S001MC-23	19-21	2	20	22.07	46	5			40	4				
S001MC-24	21-23	2	22	24.50	58	8			48	5				
S002MC													**CRS**	
S002MC-01	0-0.5	0.5	0.25	0.05	2197	25	2150	26	37	8	261	3	2007	6
S002MC-02	0.5-1	0.5	0.75	0.17	1529	18	1482	19	48	7	231	3	1995	14
S002MC-03	1-1.5	0.5	1.25	0.34	752	13	706	15	38	5	181	2	1974	22
S002MC-04	1.5-2	0.5	1.75	0.56	255	7	208	10	33	3	86	1	1946	33
S002MC-05	2-2.5	0.5	2.25	0.84	100	8	54	11	25	4	26	1	1910	46
S002MC-06	2.5-3	0.5	2.75	1.15	47	4	0	9	24	3	10	0	1866	58
S002MC-07	3-3.5	0.5	3.25	1.43	45	6			40	5	3	0	1823	63
S002MC-08	3.5-4	0.5	3.75	1.68	52	7			36	4	3	1	1785	69
S002MC-09	4-4.5	0.5	4.25	1.93	46	4			33	3	2	0	1748	77
S002MC-10	4.5-5	0.5	4.75	2.22	32	5			34	4	1	0	1708	88
S002MC-11	5-6	1	5.5	3.02	30	6			35	4			1629	149
S002MC-12	6-7	1	6.5	3.61	39	8			46	5			1527	152
S002MC-13	7-8	1	7.5	4.16	54	4			50	3			1444	165
S002MC-14	8-9	1	8.5	4.70	50	5			42	3			1365	181
S002MC-15	9-10	1	9.5	5.24	53	3			42	3			1285	198
S002MC-16	10-11	1	10.5	5.82	45	8			50	6			1203	217
S002MC-17	11-12	1	11.5	6.38	51	8			39	5			1120	234
S002MC-18	12-13	1	12.5	6.97	42	6			50	6			1036	253
S002MC-19	13-14	1	13.5	7.56	42	7			47	5			950	271
S002MC-20	14-15	1	14.5	8.16	50	5			36	4			863	289
S002MC-21	15-17	2	16	9.32	58	7			45	5			735	366
S002MC-22	17-19	2	18	10.53	56	6			46	4			562	406
S002MC-23	19-21	2	20	11.72	54	5			44	4			387	440
S002MC-24	21-23	2	22	12.92	42	5			52	4			212	477
S002MC-25	23-25	2	24	14.12	49	6			45	4			37	513
S008MC													**CRS**	
S008MC-01	0-0.5	0.5	0.25	0.07	1792	24	1742	25	50	8	342	4	2006	6
S008MC-02	0.5-1	0.5	0.75	0.15	1391	15	1340	16	46	6	299	3	1995	8
S008MC-03	1-1.5	0.5	1.25	0.25	819	9	768	11	51	5	226	2	1981	10
S008MC-04	1.5-2	0.5	1.75	0.37	483	14	432	15	44	8	184	3	1965	13
S008MC-05	2-2.5	0.5	2.25	0.49	337	8	286	10	57	5	137	2	1948	15
S008MC-06	2.5-3	0.5	2.75	0.63	204	6	153	9	57	5	54	1	1928	17
S008MC-07	3-3.5	0.5	3.25	0.79	126	9	75	11	52	6	13	1	1906	21
S008MC-08	3.5-4	0.5	3.75	0.95	92	8	41	11	47	7	4	1	1882	23
S008MC-09	4-4.5	0.5	4.25	1.15	48	8			44	7			1856	27
S008MC-10	4.5-5	0.5	4.75	1.35	65	9			53	7			1826	30
S008MC-11	5-6	1	5.5	1.79	46	6			60	5			1779	52
S008MC-12	6-7	1	6.5	2.28	52	4			38	4			1710	62
S008MC-13	7-8	1	7.5	2.76	53	8			43	7			1638	67
S008MC-14	8-9	1	8.5	3.25	56	8			53	7			1565	73
S008MC-15	9-10	1	9.5	3.78	56	6			40	4			1490	81
S008MC-16	10-11	1	10.5	4.30	53	8			46	5			1412	87
S008MC-17	11-12	1	11.5	4.83	44	8			42	7			1334	93
S008MC-18	12-13	1	12.5	5.37	60	8			39	6			1254	100
S008MC-19	13-14	1	13.5	5.93	48	7			39	6			1173	107
S008MC-20	14-15	1	14.5	6.49	40	7			47	7			1091	114
S008MC-21	15-17	2	16	7.62	44	8			37	6			965	169
S008MC-22	17-19	2	18	8.83	53	8			30	6			792	188
S008MC-23	19-21	2	20	10.09	52	7			40	5			608	206
S008MC-24	21-23	2	22	11.48	44	7			33	6			411	231
S008MC-25	23-25	2	24	12.77	47	5			44	4			213	237

Table S1. (continued)

Sample ID	Depth	Thick	Ave Depth	Dry Mass Depth	Total Pb-210	Total Pb-210 error	Unsup-ported Pb-210	Unsup-ported Pb-210 error	Ra-226	Ra-226 error	Cs-137	Cs-137 error	Selected model (top line) and average date of section	Error in years (95% confidence)
	(cm)	(cm)	(cm)	(g/cm^2)	(Bq/Kg)	(Bq/Kg)	(Bq/Kg)	(Bq/Kg)	(Bq/Kg)	(Bq/Kg)	(Bq/Kg)	(Bq/Kg)	(date)	(± years)
S011MC													**CRS**	
S011MC-01	0-0.5	0.5	0.25	0.13	1975	25	1931	26	58	10	232	3	2007	5
S011MC-02	0.5-1	0.5	0.75	0.26	1851	25	1807	26	56	8	250	3	1999	5
S011MC-03	1-1.5	0.5	1.25	0.41	1517	14	1473	14	50	5	292	2	1989	7
S011MC-04	1.5-2	0.5	1.75	0.59	1253	18	1209	19	36	6	333	3	1979	8
S011MC-05	2-2.5	0.5	2.25	0.77	978	16	934	17	61	7	387	3	1967	9
S011MC-06	2.5-3	0.5	2.75	0.97	715	14	671	15	45	6	287	3	1954	10
S011MC-07	3-3.5	0.5	3.25	1.17	367	6	323	8	46	4	120	1	1941	11
S011MC-08	3.5-4	0.5	3.75	1.36	228	10	184	11	41	6	77	2	1928	12
S011MC-09	4-4.5	0.5	4.25	1.56	186	6	142	8	49	4	64	1	1916	12
S011MC-10	4.5-5	0.5	4.75	1.75	141	8	97	9	36	5	49	1	1903	13
S011MC-11	5-6	1	5.5	2.16	86	9	42	10	37	6	13	1	1883	21
S011MC-12	6-7	1	6.5	2.57	71	7	27	8	31	5	1	0	1856	23
S011MC-13	7-8	1	7.5	3.00	52	6			41	6			1829	25
S011MC-14	8-9	1	8.5	3.39	52	7			36	5			1802	26
S011MC-15	9-10	1	9.5	3.77	42	6			47	6			1777	27
S011MC-16	10-11	1	10.5	4.15	37	7			44	6			1751	28
S011MC-17	11-12	1	11.5	4.55	44	3			35	3			1726	30
S011MC-18	12-13	1	12.5	4.96	43	6			37	5			1699	32
S011MC-19	13-14	1	13.5	5.35	45	4			35	3			1673	33
S011MC-20	14-15	1	14.5	5.73	47	5			40	4			1647	34
S011MC-21	15-17	2	16	6.49	39	6			34	5			1610	49
S011MC-22	17-19	2	18	7.28	52	7			44	5			1560	53
S011MC-23	19-21	2	20	8.07	43	5			35	4			1507	57
S011MC-24	21-23	2	22	8.88	41	6			48	5			1455	60
S011MC-25	23-25	2	24	9.73	37	6			28	4			1400	64
S012MC													**CRS**	
S012MC-01	0-0.5	0.5	0.25	0.11	1974	15	1918	17	55	6	266	2	2006	7
S012MC-02	0.5-1	0.5	0.75	0.23	1664	16	1607	18	46	6	289	3	1994	9
S012MC-03	1-1.5	0.5	1.25	0.37	1472	22	1415	23	58	10	346	4	1981	11
S012MC-04	1.5-2	0.5	1.75	0.52	1109	17	1053	18	49	8	393	4	1966	13
S012MC-05	2-2.5	0.5	2.25	0.65	884	11	827	13	49	5	346	2	1952	14
S012MC-06	2.5-3	0.5	2.75	0.78	623	15	566	16	53	9	269	3	1938	15
S012MC-07	3-3.5	0.5	3.25	0.92	417	13	360	16	54	9	137	2	1924	17
S012MC-08	3.5-4	0.5	3.75	1.06	274	12	218	14	46	9	34	2	1910	18
S012MC-09	4-4.5	0.5	4.25	1.20	148	11	92	13	54	8	8	1	1896	20
S012MC-10	4.5-5	0.5	4.75	1.35	113	6	56	10	43	4	2	0	1881	22
S012MC-11	5-6	1	5.5	1.68	92	8	36	11	61	7			1856	34
S012MC-12	6-7	1	6.5	1.99	64	10			52	7			1824	37
S012MC-13	7-8	1	7.5	2.33	72	9			52	7			1790	42
S012MC-14	8-9	1	8.5	2.69	58	5			50	4			1755	47
S012MC-15	9-10	1	9.5	3.05	65	6			48	4			1718	51
S012MC-16	10-11	1	10.5	3.40	51	8			51	7			1681	54
S012MC-17	11-12	1	11.5	3.77	51	8			44	8			1644	59
S012MC-18	12-13	1	12.5	4.15	49	5			44	4			1606	64
S012MC-19	13-14	1	13.5	4.56	55	8			53	7			1565	70
S012MC-20	14-15	1	14.5	4.99	69	11			48	8			1522	75
S012MC-21	15-17	2	16	5.89	60	8			51	6			1454	109
S012MC-22	17-19	2	18	6.83	50	9			37	7			1360	121
S012MC-23	19-21	2	20	7.77	52	6			48	4			1264	131
S012MC-24	21-23	2	22	8.64	50	8			51	6			1171	137
S012MC-25	23-25	2	24	9.46	54	9			45	7			1084	142
S012MC-26	40-42	2	41	9.46	47	8			44	6			n/a	n/a
S016MC													**CRS**	
S016MC-01	0-0.5	0.5	0.25	0.07	1685	14	1636	15	38	5	272	2	2007	7
S016MC-02	0.5-1	0.5	0.75	0.16	1349	17	1301	18	54	6	259	3	1996	10
S016MC-03	1-1.5	0.5	1.25	0.26	1084	19	1035	20	40	8	238	3	1983	14
S016MC-04	1.5-2	0.5	1.75	0.37	903	17	854	17	45	6	250	3	1968	17
S016MC-05	2-2.5	0.5	2.25	0.52	606	13	557	14	38	6	211	2	1951	23
S016MC-06	2.5-3	0.5	2.75	0.71	252	7	204	8	44	3	102	1	1928	30
S016MC-07	3-3.5	0.5	3.25	0.95	143	9	94	10	41	7	53	1	1899	41
S016MC-08	3.5-4	0.5	3.75	1.19	68	8	19	9	45	5	18	1	1867	47
S016MC-09	4-4.5	0.5	4.25	1.46	49	8			33	7	2	1	1832	55
S016MC-10	4.5-5	0.5	4.75	1.74	45	4			40	4			1795	64
S016MC-11	5-6	1	5.5	2.30	51	8			40	6			1738	97
S016MC-12	6-7	1	6.5	2.84	41	7			45	7			1664	109
S016MC-13	7-8	1	7.5	3.37	52	8			44	6			1591	123
S016MC-14	8-9	1	8.5	3.93	54	10			47	8			1517	139
S016MC-15	9-10	1	9.5	4.49	53	5			47	4			1441	153
S016MC-16	10-11	1	10.5	5.05	50	8			39	6			1366	167
S016MC-17	11-12	1	11.5	5.59	40	8			41	6			1292	179
S016MC-18	12-13	1	12.5	6.19	45	7			42	6			1215	199
S016MC-19	13-14	1	13.5	6.75	48	8			56	7			1136	211
S016MC-20	14-15	1	14.5	7.32	53	9			43	6			1059	226
S016MC-21	15-17	2	16	8.46	45	6			49	5			943	293
S016MC-22	17-19	2	18	9.62	56	8			46	7			788	325
S016MC-23	19-21	2	20	10.73	51	8			49	6			635	350
S016MC-24	21-23	2	22	11.83	46	7			41	5			485	378
S016MC-25	23-25	2	24	12.98	45	7			43	6			333	411

Table S1. (continued)

Sample ID	Depth (cm)	Thick (cm)	Ave Depth (cm)	Dry Mass Depth (g/cm^2)	Total Pb-210 (Bq/Kg)	Total Pb-210 error (Bq/Kg)	Unsup-ported Pb-210 (Bq/Kg)	Unsup-ported Pb-210 error (Bq/Kg)	Ra-226 (Bq/Kg)	Ra-226 error (Bq/Kg)	Cs-137 (Bq/Kg)	Cs-137 error (Bq/Kg)	Selected model (top line) and average date of section (date)	Error in years (95% confidence) (± years)
S019MC													**CRS**	
S019MC-01	0-0.5	0.5	0.25	0.08	1258	12	1206	16	30	5	181	2	2007	5
S019MC-02	0.5-1	0.5	0.75	0.17	919	18	867	20	35	8	194	3	1997	7
S019MC-03	1-1.5	0.5	1.25	0.26	518	15	466	18	32	8	196	3	1987	8
S019MC-04	1.5-2	0.5	1.75	0.38	421	10	369	13	36	6	167	2	1975	10
S019MC-05	2-2.5	0.5	2.25	0.49	354	8	302	12	42	5	91	1	1962	11
S019MC-06	2.5-3	0.5	2.75	0.62	243	8	191	12	46	5	17	1	1948	13
S019MC-07	3-3.5	0.5	3.25	0.79	177	12	125	15	47	6	3	1	1931	17
S019MC-08	3.5-4	0.5	3.75	0.97	103	11	51	15	54	8			1911	19
S019MC-09	4-4.5	0.5	4.25	1.18	84	7	32	11	51	4			1889	23
S019MC-10	4.5-5	0.5	4.75	1.40	60	8			49	7			1864	25
S019MC-11	5-6	1	5.5	1.92	68	10			34	5			1822	47
S019MC-12	6-7	1	6.5	2.43	58	9			57	8			1763	51
S019MC-13	7-8	1	7.5	3.01	53	8			49	7			1701	60
S019MC-14	8-9	1	8.5	3.56	55	5			53	4			1637	64
S019MC-15	9-10	1	9.5	4.12	51	6			46	5			1574	69
S019MC-16	10-11	1	10.5	4.70	38	8			58	6			1509	76
S019MC-17	11-12	1	11.5	5.32	55	5			49	4			1440	84
S019MC-18	12-13	1	12.5	5.98	47	8			40	6			1367	92
S019MC-19	13-14	1	13.5	6.64	36	8			44	8			1292	98
S019MC-20	14-15	1	14.5	7.25	43	6			39	4			1220	101
S019MC-21	15-17	2	16	8.54	52	7			47	5			1112	151
S019MC-22	17-19	2	18	9.75	51	4			47	3			969	158
S019MC-23	19-21	2	20	10.90	65	7			65	6			835	165
S019MC-24	21-23	2	22	12.12	59	5			43	3			700	180
S019MC-25	23-25	2	24	13.32	40	5			59	5			562	189
S022MC													**CRS 2-slope**	
S022MC-01	0-0.5	0.5	0.25	0.08	631	13	573	15	51	6	98	2	2009	3
S022MC-02	0.5-1	0.5	0.75	0.16	668	13	610	15	58	6	105	2	2005	4
S022MC-03	1-1.5	0.5	1.25	0.25	582	8	524	11	56	4	117	1	2000	5
S022MC-04	1.5-2	0.5	1.75	0.35	434	11	376	13	40	5	141	2	1994	5
S022MC-05	2-2.5	0.5	2.25	0.46	295	8	237	11	47	5	176	2	1988	7
S022MC-06	2.5-3	0.5	2.75	0.58	213	7	155	10	57	4	178	2	1982	8
S022MC-07	3-3.5	0.5	3.25	0.70	170	9	112	12	44	6	140	2	1975	9
S022MC-08	3.5-4	0.5	3.75	0.84	177	10	119	13	46	6	80	2	1968	9
S022MC-09	4-4.5	0.5	4.25	0.98	148	9	90	11	48	6	43	1	1963	10
S022MC-10	4.5-5	0.5	4.75	1.13	134	9	75	12	63	7	12	1	1957	12
S022MC-11	5-6	1	5.5	1.43	129	8	71	11	55	6	2	1	1948	17
S022MC-12	6-7	1	6.5	1.75	95	5	37	9	51	4			1936	20
S022MC-13	7-8	1	7.5	2.08	86	7	28	10	50	6			1922	23
S022MC-14	8-9	1	8.5	2.43	87	7	29	10	54	5			1909	26
S022MC-15	9-10	1	9.5	2.80	76	9	18	11	51	6			1894	29
S022MC-16	10-11	1	10.5	3.17	71	7	13	10	51	6			1880	32
S022MC-17	11-12	1	11.5	3.56	60	7			48	6			1864	35
S022MC-18	12-13	1	12.5	3.95	52	6			51	5			1849	39
S022MC-19	13-14	1	13.5	4.34	57	7			50	6			1833	42
S022MC-20	14-15	1	14.5	4.73	62	7			54	6			1817	45
S022MC-21	15-17	2	16	5.49	51	5			49	3			1794	58
S022MC-22	17-19	2	18	6.24	63	8			40	5			1764	64
S022MC-23	19-21	2	20	7.02	73	10			54	6			1733	71
S022MC-24	21-23	2	22	7.83	55	5			52	4			1701	78
S022MC-25	23-25	2	24	8.65	49	4			50	3			1669	84
S114MC													**Not Datable**	
S114MC-01	0-0.5	0.5	0.25	0.22	808	11	766	15	18	4	86	1		
S114MC-02	0.5-1	0.5	0.75	0.54	477	11	435	15	22	5	72	2		
S114MC-03	1-1.5	0.5	1.25	0.83	206	6	164	12	23	4	40	1		
S114MC-04	1.5-2	0.5	1.75	1.09	66	7	24	13	20	5	15	1		
S114MC-05	2-2.5	0.5	2.25	1.42	33	8			36	5	2	1		
S114MC-06	2.5-3	0.5	2.75	1.79	38	8			36	6				
S114MC-07	3-3.5	0.5	3.25	2.16	41	7			30	5				
S114MC-08	3.5-4	0.5	3.75	2.53	33	6			38	6				
S114MC-09	4-4.5	0.5	4.25	2.86	42	6			39	4				
S114MC-10	4.5-5	0.5	4.75	3.18	44	7			40	5				
S114MC-11	5-6	1	5.5	3.84	38	5			36	4				
S114MC-12	6-7	1	6.5	4.63	33	7			30	5				
S114MC-13	7-8	1	7.5	5.45	25	7			29	5				
S114MC-14	8-9	1	8.5	6.26	37	4			28	4				
S114MC-15	9-10	1	9.5	7.01	39	7			31	5				
S114MC-16	10-11	1	10.5	7.77	34	7			24	4				
S114MC-17	11-12	1	11.5	8.56	42	8			33	7				
S114MC-18	12-13	1	12.5	9.42	29	4			30	4				
S114MC-19	13-14	1	13.5	10.20	34	4			35	3				
S114MC-20	14-15	1	14.5	10.88	41	4			34	3				
S114MC-21	15-17	2	16	12.11	52	7			38	5				
S114MC-22	17-19	2	18	13.42	59	8			55	6				
S114MC-23	19-21	2	20	14.71	60	8			39	5				
S114MC-24	21-23	2	22	16.16	61	6			43	4				
S114MC-25	23-25	2	24	17.73	53	6			43	4				
S114MC-26	40-42	2	41	18.85	56	8			52	7				

Table S1. (continued)

Sample ID	Depth (cm)	Thick (cm)	Ave Depth (cm)	Dry Mass Depth (g/cm^2)	Total Pb-210 (Bq/Kg)	Total Pb-210 error (Bq/Kg)	Unsup-ported Pb-210 (Bq/Kg)	Unsup-ported Pb-210 error (Bq/Kg)	Ra-226 (Bq/Kg)	Ra-226 error (Bq/Kg)	Cs-137 (Bq/Kg)	Cs-137 error (Bq/Kg)	Selected model (top line) and average date of section (date)	Error in years (95% confidence) (± years)
M008EC													**CRS**	
M008EC-01	0-1	1	0.5	0.11	1371	27	1321	29	76	19	127	2	2008	4
M008EC-02	1-2	1	1.5	0.26	1229	45	1178	47	67	30	130	4	2002	6
M008EC-03	2-3	1	2.5	0.43	1225	40	1174	42	63	24	136	4	1994	8
M008EC-04	3-4	1	3.5	0.62	1098	40	1047	41	88	29	142	4	1986	10
M008EC-05	4-5	1	4.5	0.83	1020	85	969	85	82	19	131	4	1976	12
M008EC-06	5-6	1	5.5	1.11	734	34	683	35	52	13	129	2	1965	16
M008EC-07	6-7	1	6.5	1.49	569	33	519	35	55	19	106	3	1949	22
M008EC-08	7-8	1	7.5	1.97	246	23	196	25	36	16	69	3	1928	28
M008EC-09	8-9	1	8.5	2.45	169	27	118	29	62	17	31	2	1905	32
M008EC-10	9-10	1	9.5	2.93	92	20	42	23	69	19	12	2	1882	36
M008EC-11	10-12	2	11	3.94	63	15			51	9	4	1	1847	57
M008EC-12	12-14	2	13	5.14	31	14			54	17			1794	72
M008EC-13	14-16	2	15	6.25	55	17			41	15			1739	79
M008EC-14	16-18	2	17	7.39					76	21			1685	90
M008EC-15	18-20	2	19	8.53	57	13			38	10			1631	100
M008EC-16	20-22	2	21	9.68	43	11			46	10			1576	109
M008EC-17	22-24	2	23	10.84					52	15			1521	120
M008EC-18	24-26	2	25	11.99	52	19			38	13			1466	129
M008EC-19	26-28	2	27	13.11	44	18			50	15			1412	138
M008EC-20	28-30	2	29	14.17	59	22			49	14			1360	145
M009BC													**CRS**	
M009BC-01	0-1	1	0.5	0.21	711	15	629	17	41	8	60	2	2009	2
M009BC-02	1-2	1	1.5	0.47	647	9	565	12	41	4	63	1	2006	3
M009BC-03	2-3	1	2.5	0.75	558	14	476	16	36	7	77	2	2001	3
M009BC-04	3-4	1	3.5	1.07	424	13	342	15	44	7	102	2	1997	4
M009BC-05	4-5	1	4.5	1.45	379	11	297	13	38	6	120	2	1991	5
M009BC-06	5-6	1	5.5	1.83	337	11	255	13	31	6	133	2	1986	5
M009BC-07	6-7	1	6.5	2.21	285	14	203	16	37	6	143	2	1980	6
M009BC-08	7-8	1	7.5	2.58	298	7	216	10	36	4	155	1	1974	6
M009BC-09	8-9	1	8.5	2.95	247	7	165	10	32	4	188	2	1968	7
M009BC-10	9-10	1	9.5	3.34	204	12	122	14	39	8	211	3	1963	7
M009BC-11	10-12	2	11	4.16	172	10	90	12	38	5	182	2	1953	11
M009BC-12	12-14	2	13	4.96	171	7	89	10	38	5	68	1	1941	12
M009BC-13	14-16	2	15	5.79	139	11	56	13	43	7	16	1	1928	13
M009BC-14	16-18	2	17	6.71	116	9	34	12	58	8	2	1	1915	15
M009BC-15	18-20	2	19	7.61	108	10	26	13	36	7			1901	16
M009BC-16	20-22	2	21	8.47	103	9	21	12	45	6			1888	17
M009BC-17	22-24	2	23	9.36	89	10			45	9			1874	18
M009BC-18	24-26	2	25	10.31	81	12			35	9			1860	20
M009BC-19	26-28	2	27	11.29	72	8			35	4			1845	21
M009BC-20	28-30	2	29	12.30	86	15			30	11			1830	23
M011BC													**CIC**	
M011BC-01	0-1	1	0.5	0.14	928	19	855	20	68	11	183	3	2009	2
M011BC-02	1-2	1	1.5	0.32	875	17	801	17	59	7	176	3	2005	3
M011BC-03	2-3	1	2.5	0.53	859	17	786	17	53	8	173	3	2000	4
M011BC-04	3-4	1	3.5	0.74	789	11	716	12	57	6	177	2	1995	5
M011BC-05	4-5	1	4.5	0.96	735	15	662	15	54	7	172	3	1990	6
M011BC-06	5-6	1	5.5	1.20	684	16	611	17	39	6	174	3	1984	7
M011BC-07	6-7	1	6.5	1.45	579	16	505	17	54	9	188	3	1978	8
M011BC-08	7-8	1	7.5	1.70	522	16	449	17	43	7	207	3	1972	9
M011BC-09	8-9	1	8.5	1.96	435	16	361	16	46	9	225	3	1966	10
M011BC-10	9-10	1	9.5	2.22	361	9	288	9	46	5	221	2	1960	11
M011BC-11	10-12	2	11	2.78	300	16	227	17	55	10	180	3	1950	17
M011BC-12	12-14	2	13	3.33	237	7	163	8	56	6	105	1	1936	19
M011BC-13	14-16	2	15	3.88	172	11	99	11	55	8	31	1	1923	21
M011BC-14	16-18	2	17	4.42	111	8	38	9	52	7	3	1	1910	23
M011BC-15	18-20	2	19	4.97	96	10	22	11	52	7			1896	25
M011BC-16	20-22	2	21	5.53	79	10			57	7			1883	27
M011BC-17	22-24	2	23	6.09	75	8			44	6			1869	29
M011BC-18	24-26	2	25	6.68	71	9			49	6			1855	32
M011BC-19	26-28	2	27	7.26	70	4			54	4			1841	34
M011BC-20	28-30	2	29	7.84	70	7			53	5			1827	36
M018BC													**CRS**	
M018BC-01	0-1	1	0.5	0.13	1061	20	984	21	73	10	174	3	2007	4
M018BC-02	1-2	1	1.5	0.28	950	15	873	17	45	6	188	2	2000	6
M018BC-03	2-3	1	2.5	0.48	864	16	787	17	58	8	198	3	1990	9
M018BC-04	3-4	1	3.5	0.72	702	15	625	16	69	8	203	3	1978	11
M018BC-05	4-5	1	4.5	0.97	527	13	450	15	43	7	236	3	1965	13
M018BC-06	5-6	1	5.5	1.25	333	12	256	14	57	8	207	3	1950	16
M018BC-07	6-7	1	6.5	1.52	260	7	183	9	44	4	99	1	1935	18
M018BC-08	7-8	1	7.5	1.82	207	10	131	12	56	7	19	1	1919	20
M018BC-09	8-9	1	8.5	2.11	134	10	57	12	49	6	3	1	1903	22
M018BC-10	9-10	1	9.5	2.38	89	7	12	10	53	6			1888	23
M018BC-11	10-12	2	11	2.96	98	9	21	12	58	6			1865	35
M018BC-12	12-14	2	13	3.53	71	4			61	4			1834	39
M018BC-13	14-16	2	15	4.09	72	5			53	4			1803	42
M018BC-14	16-18	2	17	4.63	77	10			64	7			1773	45
M018BC-15	18-20	2	19	5.20	71	8			55	6			1743	49
M018BC-16	20-22	2	21	5.75	73	5			56	4			1712	52
M018BC-17	22-24	2	23	6.28	87	8			62	6			1682	56
M018BC-18	24-26	2	25	6.82	73	4			57	4			1653	59
M018BC-19	26-28	2	27	7.40	79	9			55	5			1622	64
M018BC-20	28-30	2	29	7.97	88	9			58	6			1591	67

Table S1. (continued)

Sample ID	Depth (cm)	Thick (cm)	Ave Depth (cm)	Dry Mass Depth (g/cm^2)	Total Pb-210 (Bq/Kg)	Total Pb-210 error (Bq/Kg)	Unsup-ported Pb-210 (Bq/Kg)	Unsup-ported Pb-210 error (Bq/Kg)	Ra-226 (Bq/Kg)	Ra-226 error (Bq/Kg)	Cs-137 (Bq/Kg)	Cs-137 error (Bq/Kg)	Selected model (top line) and average date of section (date)	Error in years (95% confidence) (± years)
M024BC													**CRS**	
M024BC-01	0-1	1	0.5	0.13	1034	16	962	17	50	7	207	3	2007	7
M024BC-02	1-2	1	1.5	0.28	1029	10	958	12	53	4	214	2	2000	7
M024BC-03	2-3	1	2.5	0.45	969	9	897	12	51	4	218	2	1992	7
M024BC-04	3-4	1	3.5	0.64	873	8	802	10	42	3	223	1	1983	7
M024BC-05	4-5	1	4.5	0.84	783	15	711	16	43	6	250	3	1972	8
M024BC-06	5-6	1	5.5	1.03	664	14	592	15	41	6	283	3	1962	9
M024BC-07	6-7	1	6.5	1.25	551	14	480	15	52	7	271	3	1951	10
M024BC-08	7-8	1	7.5	1.48	421	13	350	14	39	7	177	3	1940	11
M024BC-09	8-9	1	8.5	1.72	272	13	200	15	48	7	80	2	1927	13
M024BC-10	9-10	1	9.5	1.98	173	10	102	12	48	6	30	1	1914	14
M024BC-11	10-12	2	11	2.50	130	6	58	9	53	4	13	1	1894	23
M024BC-12	12-14	2	13	3.03	95	9	23	12	51	6			1867	25
M024BC-13	14-16	2	15	3.56	82	5	10	8	57	4			1839	27
M024BC-14	16-18	2	17	4.10	71	8			45	7			1811	29
M024BC-15	18-20	2	19	4.63	82	9			52	6			1783	31
M024BC-16	20-22	2	21	5.18	63	8			48	5			1755	33
M024BC-17	22-24	2	23	5.75	79	9			58	6			1726	36
M024BC-18	24-26	2	25	6.33	65	8			52	6			1696	38
M024BC-19	26-28	2	27	6.92	72	7			49	5			1666	40
M024BC-20	28-30	2	29	7.52	71	5			60	4			1635	43
M028MC													**Not Datable**	
M028MC-01	0-1	1	0.5	0.51	286	8	251	11	32	4	43	1		
M028MC-02	1-2	1	1.5	1.31	94	6	59	11	16	4	15	1		
M028MC-03	2-3	1	2.5	2.35	20	4			23	4				
M028MC-04	3-4	1	3.5	3.42	19	3			18	2				
M028MC-05	4-5	1	4.5	4.33	24	3			21	2				
M028MC-06	5-6	1	5.5	5.23	33	6			38	5				
M028MC-07	6-7	1	6.5	6.05	32	4			31	3				
M028MC-08	7-8	1	7.5	6.83	40	5			30	3				
M028MC-09	8-9	1	8.5	7.66	44	7			36	5				
M028MC-10	9-10	1	9.5	8.45	40	5			35	4				
M028MC-11	10-12	2	11	9.94	37	3			35	3				
M028MC-12	12-14	2	13	11.47	32	5			36	4				
M028MC-13	14-16	2	15	13.00	44	6			39	5				
M028MC-14	16-18	2	17	14.61	38	4			32	4				
M028MC-15	18-20	2	19	16.28	41	3			30	3				
M028MC-16	20-22	2	21	17.99	45	7			36	5				
M028MC-17	22-24	2	23	19.55	33	6			36	5				
M032BC													**CRS**	
M032BC-01	0-1	1	0.5	0.10	1312	14	1237	16	69	7	158	2	2008	4
M032BC-02	1-2	1	1.5	0.23	1203	22	1128	23	71	10	161	3	2002	5
M032BC-03	2-3	1	2.5	0.39	1115	24	1041	25	72	11	165	3	1994	7
M032BC-04	3-4	1	3.5	0.55	975	20	901	21	56	9	173	3	1985	9
M032BC-05	4-5	1	4.5	0.73	883	20	808	22	47	10	182	3	1976	11
M032BC-06	5-6	1	5.5	0.91	751	21	676	23	59	10	206	3	1966	12
M032BC-07	6-7	1	6.5	1.10	602	14	527	16	64	8	193	2	1956	14
M032BC-08	7-8	1	7.5	1.30	454	19	379	20	42	11	153	3	1946	16
M032BC-09	8-9	1	8.5	1.51	317	13	242	15	49	7	84	2	1935	18
M032BC-10	9-10	1	9.5	1.73	236	8	161	11	51	5	16	1	1923	20
M032BC-11	10-12	2	11	2.18	191	7	116	10	52	5	2	0	1905	30
M032BC-12	12-14	2	13	2.67	134	11	59	13	46	7			1879	35
M032BC-13	14-16	2	15	3.17	85	6	10	9	50	4			1852	39
M032BC-14	16-18	2	17	3.70	75	9			64	8			1824	44
M032BC-15	18-20	2	19	4.23	81	6			53	4			1796	48
M032BC-16	20-22	2	21	4.79	63	10			57	8			1766	54
M032BC-17	22-24	2	23	5.34	79	11			52	8			1736	58
M032BC-18	24-26	2	25	5.90	68	12			46	7			1706	63
M032BC-19	26-28	2	27	6.47	83	12			70	10			1675	67
M032BC-20	28-30	2	29	7.03	75	10			61	7			1644	72
M041MC													**CRS**	
M041MC-01	0-1	1	0.5	0.11	1359	13	1291	17	84	7	158	2	2009	3
M041MC-02	1-2	1	1.5	0.26	1265	23	1197	26	96	11	165	3	2003	5
M041MC-03	2-3	1	2.5	0.43	1039	21	970	24	59	11	170	3	1996	6
M041MC-04	3-4	1	3.5	0.61	830	18	762	21	59	9	190	3	1988	8
M041MC-05	4-5	1	4.5	0.80	684	20	616	23	51	11	209	4	1979	10
M041MC-06	5-6	1	5.5	1.00	629	20	561	23	65	9	216	3	1971	11
M041MC-07	6-7	1	6.5	1.21	494	19	426	22	50	11	187	3	1961	12
M041MC-08	7-8	1	7.5	1.42	363	17	295	21	52	9	129	3	1952	14
M041MC-09	8-9	1	8.5	1.66	281	9	213	15	62	7	51	1	1942	16
M041MC-10	9-10	1	9.5	1.89	240	13	172	18	65	11	17	1	1931	17
M041MC-11	10-12	2	11	2.36	183	8	114	14	56	5	4	1	1915	26
M041MC-12	12-14	2	13	2.86	135	13	67	18	53	9			1893	29
M041MC-13	14-16	2	15	3.37	104	9	36	15	52	7			1870	33
M041MC-14	16-18	2	17	3.91	85	6	17	13	62	5	1	0	1846	37
M041MC-15	18-20	2	19	4.44	71	10	3	15	44	6			1822	40
M041MC-16	20-22	2	21	5.00	63	10			56	7			1798	44
M041MC-17	22-24	2	23	5.54	60	5			54	4			1773	47
M041MC-18	24-26	2	25	6.08	63	10			55	8			1748	51
M041MC-19	26-28	2	27	6.62	88	11			68	9			1724	54
M041MC-20	28-30	2	29	7.19	67	8			54	6			1699	58

Table S1. (continued)

Sample ID	Depth (cm)	Thick (cm)	Ave Depth (cm)	Dry Mass Depth (g/cm^2)	Total Pb-210 (Bq/Kg)	Total Pb-210 error (Bq/Kg)	Unsup-ported Pb-210 (Bq/Kg)	Unsup-ported Pb-210 error (Bq/Kg)	Ra-226 (Bq/Kg)	Ra-226 error (Bq/Kg)	Cs-137 (Bq/Kg)	Cs-137 error (Bq/Kg)	Selected model (top line) and average date of section (date)	Error in years (95% confidence) (± years)
M047BC													**CRS**	
M047BC-01	0-1	1	0.5	0.12	1354	29	1247	32	100	18	152	3	2009	2
M047BC-02	1-2	1	1.5	0.28	1185	44	1078	45	64	29	125	4	2004	3
M047BC-03	2-3	1	2.5	0.46	1165	39	1058	41	93	18	158	3	1999	4
M047BC-04	3-4	1	3.5	0.66	1043	46	936	48	115	31	181	5	1993	5
M047BC-05	4-5	1	4.5	0.88	846	24	739	27	55	17	190	3	1986	5
M047BC-06	5-6	1	5.5	1.10	759	43	652	45	98	32	210	5	1979	6
M047BC-07	6-7	1	6.5	1.34	646	38	540	40	92	28	218	5	1972	7
M047BC-08	7-8	1	7.5	1.57	438	44	331	45	94	29	177	5	1964	7
M047BC-09	8-9	1	8.5	1.81	400	20	293	23	70	13	104	2	1956	8
M047BC-10	9-10	1	9.5	2.07	333	28	227	31	77	16	49	2	1948	9
M047BC-11	10-12	2	11	2.59	301	32	195	34	96	24	10	2	1936	14
M047BC-12	12-14	2	13	3.13	236	33	130	35	59	20			1919	16
M047BC-13	14-16	2	15	3.73	110	23			76	25			1901	18
M047BC-14	16-18	2	17	4.35	129	53			96	41			1881	20
M047BC-15	18-20	2	19	4.95	100	17			54	15			1861	20
M047BC-16	20-22	2	21	5.55	110	29			96	25			1842	22
M047BC-17	22-24	2	23	6.16	102	26			73	18			1823	23
M047BC-18	24-26	2	25	6.77	90	31			92	25			1803	25
M047BC-19	26-28	2	27	7.39					73	22			1783	26
M047BC-20	28-30	2	29	8.01	106	17			71	16			1763	27
M050BC													**CRS 2-slope**	
M050BC-01	0-1	1	0.5	0.05	1587	114	1478	115	187	51	75	5	2010	1
M050BC-02	1-2	1	1.5	0.12	1481	65	1373	66	98	30	80	4	2009	1
M050BC-03	2-3	1	2.5	0.20	1389	37	1280	39	115	26	87	3	2007	1
M050BC-04	3-4	1	3.5	0.28	1255	52	1146	53	88	24	97	4	2005	1
M050BC-05	4-5	1	4.5	0.38	992	40	883	42	90	20	114	3	2003	2
M050BC-06	5-6	1	5.5	0.49	854	28	745	31	149	23	123	3	2001	2
M050BC-07	6-7	1	6.5	0.61	766	42	657	44	129	31	123	4	1998	2
M050BC-08	7-8	1	7.5	0.73	936	46	827	48	77	35	141	4	1993	5
M050BC-09	8-9	1	8.5	0.86	954	49	845	51	135	32	159	5	1987	7
M050BC-10	9-10	1	9.5	1.01	881	25	772	28	128	18	174	3	1980	8
M050BC-11	10-12	2	11	1.30	795	40	686	42	140	32	216	5	1969	15
M050BC-12	12-14	2	13	1.60	652	26	543	29	138	19	200	3	1953	17
M050BC-13	14-16	2	15	1.93	503	19	394	23	103	11	115	2	1937	21
M050BC-14	16-18	2	17	2.27	416	29	307	32	112	19	46	2	1920	24
M050BC-15	18-20	2	19	2.58	244	37	135	39	101	14	16	1	1904	26
M050BC-16	20-22	2	21	2.90	206	26	97	30	118	21	8	2	1888	29
M050BC-17	22-24	2	23	3.23	153	27	44	30	126	21	3	1	1871	32
M050BC-18	24-26	2	25	3.62	137	16	28	20	66	11	2	1	1852	37
M050BC-19	26-28	2	27	4.03	109	13			65	10	3	1	1832	42

Table S1. (continued)

Sample ID	Depth (cm)	Thick (cm)	Ave Depth (cm)	Dry Mass Depth (g/cm^2)	Total Pb-210 (Bq/Kg)	Total Pb-210 error (Bq/Kg)	Unsup-ported Pb-210 (Bq/Kg)	Unsup-ported Pb-210 error (Bq/Kg)	Ra-226 (Bq/Kg)	Ra-226 error (Bq/Kg)	Cs-137 (Bq/Kg)	Cs-137 error (Bq/Kg)	Selected model (top line) and average date of section (date)	Error in years (95% confidence) (± years)
H001MC													**CIC**	
H001MC-01	0-1	1	0.5	0.09	471	6	428	7	43	4	47	1	2012	0
H001MC-02	1-2	1	1.5	0.20	460	15	434	17	26	8	49	2	2012	1
H001MC-03	2-3	1	2.5	0.32	454	7	409	8	44	4	48	1	2011	1
H001MC-04	3-4	1	3.5	0.47	445	7	403	8	42	4	50	1	2010	1
H001MC-05	4-5	1	4.5	0.63	429	8	399	9	30	4	49	1	2009	1
H001MC-06	5-6	1	5.5	0.81	401	7	357	8	44	4	47	1	2008	1
H001MC-07	6-7	1	6.5	0.99	435	13	390	15	46	8	48	2	2007	2
H001MC-08	7-8	1	7.5	1.18	446	6	399	7	47	4	49	1	2006	2
H001MC-09	8-9	1	8.5	1.38	418	12	368	14	50	7	50	1	2004	2
H001MC-10	9-10	1	9.5	1.58	420	16	371	18	49	9	52	2	2003	2
H001MC-11	10-11	1	10.5	1.79	409	7	365	9	44	5	52	1	2002	2
H001MC-12	11-12	1	11.5	2.00	389	14	346	15	43	7	55	2	2000	3
H001MC-13	12-13	1	12.5	2.22	377	12	328	14	49	7	54	2	1999	3
H001MC-14	13-14	1	13.5	2.43	381	13	343	15	38	8	56	2	1998	3
H001MC-15	14-15	1	14.5	2.66	345	11	302	13	43	7	60	1	1996	3
H001MC-16	15-17	2	16	3.11	322	9	277	10	45	4	65	1	1994	4
H001MC-17	17-19	2	18	3.59	306	20	266	21	40	7	66	2	1991	5
H001MC-18	19-21	2	20	4.09	237	26	191	27	46	8	72	2	1988	6
H001MC-19	21-23	2	22	4.59	170	34	136	35	34	8	83	2	1985	6
H001MC-20	23-25	2	24	5.09	175	24	125	25	50	6	86	2	1981	7
H001MC-21	25-27	2	26	5.61	225	7	183	8	41	4	94	1	1978	7
H001MC-22	27-29	2	28	6.15	201	11	150	14	52	8	96	2	1975	8
H001MC-23	29-31	2	30	6.70	187	12	137	14	51	8	100	2	1971	8
H001MC-24	31-33	2	32	7.26	187	6	139	7	48	4	108	1	1968	9
H001MC-25	33-35	2	34	7.85	149	12	114	15	35	8	99	2	1964	10
H006MC													**CRS 2-slope**	
H006MC-01	0-1	1	0.5	0.09	1301	12	1243	13	52	5	126	1	2011	2
H006MC-02	1-2	1	1.5	0.20	1186	13	1128	14	72	7	135	2	2008	2
H006MC-03	2-3	1	2.5	0.36	976	12	918	14	55	6	148	2	2004	3
H006MC-04	3-4	1	3.5	0.55	785	8	727	10	54	4	182	1	1999	4
H006MC-05	4-5	1	4.5	0.76	670	12	612	14	54	6	197	2	1993	5
H006MC-06	5-6	1	5.5	1.00	601	8	543	10	50	4	203	2	1986	6
H006MC-07	6-7	1	6.5	1.25	484	5	426	8	50	3	241	1	1978	7
H006MC-08	7-8	1	7.5	1.52	451	9	393	11	49	5	266	2	1970	8
H006MC-09	8-9	1	8.5	1.81	354	8	296	10	48	5	284	2	1961	9
H006MC-10	9-10	1	9.5	2.09	295	10	237	12	50	6	247	3	1952	10
H006MC-11	10-11	1	10.5	2.40	244	10	186	11	56	6	139	2	1929	51
H006MC-12	11-12	1	11.5	2.72	155	9	97	11	44	6	38	1	1892	81
H006MC-13	12-13	1	12.5	3.02	96	5	38	7	47	4	8	0	1855	106
H006MC-14	13-14	1	13.5	3.32	70	4	12	7	44	4	3	0	1819	133
H006MC-15	14-15	1	14.5	3.65	59	6			54	5			1781	164
H006MC-16	15-17	2	16	4.28	50	7			44	5			1723	239
H006MC-17	17-19	2	18	4.92	50	7			48	6			1646	296
H006MC-18	19-21	2	20	5.55	66	5			49	4			1570	351
H006MC-19	21-23	2	22	6.17	66	5			50	4			1495	407
H006MC-20	23-25	2	24	6.81	53	9			60	7			1419	464
H006MC-21	25-27	2	26	7.47	54	7			49	5			1341	524
H006MC-22	27-29	2	28	8.13	55	10			43	7			1262	583
H006MC-23	29-31	2	30	8.78	64	9			53	6			1183	641
H006MC-24	31-33	2	32	9.42	59	8			53	7			1105	698
H006MC-25	33-35	2	34	10.06	61	3			54	3			1028	755
H012MC													**CIC**	
H012MC-01	0-1	1	0.5	0.10	1116	13	1060	15	56	8	94	1	2012	1
H012MC-02	1-2	1	1.5	0.26	1024	37	978	42	46	19	111	5	2010	2
H012MC-03	2-3	1	2.5	0.44	878	22	810	25	68	12	139	3	2007	2
H012MC-04	3-4	1	3.5	0.63	764	35	699	40	65	20	161	5	2003	3
H012MC-05	4-5	1	4.5	0.84	752	11	696	12	56	5	188	2	2000	3
H012MC-06	5-6	1	5.5	1.07	690	28	646	31	44	11	208	5	1996	4
H012MC-07	6-7	1	6.5	1.32	633	25	586	27	47	12	222	4	1992	4
H012MC-08	7-8	1	7.5	1.56	575	19	535	22	41	11	233	4	1987	5
H012MC-09	8-9	1	8.5	1.81	496	16	449	18	47	8	260	3	1983	5
H012MC-10	9-10	1	9.5	2.06	458	15	393	19	65	10	279	3	1979	6
H012MC-11	10-11	1	10.5	2.32	433	14	376	16	57	9	303	3	1974	6
H012MC-12	11-12	1	11.5	2.57	416	18	341	22	75	13	330	4	1970	7
H012MC-13	12-13	1	12.5	2.82	345	15	309	18	36	10	336	4	1965	7
H012MC-14	13-14	1	13.5	3.07	326	8	270	10	55	7	272	2	1961	7
H012MC-15	14-15	1	14.5	3.32	305	6	252	7	53	3	211	1	1957	8
H012MC-16	15-17	2	16	3.89	250	14	203	16	47	9	98	2	1949	12
H012MC-17	17-19	2	18	4.47	192	9	138	11	54	7	32	1	1939	13
H012MC-18	19-21	2	20	5.04	141	11	80	13	61	6	8	1	1929	14
H012MC-19	21-23	2	22	5.62	96	8	51	9	44	5	2	1	1919	15
H012MC-20	23-25	2	24	6.20	77	7	27	9	50	5			1909	16
H012MC-21	25-27	2	26	6.78									1899	17
H012MC-22	27-29	2	28	7.34									1889	18
H012MC-23	29-31	2	30	7.91									1879	19
H012MC-24	31-33	2	32	8.50									1869	20
H012MC-25	33-35	2	34	4.47										

Table S1. (continued)

Sample ID	Depth (cm)	Thick (cm)	Ave Depth (cm)	Dry Mass Depth (g/cm^2)	Total Pb-210 (Bq/Kg)	Total Pb-210 error (Bq/Kg)	Unsup-ported Pb-210 (Bq/Kg)	Unsup-ported Pb-210 error (Bq/Kg)	Ra-226 (Bq/Kg)	Ra-226 error (Bq/Kg)	Cs-137 (Bq/Kg)	Cs-137 error (Bq/Kg)	Selected model (top line) and average date of section (date)	Error in years (95% confidence) (± years)
H032MC													**CRS**	
H032MC-01	0-1	1	0.5	0.10	1126	21	1049	27	64	9	122	3	2012	3
H032MC-02	1-2	1	1.5	0.24	1085	17	1008	25	50	7	164	3	2009	3
H032MC-03	2-3	1	2.5	0.40	906	15	828	23	55	8	196	3	2005	3
H032MC-04	3-4	1	3.5	0.59	857	16	779	24	70	9	215	3	2002	3
H032MC-05	4-5	1	4.5	0.79	818	9	740	20	63	4	225	2	1997	4
H032MC-06	5-6	1	5.5	1.00	730	14	652	23	55	7	238	3	1993	4
H032MC-07	6-7	1	6.5	1.22	691	14	614	23	57	8	260	3	1988	5
H032MC-08	7-8	1	7.5	1.45	631	13	553	22	62	7	285	3	1982	5
H032MC-09	8-9	1	8.5	1.68	521	12	443	22	57	8	322	3	1977	6
H032MC-10	9-10	1	9.5	1.92	463	12	385	22	63	8	353	3	1972	6
H032MC-11	10-11	1	10.5	2.15	399	10	322	20	57	5	372	3	1967	7
H032MC-12	11-12	1	11.5	2.39	341	13	264	22	63	8	320	3	1961	7
H032MC-13	12-13	1	12.5	2.63	311	12	233	21	48	7	207	3	1956	8
H032MC-14	13-14	1	13.5	2.87	322	6	244	19	64	4	109	1	1950	8
H032MC-15	14-15	1	14.5	3.12	241	11	163	21	38	7	34	1	1945	9
H032MC-16	15-17	2	16	3.61	228	8	150	19	73	6	10	1	1937	12
H032MC-17	17-19	2	18	4.10	198	5	121	19	58	3			1925	13
H032MC-18	19-21	2	20	4.58	171	10	93	21	67	8			1914	14
H032MC-19	21-23	2	22	5.07	126	11	49	21	60	7			1903	15
H032MC-20	23-25	2	24	5.56	143	9	65	20	57	6			1892	16
H032MC-21	25-27	2	26	6.07	117	6	39	19	65	5			1881	17
H032MC-22	27-29	2	28	6.59	88	7			59	6			1869	18
H032MC-23	29-31	2	30	7.12	89	7			66	6			1857	19
H032MC-24	31-33	2	32	7.65	51	13			59	8			1845	20
H032MC-25	33-35	2	34	8.19	83	5			59	4			1833	21
H037MC													**Not Datable**	
H037MC-01	0-1	1	0.5	0.15	1107	18	1058	19	36	7	143	2		
H037MC-02	1-2	1	1.5	0.39	737	9	689	12	43	4	122	1		
H037MC-03	2-3	1	2.5	0.84	288	11	239	13	32	6	82	2		
H037MC-04	3-4	1	3.5	1.30	96	6	47	9	51	5	29	1		
H037MC-05	4-5	1	4.5	1.72	63	5	14	9	40	4	2	0		
H037MC-06	5-6	1	5.5	2.10	128	9	79	11	112	7				
H037MC-07	6-7	1	6.5	2.44	86	12	38	14	67	9				
H037MC-08	7-8	1	7.5	2.84	52	6			34	5				
H037MC-09	8-9	1	8.5	3.27	51	5			40	4				
H037MC-10	9-10	1	9.5	3.71	50	9			31	5				
H037MC-11	10-11	1	10.5	4.14	39	6			39	4				
H037MC-12	11-12	1	11.5	4.56	43	4			41	3				
H037MC-13	12-13	1	12.5	4.94	42	5			40	5				
H037MC-14	13-14	1	13.5	5.33	46	6			37	4				
H037MC-15	14-15	1	14.5	5.70	48	5			46	4				
H037MC-16	15-17	2	16	6.43	48	5			41	4				
H037MC-17	17-19	2	18	7.16	55	6			41	5				
H037MC-18	19-21	2	20	7.92	65	6			46	5				
H037MC-19	21-23	2	22	8.67	54	5			48	4				
H037MC-20	23-25	2	24	9.48	41	6			50	5				
H037MC-21	25-27	2	26											
H037MC-22	27-29	2	28											
H037MC-23	29-31	2	30											
H037MC-24	31-33	2	32											
H038MC													**CRS**	
H038MC-01	0-0.5	0.5	0.25	0.06	1318	21	1272	22	65	10	172	3	2010	5
H038MC-02	0.5-1	0.5	0.75	0.13	1159	10	1112	10	60	5	161	1	2002	8
H038MC-03	1-1.5	0.5	1.25	0.21	1025	18	978	18	59	9	155	3	1993	10
H038MC-04	1.5-2	0.5	1.75	0.32	863	10	817	11	57	5	159	2	1982	15
H038MC-05	2-2.5	0.5	2.25	0.46	612	13	565	13	55	7	131	2	1968	20
H038MC-06	2.5-3	0.5	2.75	0.64	369	10	323	11	34	5	87	2	1950	28
H038MC-07	3-3.5	0.5	3.25	0.86	230	7	183	8	48	5	63	1	1927	36
H038MC-08	3.5-4	0.5	3.75	1.10	93	8	46	8	31	7	21	1	1900	44
H038MC-09	4-4.5	0.5	4.25	1.34	52	8			35	5	6	1	1872	51
H038MC-10	4.5-5	0.5	4.75	1.60	51	8			41	6			1844	58
H038MC-11	5-6	1	5.5	2.09	42	7			47	6			1801	85
H038MC-12	6-7	1	6.5	2.59	43	7			38	5			1744	99
H038MC-13	7-8	1	7.5	3.10	47	7			36	5			1685	114
H038MC-14	8-9	1	8.5	3.64	47	6			46	4			1625	130
H038MC-15	9-10	1	9.5	4.25	48	4			43	3			1559	150
H038MC-16	10-11	1	10.5	4.84	46	5			39	4			1490	166
H038MC-17	11-12	1	11.5	5.45	47	6			36	5			1421	183
H038MC-18	12-13	1	12.5	6.01									1354	196
H038MC-19	13-14	1	13.5	6.57	43	4			36	3			1289	211
H038MC-20	14-15	1	14.5	7.10	47	4			43	4			1227	223
H038MC-21	15-17	2	16	8.13									1137	280
H038MC-22	17-19	2	18	9.14									1020	307
H038MC-23	19-21	2	20	10.11									906	331
H038MC-24	21-23	2	22	11.05									797	354
H038MC-25	23-25	2	24	11.99									688	381

Table S1. (continued)

Sample ID	Depth	Thick	Ave Depth	Dry Mass Depth	Total Pb-210	Total Pb-210 error	Unsup-ported Pb-210	Unsup-ported Pb-210 error	Ra-226	Ra-226 error	Cs-137	Cs-137 error	Selected model (top line) and average date of section	Error in years (95% confidence)
	(cm)	(cm)	(cm)	(g/cm^2)	(Bq/Kg)	(Bq/Kg)	(Bq/Kg)	(Bq/Kg)	(Bq/Kg)	(Bq/Kg)	(Bq/Kg)	(Bq/Kg)	(date)	(± years)
H048MC													**CRS**	
H048MC-01	0-1	1	0.5	0.13	1074	20	1000	21	54	10	174	3	2009	6
H048MC-02	1-2	1	1.5	0.36	820	20	746	21	62	10	208	3	1998	11
H048MC-03	2-3	1	2.5	0.61	643	19	569	21	47	10	245	4	1983	15
H048MC-04	3-4	1	3.5	0.88	555	19	480	20	53	11	300	4	1968	19
H048MC-05	4-5	1	4.5	1.15	426	10	352	12	49	7	285	2	1952	22
H048MC-06	5-6	1	5.5	1.43	353	12	278	14	150	8	209	2	1935	26
H048MC-07	6-7	1	6.5	1.73	322	15	248	16	40	11	79	2	1917	31
H048MC-08	7-8	1	7.5	2.05	236	14	162	16	45	8	27	2	1899	35
H048MC-09	8-9	1	8.5	2.35	157	8	83	10	53	6	3	1	1880	39
H048MC-10	9-10	1	9.5	2.67	114	11	40	13	37	9			1861	43
H048MC-11	10-11	1	10.5	2.99	90	9	16	12	49	7			1842	47
H048MC-12	11-12	1	11.5	3.32	82	11	8	13	36	9			1823	52
H048MC-13	12-13	1	12.5	3.65	62	9			45	6			1802	56
H048MC-14	13-14	1	13.5	4.03	80	8			59	7			1781	62
H048MC-15	14-15	1	14.5	4.39	83	14			76	10			1759	66
H048MC-16	15-17	2	16	5.09	76	5			56	4			1727	85
H048MC-17	17-19	2	18	5.75	76	8			59	6			1686	92
H048MC-18	19-21	2	20	6.46	71	5			58	4			1645	102
H048MC-19	21-23	2	22	7.16	73	7			92	5			1602	111
H048MC-20	23-25	2	24	7.85									1560	119
H048MC-21	25-27	2	26	8.56									1518	129
H048MC-22	27-29	2	28	9.30									1474	138
H048MC-23	29-31	2	30	10.08									1428	150
H048MC-24	31-33	2	32	10.90									1380	161
H048MC-25	33-35	2	34											
H061MC													**CRS**	
H061MC-01	0-0.5	0.5	0.25	0.04	1239	23	1197	24	57	15	189	3	2010	4
H061MC-02	0.5-1	0.5	0.75	0.09	1140	39	1098	40	39	15	196	6	2002	8
H061MC-03	1-1.5	0.5	1.25	0.16	994	20	952	21	43	10	191	3	1993	11
H061MC-04	1.5-2	0.5	1.75	0.25	783	9	741	11	47	6	186	2	1981	16
H061MC-05	2-2.5	0.5	2.25	0.38	468	15	425	16	43	8	157	2	1963	24
H061MC-06	2.5-3	0.5	2.75	0.55	267	8	225	10	33	4	129	1	1939	32
H061MC-07	3-3.5	0.5	3.25	0.77	108	9	66	11	28	6	57	1	1908	44
H061MC-08	3.5-4	0.5	3.75	0.97	58	5	15	8	31	5	21	1	1875	50
H061MC-09	4-4.5	0.5	4.25	1.18	38	6			29	4	6	1	1842	57
H061MC-10	4.5-5	0.5	4.75	1.39	38	7			36	5			1810	64
H061MC-11	5-6	1	5.5	1.80	37	5			32	4			1761	95
H061MC-12	6--7	1	6.5	2.22	45	8			32	6			1695	110
H061MC-13	7-8	1	7.5	2.63	37	7			37	5			1629	124
H061MC-14	8-9	1	8.5	3.10	38	5			33	4			1559	144
H061MC-15	9-10	1	9.5	3.57	35	5			33	4			1486	161
H061MC-16	10-11	1	10.5	3.99	44	5			36	4			1415	171
H061MC-17	11-12	1	11.5	4.41	51	7			37	5			1349	186
H061MC-18	12-13	1	12.5	4.80	52	5			23	4			1285	197
H061MC-19	13-14	1	13.5	5.23	49	8			39	7			1220	215
H061MC-20	14-15	1	14.5	5.64	45	7			18	5			1153	228
H061MC-21	15-17	2	16	6.50									1053	292
H061MC-22	17-19	2	18	7.31									922	317
H061MC-23	19-21	2	20	8.12									793	345
H061MC-24	21-23	2	22	9.09									652	391
H061MC-25	23-25	2	24	10.47									467	472
H095MC													**CRS**	
H095MC-01	0-1	1	0.5	0.09	1247	22	1199	24	70	10	179	3	2009	5
H095MC-02	1-2	1	1.5	0.22	1060	17	1011	20	68	6	190	3	2001	10
H095MC-03	2-3	1	2.5	0.42	798	13	750	17	75	6	164	2	1989	17
H095MC-04	3-4	1	3.5	0.71	537	7	489	13	72	4	139	1	1972	27
H095MC-05	4-5	1	4.5	1.11	294	7	246	13	56	4	86	1	1947	41
H095MC-06	5-6	1	5.5	1.70	78	7	30	13	36	4	22	1	1911	62
H095MC-07	6-7	1	6.5	2.28	33	3			31	2	4	0	1869	75
H095MC-08	7-8	1	7.5	2.81	46	5			36	4			1829	86
H095MC-09	8-9	1	8.5	3.41	34	4			32	3			1789	103
H095MC-10	9-10	1	9.5	3.87	62	5			40	4			1751	109
H095MC-11	10-11	1	10.5	4.31	50	5			46	4			1718	119
H095MC-12	11-12	1	11.5	4.77	41	5			36	4			1686	130
H095MC-13	12-13	1	12.5	5.21	50	6			43	4			1654	141
H095MC-14	13-14	1	13.5	5.64	58	4			47	3			1622	150
H095MC-15	14-15	1	14.5	6.11	61	8			47	6			1590	163
H095MC-16	15-17	2	16	7.28									1531	216
H095MC-17	17-19	2	18	8.42									1448	242
H095MC-18	19-21	2	20	9.52									1367	267
H095MC-19	21-23	2	22	10.56									1290	290
H095MC-20	23-25	2	24	11.76									1209	324
H095MC-21	25-27	2	26	13.28									1111	373
H095MC-22	27-29	2	28	14.35									1018	381
H095MC-23	29-31	2	30	15.41									942	407
H095MC-24	31-33	2	32	16.31									871	422
H095MC-25	33-35	2	34	17.13									809	439

Table S1. (continued)

Sample ID	Depth (cm)	Thick (cm)	Ave Depth (cm)	Dry Mass Depth (g/cm^2)	Total Pb-210 (Bq/Kg)	Total Pb-210 error (Bq/Kg)	Unsup-ported Pb-210 (Bq/Kg)	Unsup-ported Pb-210 error (Bq/Kg)	Ra-226 (Bq/Kg)	Ra-226 error (Bq/Kg)	Cs-137 (Bq/Kg)	Cs-137 error (Bq/Kg)	Selected model (top line) and average date of section (date)	Error in years (95% confidence) (± years)
ON02MC													**CRS**	
ON02MC-01	0-1	1	0.5	0.10	873	24	810	24	91	14	76	3	2011	3
ON02MC-02	1-2	1	1.5	0.25	814	19	751	20	98	11	75	2	2004	5
ON02MC-03	2-3	1	2.5	0.43	663	21	601	22	90	11	94	3	1995	6
ON02MC-04	3-4	1	3.5	0.62	451	20	389	21	95	12	127	3	1985	7
ON02MC-05	4-5	1	4.5	0.83	305	19	243	19	66	11	188	3	1973	8
ON02MC-06	5-6	1	5.5	1.08	238	11	176	13	71	7	133	2	1961	10
ON02MC-07	6-7	1	6.5	1.40	171	9	108	11	70	6	30	1	1945	13
ON02MC-08	7-8	1	7.5	1.77	147	12	84	13	102	7	2	1	1926	15
ON02MC-09	8-9	1	8.5	2.15	74	8			75	6			1905	16
ON02MC-10	9-10	1	9.5	2.52	71	7			45	6			1884	17
ON02MC-11	10-12	2	11	3.27	79	10			55	5			1853	30
ON02MC-12	12-14	2	13	3.98	61	8			49	5			1812	30
ON02MC-13	14-16	2	15	4.69	93	10			47	6			1773	32
ON02MC-14	16-18	2	17	5.43	70	8			43	5			1732	35
ON02MC-15	18-20	2	19	6.18	66	8			44	5			1691	38
ON02MC-16	20-22	2	21	6.96	68	5			46	4			1648	40
ON02MC-17	22-24	2	23	7.73	55	8			52	6			1605	42
ON02MC-18	24-26	2	25	8.49	68	6			46	5			1563	44
ON02MC-19	26-28	2	27	9.25	56	4			47	3			1520	46
ON02MC-20	28-30	2	29	10.04	64	6			42	4			1477	49
ON02MC-21	30-32	2	31	10.82	56	6			34	4			1434	51
ON02MC-22	32-34	2	33	11.57	56	9			52	7			1391	52
ON02MC-23	34-36	2	35	12.34	58	7			55	5			1349	54
ON02MC-24	36-38	2	37	13.09	63	5			46	4			1306	56
ON02MC-25	38-40	2	39	13.90	68	6			39	4			1263	60
ON06MC													**CIC**	
ON06MC-01	0-1	1	0.5	0.26	331	8	294	8	44	5	9	1	2013	1
ON06MC-02	1-2	1	1.5	0.64	272	12	235	12	46	9	9	1	2012	1
ON06MC-03	2-3	1	2.5	1.06	304	16	268	16	38	9	10	1	2010	1
ON06MC-04	3-4	1	3.5	1.46	293	15	257	15	50	8	8	1	2008	2
ON06MC-05	4-5	1	4.5	1.87	295	7	259	7	41	5	10	1	2007	2
ON06MC-06	5-6	1	5.5	2.31	295	16	259	16	38	12	9	1	2005	2
ON06MC-07	6-7	1	6.5	2.76	297	14	261	14	42	9	10	1	2003	3
ON06MC-08	7-8	1	7.5	3.22	205	10	169	10	22	7	8	1	2001	3
ON06MC-09	8-9	1	8.5	3.68	291	8	255	8	33	6	13	1	1999	3
ON06MC-10	9-10	1	9.5	4.12	315	18	279	18	47	12	14	2	1997	3
ON06MC-11	10-12	2	11	5.03	207	7	171	8	34	6	9	1	1994	5
ON06MC-12	12-14	2	13	5.99	187	12	151	13	46	9	13	1	1990	5
ON06MC-13	14-16	2	15	7.05	190	13	154	13	40	10	16	1	1986	6
ON06MC-14	16-18	2	17	8.17	170	7	134	7	32	5	15	1	1982	7
ON06MC-15	18-20	2	19	9.46	127	13	91	13	32	8	18	1	1976	8
ON06MC-16	20-22	2	21	10.78	110	11	74	11	28	6	13	1	1971	9
ON06MC-17	22-24	2	23	12.29	89	7	53	8	19	4	14	1	1965	10
ON06MC-18	24-26	2	25	13.53	102	11	66	11	33	7	24	1	1959	10
ON06MC-19	26-28	2	27	14.85	77	10	41	10	25	6	28	1	1954	11
ON06MC-20	28-30	2	29	16.14	83	6	47	7	35	4	39	1	1948	12
ON06MC-21	30-32	2	31	17.41	80	6	44	6	33	4	42	1	1943	12
ON13MC													**CRS**	
ON13MC-01	0-1	1	0.5	0.08	1215	26	1149	30	109	14	76	3	2011	3
ON13MC-02	1-2	1	1.5	0.19	999	19	933	24	104	10	78	2	2006	5
ON13MC-03	2-3	1	2.5	0.36	738	11	672	18	67	6	91	1	1998	8
ON13MC-04	3-4	1	3.5	0.55	472	17	406	22	66	10	98	2	1988	11
ON13MC-05	4-5	1	4.5	0.76	371	11	305	19	65	7	150	2	1977	13
ON13MC-06	5-6	1	5.5	0.96	327	8	261	17	55	5	188	2	1966	15
ON13MC-07	6-7	1	6.5	1.16	238	23	173	27	40	13	187	4	1955	17
ON13MC-08	7-8	1	7.5	1.37	224	19	158	24	41	11	165	4	1943	20
ON13MC-09	8-9	1	8.5	1.61	255	19	189	24	37	11	98	3	1931	23
ON13MC-10	9-10	1	9.5	1.89	143	16	77	22	42	10	19	2	1916	27
ON13MC-11	10-12	2	11	2.49	75	16			80	12			1892	42
ON13MC-12	12-14	2	13	3.15	81	12			60	9			1857	50
ON13MC-13	14-16	2	15	3.76	75	11			39	8			1821	55
ON13MC-14	16-18	2	17	4.33	38	9			48	8			1788	59
ON13MC-15	18-20	2	19	4.87	40	8			43	8			1758	64
ON13MC-16	20-22	2	21	5.46	67	6			44	5			1726	71
ON13MC-17	22-24	2	23	6.04	72	12			66	9			1694	77
ON13MC-18	24-26	2	25	6.63	80	8			47	6			1661	83
ON13MC-19	26-28	2	27	7.25	72	5			51	4			1627	90
ON13MC-20	28-30	2	29	7.86	75	8			52	5			1593	96
ON13MC-21	30-32	2	31	8.49	77	8			47	6			1559	103
ON13MC-22	32-34	2	33	9.15	53	9			52	6			1523	110
ON13MC-23	34-36	2	35	9.84	73	8			43	5			1485	118
ON13MC-24	36-38	2	37	10.49	73	5			46	4			1448	124
ON13MC-25	38-40	2	39	11.15	76	7			56	5			1411	130
ON17MC													**CRS**	
ON17MC-01	0-1	1	0.5	0.09	1217	31	1144	32	55	13	66	2	2012	2
ON17MC-02	1-2	1	1.5	0.18	1026	24	952	25	60	11	68	2	2009	2
ON17MC-03	2-3	1	2.5	0.31	878	22	805	24	69	11	73	2	2006	3
ON17MC-04	3-4	1	3.5	0.47	638	19	564	21	60	11	76	2	2001	4
ON17MC-05	4-5	1	4.5	0.67	408	19	334	21	63	12	96	3	1996	5
ON17MC-06	5-6	1	5.5	0.87	339	18	266	20	55	11	136	3	1989	5
ON17MC-07	6-7	1	6.5	1.05	288	19	214	21	57	12	152	3	1983	6
ON17MC-08	7-8	1	7.5	1.23	291	18	217	20	54	11	177	3	1978	6
ON17MC-09	8-9	1	8.5	1.42	260	20	186	22	52	11	196	3	1972	7
ON17MC-10	9-10	1	9.5	1.62	242	16	168	18	67	13	187	3	1966	7

Table S1. (continued)

Sample ID	Depth (cm)	Thick (cm)	Ave Depth (cm)	Dry Mass Depth (g/cm^2)	Total Pb-210 (Bq/Kg)	Total Pb-210 error (Bq/Kg)	Unsup-ported Pb-210 (Bq/Kg)	Unsup-ported Pb-210 error (Bq/Kg)	Ra-226 (Bq/Kg)	Ra-226 error (Bq/Kg)	Cs-137 (Bq/Kg)	Cs-137 error (Bq/Kg)	Selected model (top line) and average date of section (date)	Error in years (95% confidence) (± years)
ON17MC-11	10-12	2	11	2.10	202	16	128	18	62	11	103	3	1955	13
ON17MC-12	12-14	2	13	2.62	155	16	82	19	61	11	24	2	1939	15
ON17MC-13	14-16	2	15	3.17	128	13	54	16	59	9			1922	17
ON17MC-14	16-18	2	17	3.73	86	11			60	7			1905	19
ON17MC-15	18-20	2	19	4.32	84	10			57	8			1887	21
ON17MC-16	20-22	2	21	4.90	75	7			41	6			1868	22
ON17MC-17	22-24	2	23	5.46	74	5			48	3			1850	23
ON17MC-18	24-26	2	25	5.99	68	8			56	5			1833	24
ON17MC-19	26-28	2	27	6.54	78	6			55	4			1816	26
ON17MC-20	28-30	2	29	7.09	62	5			47	4			1799	27
ON17MC-21	30-32	2	31	7.64	63	7			51	5			1781	29
ON25MC													**CRS**	
ON25MC-01	0-1	1	0.5	0.07	1342	28	1267	29	76	13	59	3	2012	2
ON25MC-02	1-2	1	1.5	0.17	1260	34	1151	36	109	16	63	3	2009	2
ON25MC-03	2-3	1	2.5	0.30	1002	24	931	26	71	11	66	2	2005	3
ON25MC-04	3-4	1	3.5	0.46	755	24	679	25	76	12	65	2	1999	4
ON25MC-05	4-5	1	4.5	0.66	455	25	390	27	65	13	83	3	1992	5
ON25MC-06	5-6	1	5.5	0.86	384	27	311	28	73	13	132	4	1984	6
ON25MC-07	6-7	1	6.5	1.06	315	21	263	23	52	13	188	4	1977	6
ON25MC-08	7-8	1	7.5	1.26	297	14	238	17	59	9	216	3	1969	7
ON25MC-09	8-9	1	8.5	1.47	254	13	189	16	65	8	180	2	1961	8
ON25MC-10	9-10	1	9.5	1.71	201	23	149	25	52	15	99	3	1953	9
ON25MC-11	10-12	2	11	2.23	127	21	96	23	31	13	15	2	1938	15
ON25MC-12	12-14	2	13	2.76	108	17	54	20	54	12	3	1	1918	17
ON25MC-13	14-16	2	15	3.30	73	13			45	8			1897	18
ON25MC-14	16-18	2	17	3.83	80	13			43	9			1877	19
ON25MC-15	18-20	2	19	4.36	94	12			28	8			1857	21
ON25MC-16	20-22	2	21	4.91	60	10			53	8			1836	22
ON25MC-17	22-24	2	23	5.47	74	6			48	5			1815	24
ON25MC-18	24-26	2	25	6.05	74	8			42	6			1793	26
ON25MC-19	26-28	2	27	6.63	79	7			48	5			1771	27
ON25MC-20	28-30	2	29	7.21	66	6			47	4			1748	29
ON25MC-21	30-32	2	31	7.78	73	8			37	5			1726	30
ON25MC-22	32-34	2	33	8.37	74	8			41	5			1704	32
ON25MC-23	34-36	2	35	9.00	66	6			43	4			1681	34
ON25MC-24	36-38	2	37	9.60	56	9			40	6			1657	35
ON25MC-25	38-40	2	39	10.20	65	7			43	4			1634	36
ON30MC													**CRS**	
ON30MC-01	0-1	1	0.5	0.07	1357	28	1278	30	105	15	56	2	2012	2
ON30MC-02	1-2	1	1.5	0.14	1250	21	1171	24	81	11	59	2	2009	2
ON30MC-03	2-3	1	2.5	0.25	1038	12	959	17	88	6	66	1	2006	3
ON30MC-04	3-4	1	3.5	0.39	799	19	720	22	63	11	79	2	2001	4
ON30MC-05	4-5	1	4.5	0.59	547	17	467	20	63	10	107	2	1994	6
ON30MC-06	5-6	1	5.5	0.79	377	13	297	17	65	9	143	2	1986	7
ON30MC-07	6-7	1	6.5	1.00	326	15	247	19	67	12	187	3	1978	8
ON30MC-08	7-8	1	7.5	1.18	304	9	224	15	60	7	232	2	1971	8
ON30MC-09	8-9	1	8.5	1.38	291	15	211	19	55	12	179	3	1963	9
ON30MC-10	9-10	1	9.5	1.58	212	15	133	19	49	11	96	3	1955	10
ON30MC-11	10-12	2	11	2.07	168	10	89	15	63	6	22	1	1941	18
ON30MC-12	12-14	2	13	2.57	152	7	73	14	46	5	2	1	1922	20
ON30MC-13	14-16	2	15	3.09	106	14	27	18	61	9			1902	23
ON30MC-14	16-18	2	17	3.63	102	9			41	7			1881	25
ON30MC-15	18-20	2	19	4.17	98	6			57	5			1860	27
ON30MC-16	20-22	2	21	4.71	88	5			51	4			1838	30
ON30MC-17	22-24	2	23	5.27	78	7			60	5			1817	32
ON30MC-18	24-26	2	25	5.84	73	8			45	7			1795	35
ON30MC-19	26-28	2	27	6.42	78	7			47	6			1772	37
ON30MC-20	28-30	2	29	6.99	70	6			54	4			1749	39
ON30MC-21	30-32	2	31	7.59	78	7			60	7			1726	42
ON30MC-22	32-34	2	33	8.18	72	5			48	4			1703	45
ON30MC-23	34-36	2	35	8.79	72	6			47	4			1679	47
ON30MC-24	36-38	2	37	9.41	62	10			38	7			1655	50
ON36MC													**CRS**	
ON36MC-01	0-1	1	0.5	0.12	902	22	823	22	34	9	32	2	2012	3
ON36MC-02	1-2	1	1.5	0.28	761	9	682	9	36	4	41	1	2007	5
ON36MC-03	2-3	1	2.5	0.48	610	17	532	17	38	10	69	2	2002	7
ON36MC-04	3-4	1	3.5	0.71	458	13	380	14	26	6	89	2	1995	9
ON36MC-05	4-5	1	4.5	0.94	423	17	345	17	38	9	124	3	1988	10
ON36MC-06	5-6	1	5.5	1.16	334	9	256	9	46	5	177	2	1982	12
ON36MC-07	6-7	1	6.5	1.38	302	14	224	14	44	9	209	3	1975	14
ON36MC-08	7-8	1	7.5	1.59	265	13	187	13	45	7	226	3	1968	15
ON36MC-09	8-9	1	8.5	1.81	248	10	170	10	47	6	198	2	1962	17
ON36MC-10	9-10	1	9.5	2.04	230	8	152	9	51	5	195	2	1955	19
ON36MC-11	10-12	2	11	2.50	228	10	150	10	45	6	184	2	1944	26
ON36MC-12	12-14	2	13	3.01	179	10	100	10	47	6	84	1	1930	30
ON36MC-13	14-16	2	15	3.61	164	7	85	7	37	5	32	1	1913	36
ON36MC-14	16-18	2	17	4.26	136	8	57	8	45	6	13	1	1894	42
ON36MC-15	18-20	2	19	4.92	117	8	38	8	47	5	3	1	1874	47
ON36MC-16	20-22	2	21	5.58	100	12	21	12	30	7			1854	52
ON36MC-17	22-24	2	23	6.21	80	10	2	10	41	7			1834	56
ON36MC-18	24-26	2	25	6.85	85	6			39	4			1815	61
ON36MC-19	26-28	2	27	7.46	86	9			36	6			1796	65
ON36MC-20	28-30	2	29	8.10	65	9			32	6			1777	70
ON36MC-21	30-32	2	31	8.74	72	8			50	5			1757	75
ON36MC-22	32-34	2	33	9.37	80	9			47	6			1738	80
ON36MC-23	34-36	2	35	10.02	82	10			43	7			1718	85
ON36MC-24	36-38	2	37	10.71	47	7			48	5			1698	91
ON36MC-25	38-40	2	39	11.43	60	8			45	6			1677	97

Table S1. (continued)

Sample ID	Depth (cm)	Thick (cm)	Ave Depth (cm)	Dry Mass Depth (g/cm^2)	Total Pb-210 (Bq/Kg)	Total Pb-210 error (Bq/Kg)	Unsup-ported Pb-210 (Bq/Kg)	Unsup-ported Pb-210 error (Bq/Kg)	Ra-226 (Bq/Kg)	Ra-226 error (Bq/Kg)	Cs-137 (Bq/Kg)	Cs-137 error (Bq/Kg)	Selected model (top line) and average date of section (date)	Error in years (95% confidence) (± years)
ER09MC													**CIC**	
ER09MC-01	0-2	2	1	0.36	440	12	389	12	55	7	12	1	2014	1
ER09MC-02	2-4	2	3	0.95	332	9	280	10	55	6	16	1	2013	1
ER09MC-03	4-6	2	5	1.54	316	15	265	15	56	9	19	2	2012	1
ER09MC-04	6-8	2	7	2.12	316	12	264	12	50	7	17	1	2010	1
ER09MC-05	8-10	2	9	2.77	296	8	244	8	43	5	15	1	2009	2
ER09MC-06	10-12	2	11	3.47	297	8	246	9	56	5	18	1	2008	2
ER09MC-07	12-14	2	13	4.15	252	13	201	13	53	7	19	1	2006	2
ER09MC-08	14-16	2	15	4.82	302	14	250	14	49	8	19	1	2005	2
ER09MC-09	16-18	2	17	5.53	271	11	219	12	43	6	19	1	2003	3
ER09MC-10	18-20	2	19	6.27	281	7	230	7	52	5	17	1	2001	3
ER09MC-11	20-22	2	21	6.99	276	11	225	11	48	7	19	1	2000	3
ER09MC-12	22-24	2	23	7.76	240	14	189	14	45	8	16	1	1998	4
ER09MC-13	24-26	2	25	8.55	240	11	189	11	51	7	19	1	1996	4
ER09MC-14	26-28	2	27	9.32	244	12	192	12	46	8	16	1	1995	4
ER09MC-15	28-30	2	29	10.10	228	7	176	7	49	4	18	1	1993	4
ER09MC-16	30-32	2	31	10.86	221	10	170	10	58	7	20	1	1991	5
ER09MC-17	32-34	2	33	11.62	191	14	140	14	53	10	19	1	1990	5
ER09MC-18	34-36	2	35	12.42	199	17	148	17	56	11	23	2	1988	5
ER09MC-19	36-38	2	37	13.17	194	9	143	10	61	7	32	1	1986	6
ER09MC-20	38-40	2	39	13.95	180	11	129	11	48	7	34	1	1984	6
ER09MC-21	40-42	2	41	14.75	163	11	111	11	44	7	36	1	1983	6
ER09MC-22	42-44	2	43	15.56	169	11	118	11	58	8	44	1	1981	6
ER15MC													**CIC**	
ER15MC-01	0-2	2	1	0.58	274	8	233	8	44	5	8	1	2014	1
ER15MC-02	2-4	2	3	1.42	261	9	220	9	47	6	8	1	2013	1
ER15MC-03	4-6	2	5	2.28	257	12	216	12	55	8	7	1	2011	2
ER15MC-04	6-8	2	7	3.16	198	8	157	8	35	5	8	1	2010	2
ER15MC-05	8-10	2	9	4.09	208	11	166	11	41	7	10	1	2008	3
ER15MC-06	10-12	2	11	4.99	232	7	190	7	51	5	13	1	2007	3
ER15MC-07	12-14	2	13	5.94	184	10	143	10	39	6	12	1	2005	3
ER15MC-08	14-16	2	15	6.86	181	14	139	14	48	9	12	1	2004	4
ER15MC-09	16-18	2	17	7.85	201	11	160	11	43	6	11	1	2002	4
ER15MC-10	18-20	2	19	8.84	153	12	111	12	42	8	12	1	2000	5
ER15MC-11	20-22	2	21	9.90	160	7	118	7	42	4	11	1	1999	5
ER15MC-12	22-24	2	23	10.91	153	10	112	10	37	6	14	1	1997	6
ER15MC-13	24-26	2	25	11.92	155	12	113	13	42	8	12	1	1995	6
ER15MC-14	26-28	2	27	12.92	164	12	122	12	34	8	14	1	1993	7
ER15MC-15	28-30	2	29	13.89	164	10	123	11	55	7	18	1	1992	7
ER15MC-16	30-32	2	31	14.84	164	12	122	12	29	8	18	1	1990	7
ER15MC-17	32-34	2	33	15.79	142	12	101	12	41	6	19	1	1989	8
ER15MC-18	34-36	2	35	16.74	141	11	99	11	34	7	23	1	1987	8
ER15MC-19	36-38	2	37	17.70	152	10	111	10	36	7	24	1	1985	9
ER15MC-20	38-40	2	39	18.69	132	12	90	12	40	7	26	1	1984	9
ER15MC-21	40-42	2	41	19.65	129	11	87	11	38	7	34	2	1982	10
ER37MC													**CIC**	
ER37MC-01	0-2	2	1	0.32	440	16	381	17	57	12	21	1	2013	3
ER37MC-02	2-4	2	3	0.77	437	23	378	23	106	12	22	2	2011	3
ER37MC-03	4-6	2	5	1.29	363	14	304	14	61	9	26	1	2007	3
ER37MC-04	6-8	2	7	1.86	318	12	259	12	63	8	23	1	2003	4
ER37MC-05	8-10	2	9	2.44	357	14	298	14	58	9	24	1	1999	4
ER37MC-06	10-12	2	11	3.04	318	8	259	8	53	5	25	1	1995	5
ER37MC-07	12-14	2	13	3.67	279	12	220	12	65	7	29	1	1991	5
ER37MC-08	14-16	2	15	4.29	260	12	201	12	46	7	41	1	1986	6
ER37MC-09	16-18	2	17	4.88	278	13	219	13	58	8	45	2	1982	6
ER37MC-10	18-20	2	19	5.43	256	12	196	13	55	8	55	2	1978	7
ER37MC-11	20-22	2	21	5.99	240	12	181	12	63	9	61	2	1974	7
ER37MC-12	22-24	2	23	6.55	232	9	173	9	61	6	71	1	1970	8
ER37MC-13	24-26	2	25	7.08	207	12	148	12	68	8	106	2	1966	8
ER37MC-14	26-28	2	27	7.62	183	13	124	13	51	8	102	2	1962	9
ER37MC-15	28-30	2	29	8.21	154	12	95	12	61	8	54	2	1958	9
ER37MC-16	30-32	2	31	8.85	127	10	68	10	54	6	13	1	1954	10
ER37MC-17	32-34	2	33	9.49	114	8	55	8	51	6	5	1	1949	11
ER37MC-18	34-36	2	35	10.15	112	10	53	11	50	8			1945	11
ER37MC-19	36-38	2	37	10.83	95	10	36	10	53	8			1940	12
ER37MC-20	38-40	2	39	11.51	103	10	44	10	54	7			1935	12
ER37MC-21	40-42	2	41	12.19	97	10	38	10	75	8			1930	13
ER37MC-22	42-44	2	43	12.89	81	9	22	9	51	7			1925	14
ER37MC-23	44-46	2	45	13.62	87	6	28	6	58	4			1920	14
ER37MC-24	46-48	2	47	14.37	92	9	33	9	45	7			1915	15

Table S1. (continued)

Sample ID	Depth (cm)	Thick (cm)	Ave Depth (cm)	Dry Mass Depth (g/cm^2)	Total Pb-210 (Bq/Kg)	Total Pb-210 error (Bq/Kg)	Unsup-ported Pb-210 (Bq/Kg)	Unsup-ported Pb-210 error (Bq/Kg)	Ra-226 (Bq/Kg)	Ra-226 error (Bq/Kg)	Cs-137 (Bq/Kg)	Cs-137 error (Bq/Kg)	Selected model (top line) and average date of section (date)	Error in years (95% confidence) (± years)
ER73MC													**CIC**	
ER73MC-01	0-2	2	1	0.27	470	15	415	15	44	9	28	1	2014	1
ER73MC-02	2-4	2	3	0.70	421	17	365	18	72	12	31	2	2011	2
ER73MC-03	4-6	2	5	1.20	368	6	312	6	63	5	34	1	2008	3
ER73MC-04	6-8	2	7	1.72	348	14	292	14	52	7	34	1	2005	3
ER73MC-05	8-10	2	9	2.24	289	18	234	18	58	10	35	2	2002	4
ER73MC-06	10-12	2	11	2.79	271	12	216	12	68	7	42	1	1998	5
ER73MC-07	12-14	2	13	3.35	273	11	218	11	46	7	42	1	1995	5
ER73MC-08	14-16	2	15	3.90	273	11	217	12	52	7	45	1	1991	6
ER73MC-09	16-18	2	17	4.41	269	14	213	14	47	9	61	2	1988	6
ER73MC-10	18-20	2	19	4.93	230	11	174	12	51	8	71	2	1984	7
ER73MC-11	20-22	2	21	5.45	220	14	164	14	55	9	80	2	1981	7
ER73MC-12	22-24	2	23	5.95	241	14	185	14	64	9	92	2	1978	8
ER73MC-13	24-26	2	25	6.46	221	13	166	13	49	8	129	2	1974	8
ER73MC-14	26-28	2	27	6.99	208	16	153	16	63	10	152	3	1971	9
ER73MC-15	28-30	2	29	7.50	191	13	135	13	48	8	134	3	1968	9
ER73MC-16	30-32	2	31	8.06	163	9	107	9	50	6	103	2	1964	10
ER73MC-17	32-34	2	33	8.66	165	13	109	13	50	9	49	2	1961	10
ER73MC-18	34-36	2	35	9.26	150	10	94	10	61	7	9	1	1957	11
ER73MC-19	36-38	2	37	9.88	106	13	51	13	62	9			1953	12
ER73MC-20	38-40	2	39	10.52	98	12	42	12	60	8			1949	12
ER73MC-21	40-42	2	41	11.20	100	10	45	11	47	8			1944	13
ER73MC-22	42-44	2	43	11.87	99	13	43	13	62	9			1940	14
ER78MC													**CIC**	
ER78MC-01	0-2	2	1	0.36	348	12	289	13	48	7	16	1	2012	17
ER78MC-02	2-4	2	3	0.95	341	12	282	13	61	7	18	1	2007	17
ER78MC-03	4-6	2	5	1.62	283	11	224	13	58	7	21	1	2000	17
ER78MC-04	6-8	2	7	2.34	214	7	155	9	49	5	29	1	1992	17
ER78MC-05	8-10	2	9	3.05	222	13	163	14	55	9	32	1	1984	17
ER78MC-06	10-12	2	11	3.67	213	11	154	13	51	8	47	1	1977	17
ER78MC-07	12-14	2	13	4.29	191	11	132	12	53	8	84	2	1970	17
ER78MC-08	14-16	2	15	5.01	137	11	78	12	39	7	53	2	1962	17
ER78MC-09	16-18	2	17	5.74	115	10	56	12	43	6	18	1	1954	17
ER78MC-10	18-20	2	19	6.55	98	6	39	8	52	5	7	1	1946	17
ER78MC-11	20-22	2	21	7.35	95	8	36	9	37	6	3	1	1937	17
ER78MC-12	22-24	2	23	8.15	91	11	32	12	44	8			1928	17
ER78MC-13	24-26	2	25	8.97	76	8	17	9	56	6			1919	17
ER78MC-14	26-28	2	27	9.78	71	9	12	10	48	6			1910	18
ER78MC-15	28-30	2	29	10.66	56	5			51	3			1900	20
ER78MC-16	30-32	2	31	11.63	65	7			41	5			1890	21
ER78MC-17	32-34	2	33	12.80	68	4			50	3			1878	24
ER78MC-18	34-36	2	35	14.01	59	5			52	4			1865	26
ER78MC-19	36-38	2	37	15.26	53	5			44	4			1851	28
ER78MC-20	38-40	2	39	16.50	54	5			44	4			1837	30
ER92MC													**CIC**	
ER92MC-01	0-2	2	1	0.46	248	10	200	12	61	8	21	1	2013	2
ER92MC-02	2-4	2	3	1.12	240	11	192	12	62	7	22	1	2011	3
ER92MC-03	4-6	2	5	1.89	231	12	183	13	61	8	23	1	2007	4
ER92MC-04	6-8	2	7	2.76	167	11	119	12	42	7	18	1	2003	5
ER92MC-05	8-10	2	9	3.71	179	10	131	11	60	7	20	1	1999	6
ER92MC-06	10-12	2	11	4.62	173	12	125	13	38	7	22	1	1994	7
ER92MC-07	12-14	2	13	5.50	172	7	124	9	54	5	23	1	1990	7
ER92MC-08	14-16	2	15	6.48	169	10	121	11	43	8	25	1	1985	8
ER92MC-09	16-18	2	17	7.48	136	9	88	11	46	7	28	1	1980	9
ER92MC-10	18-20	2	19	8.52	116	10	68	11	49	7	30	1	1975	10
ER92MC-11	20-22	2	21	9.55	109	11	61	12	43	6	33	1	1970	11
ER92MC-12	22-24	2	23	10.59	103	9	55	11	42	7	39	1	1965	12
ER92MC-13	24-26	2	25	11.66	87	9	39	10	53	7	34	1	1960	13
ER92MC-14	26-28	2	27	12.86	75	5	28	7	46	4	26	1	1955	15
ER92MC-15	28-30	2	29	14.30	58	8			35	7	10	1	1948	17
ER92MC-16	30-32	2	31	15.94	50	7			38	4	3	1	1941	19
ER92MC-17	32-34	2	33	17.63	44	8			42	6			1933	21
ER92MC-18	34-36	2	35	19.40	46	4			43	3			1924	22
ER92MC-19	36-38	2	37	21.22	39	6			37	4			1915	24
ER92MC-20	38-40	2	39	23.07	51	6			41	4			1906	26
ER92MC-21	40-42	2	41	24.96	51	5			41	4			1897	28
ER92MC-22	42-44	2	43	26.84	44	5			42	4			1888	30

Table S2.

Sample ID	Depth cm	Thick cm	Ave depth cm	Dry mass depth (g/cm^2)	Total Pb-210 (Bq/kg)	Total Pb-210 error (Bq/kg)	Unsupported Pb-210 (Bq/kg)	Unsupported Pb-210 error (Bq/kg)	Ra-226 (Bq/kg)	Ra-226 error (Bq/kg)	Cs-137 (Bq/kg)	Cs-137 error (Bq/kg)	Average Date of Section (year A.D.)	95% confidence error (± years)
2014-ER15MC (Composite core)														
2014-ER15MC-01	0-2	2	1	0.576	274	8	233	8	44	5	8	1	2013.9	0.7
2014-ER15MC-02	2-4	2	3	1.420	261	9	220	9	47	6	8	1	2012.7	1.3
2014-ER15MC-03	4-6	2	5	2.280	257	12	216	12	55	8	7	1	2011.3	1.7
2014-ER15MC-04	6-8	2	7	3.163	198	8	157	8	35	5	8	1	2009.8	2.1
2013-ER15MC-05	8-10	2	9	4.090	208	11	166	11	41	7	10	1	2008.3	2.6
2013-ER15MC-06	10-12	2	11	4.991	232	7	190	7	51	5	13	1	2006.7	3.0
2013-ER15MC-07	12-14	2	13	5.943	184	10	143	10	39	6	12	1	2005.2	3.4
2013-ER15MC-08	14-16	2	15	6.864	181	14	139	14	48	9	12	1	2003.6	3.8
2013-ER15MC-09	16-18	2	17	7.845	201	11	160	11	43	6	11	1	2002.0	4.3
2013-ER15MC-10	18-20	2	19	8.841	153	12	111	12	42	8	12	1	2000.3	4.8
2013-ER15MC-11	20-22	2	21	9.901	160	7	118	7	42	4	11	1	1998.6	5.3
2013-ER15MC-12	22-24	2	23	10.909	153	10	112	10	37	6	14	1	1996.8	5.7
2013-ER15MC-13	24-26	2	25	11.917	155	12	113	13	42	8	12	1	1995.1	6.1
2013-ER15MC-14	26-28	2	27	12.915	164	12	122	12	34	8	14	1	1993.4	6.6
2013-ER15MC-15	28-30	2	29	13.887	164	10	123	11	55	7	18	1	1991.8	7.0
2013-ER15MC-16	30-32	2	31	14.845	164	12	122	12	29	8	18	1	1990.1	7.4
2013-ER15MC-17	32-34	2	33	15.787	142	12	101	12	41	6	19	1	1988.5	7.8
2013-ER15MC-18	34-36	2	35	16.745	141	11	99	11	34	7	23	1	1986.9	8.2
2013-ER15MC-19	36-38	2	37	17.697	152	10	111	10	36	7	24	1	1985.3	8.6
2013-ER15MC-20	38-40	2	39	18.686	132	12	90	12	40	7	26	1	1983.7	9.1
2013-ER15MC-21	40-42	2	41	19.655	129	11	87	11	38	7	34	2	1982.0	9.5
2014-ER15MC-A (Subcore A)														
2014-ER15MC-A1	0-2	2	1	0.485	272	8	232	8	44	5	7	1	2014.0	0.8
2014-ER15MC-A2	2-4	2	3	1.296	241	10	200	10	41	6	7	1	2012.8	1.6
2014-ER15MC-A3	4-6	2	5	2.130	233	11	193	11	43	7	9	1	2011.4	2.2
2014-ER15MC-A4	6-8	2	7	3.026	200	10	159	10	45	6	9	1	2009.8	2.8
2014-ER15MC-A5	8-10	2	9	3.958	213	10	173	10	40	6	9	1	2008.2	3.5
2014-ER15MC-A6	10-12	2	11	4.917	181	6	140	6	41	4	9	0	2006.5	4.2
2014-ER15MC-A7	12-14	2	13	5.837	183	10	142	10	38	7	13	1	2004.9	4.8
2014-ER15MC-A8	14-16	2	15	6.775	183	11	142	11	34	7	12	1	2003.2	5.4
2014-ER15MC-A9	16-18	2	17	7.722	159	10	118	10	42	6	11	1	2001.5	6.1
2014-ER15MC-A10	18-20	2	19	8.789	146	9	106	9	40	6	9	1	1999.8	6.9
2014-ER15MC-A11	20-22	2	21	9.793	162	6	121	6	44	4	12	1	1997.9	7.5
2014-ER15MC-A12	22-24	2	23	10.789	138	9	98	9	36	6	13	1	1996.1	8.2
2014-ER15MC-A13	24-26	2	25	11.796	157	11	116	11	32	7	11	1	1994.4	8.9
2014-ER15MC-A14	26-28	2	27	12.784	139	9	98	9	45	6	10	1	1992.6	9.5
2014-ER15MC-A15	28-30	2	29	13.720	149	11	109	11	33	7	16	1	1990.9	10.1
2014-ER15MC-A16	30-32	2	31	14.678	151	6	111	6	46	4	16	1	1989.2	10.8
2014-ER15MC-A17	32-34	2	33	15.594	161	7	121	7	48	5	19	1	1987.5	11.3
2014-ER15MC-A18	34-36	2	35	16.515	138	9	98	10	37	6	20	1	1985.9	12.0
2014-ER15MC-A19	36-38	2	37	17.450	142	10	102	10	38	7	23	1	1984.3	12.6
2014-ER15MC-B (Subcore B)														
2013-ER15MC-B1	0-2	2	1	0.699	238	8	197	8	46	5	6	1	2013.8	1.1
2013-ER15MC-B2	2-4	2	3	1.572	229	11	188	11	36	6	5	1	2012.5	1.8
2014-ER15MC-B3	4-6	2	5	2.422	232	12	191	12	47	8	6	1	2011.0	2.4
2014-ER15MC-B4	6-8	2	7	3.317	228	11	187	11	23	7	8	1	2009.5	3.1
2014-ER15MC-B5	8-10	2	9	4.230	208	10	167	10	45	7	8	1	2008.0	3.7
2014-ER15MC-B6	10-12	2	11	5.186	199	7	157	7	45	4	12	1	2006.4	4.4
2014-ER15MC-B7	12-14	2	13	6.118	202	11	161	11	42	7	14	1	2004.8	5.0
2014-ER15MC-B8	14-16	2	15	7.075	187	11	146	11	30	8	14	1	2003.2	5.7
2014-ER15MC-B9	16-18	2	17	8.046	198	11	157	11	46	7	11	1	2001.5	6.4
2014-ER15MC-B10	18-20	2	19	9.108	154	10	113	10	39	7	11	1	1999.8	7.2
2014-ER15MC-B11	20-22	2	21	10.121	165	7	123	7	41	4	14	1	1998.0	7.9
2014-ER15MC-B12	22-24	2	23	11.121	129	9	87	9	48	7	15	1	1996.3	8.6
2014-ER15MC-B13	24-26	2	25	12.159	142	11	101	11	31	7	14	1	1994.6	9.3
2014-ER15MC-B14	26-28	2	27	13.172	148	9	107	9	41	6	15	1	1992.8	10.0
2014-ER15MC-B15	28-30	2	29	14.117	154	6	113	6	46	4	18	1	1991.1	10.6
2014-ER15MC-B16	30-32	2	31	15.058	157	8	116	8	49	5	17	1	1989.5	11.3
2014-ER15MC-B17	32-34	2	33	16.012	153	10	112	10	42	7	20	1	1987.9	11.9
2014-ER15MC-B18	34-36	2	35	16.962	160	10	119	11	43	7	23	1	1986.3	12.6
2014-ER15MC-B19	36-38	2	37	17.923	143	6	102	6	41	4	25	1	1984.7	13.3
2014-ER15MC-C (Subcore C)														
2014-ER15MC-C1	0-2	2	1	0.520	264	6	220	6	45	3	7	0	2013.9	0.8
2014-ER15MC-C2	2-4	2	3	1.359	246	10	203	10	45	6	6	1	2012.7	1.7
2014-ER15MC-C3	4-6	2	5	2.179	218	11	175	11	38	7	8	1	2011.1	2.3
2014-ER15MC-C4	6-8	2	7	3.010	212	10	169	10	29	6	8	1	2009.6	2.9
2014-ER15MC-C5	8-10	2	9	3.962	203	6	160	6	39	4	9	1	2007.9	3.7
2014-ER15MC-C6	10-12	2	11	4.885	207	11	164	11	41	7	12	1	2006.2	4.3
2014-ER15MC-C7	12-14	2	13	5.821	192	10	149	10	44	7	12	1	2004.4	5.0
2014-ER15MC-C8	14-16	2	15	6.771	203	11	160	11	46	7	12	1	2002.7	5.6
2014-ER15MC-C9	16-18	2	17	7.718	164	9	120	9	47	6	11	1	2000.9	6.3
2014-ER15MC-C10	18-20	2	19	8.770	134	7	90	7	40	4	10	1	1999.0	7.1
2014-ER15MC-C11	20-22	2	21	9.780	151	11	108	11	38	7	12	1	1997.1	7.8
2014-ER15MC-C12	22-24	2	23	10.736	168	10	124	10	44	7	14	1	1995.3	8.4
2014-ER15MC-C13	24-26	2	25	11.701	149	10	106	10	50	7	10	1	1993.5	9.1
2014-ER15MC-C14	26-28	2	27	12.685	141	10	98	10	48	7	11	1	1991.7	9.8
2014-ER15MC-C15	28-30	2	29	13.651	148	10	105	10	37	6	14	1	1989.8	10.5
2014-ER15MC-C16	30-32	2	31	14.610	153	6	110	6	51	4	16	1	1988.0	11.2
2014-ER15MC-C17	32-34	2	33	15.558	157	10	114	11	36	7	20	1	1986.3	11.8
2014-ER15MC-C18	34-36	2	35	16.508	133	12	90	12	50	8	19	1	1984.5	12.5
2014-ER15MC-C19	36-38	2	37	17.432	146	9	102	9	51	6	26	1	1982.7	13.1
2014-ER15MC-D (Subcore D)														
2013-ER15MC-D1	0-2	2	1	0.547	246	10	199	10	47	6	7	1	2013.8	1.1
2013-ER15MC-D2	2-4	2	3	1.379	229	10	192	10	37	6	6	1	2012.3	2.2
2014-ER15MC-D3	4-6	2	5	2.219	192	10	145	10	48	6	7	1	2010.6	3.0
2014-ER15MC-D4	6-8	2	7	3.088	201	6	167	6	34	4	9	1	2008.7	3.9
2014-ER15MC-D5	8-10	2	9	4.030	190	9	147	9	44	6	8	1	2006.8	4.9
2014-ER15MC-D6	10-12	2	11	4.975	204	10	162	10	41	6	12	1	2004.8	5.8
2014-ER15MC-D7	12-14	2	13	5.957	184	11	140	11	44	7	11	1	2002.7	6.8
2014-ER15MC-D8	14-16	2	15	6.909	175	9	138	9	37	6	12	1	2000.6	7.7
2014-ER15MC-D9	16-18	2	17	7.862	204	8	157	8	47	5	15	1	1998.6	8.6
2014-ER15MC-D10	18-20	2	19	8.920	129	10	88	10	41	6	10	1	1996.5	9.7
2014-ER15MC-D11	20-22	2	21	9.908	176	10	137	10	39	6	14	1	1994.3	10.6
2014-ER15MC-D12	22-24	2	23	10.838	168	9	133	10	35	7	14	1	1992.2	11.4
2014-ER15MC-D13	24-26	2	25	11.834	159	11	105	11	54	7	14	1	1990.2	12.5
2014-ER15MC-D14	26-28	2	27	12.829	141	10	111	10	30	6	14	1	1988.0	13.4
2014-ER15MC-D15	28-30	2	29	13.785	139	6	93	6	46	4	19	1	1985.9	14.3
2014-ER15MC-D16	30-32	2	31	14.775	162	10	119	10	43	7	19	1	1983.9	15.3
2014-ER15MC-D17	32-34	2	33	15.773	108	13	61	13	47	9	22	2	1981.7	16.3
2014-ER15MC-D18	34-36	2	35	16.733	136	8	93	8	42	5	23	1	1979.6	17.1
2014-ER15MC-D19	36-38	2	37	17.704	120	9	80	9	39	6	24	1	1977.6	18.1

Table S2. (continued)

Sample ID	Depth cm	Thick cm	Ave Depth cm	Dry mass depth (g/cm2)	Total Pb-210 (Bq/Kg)	Total Pb-210 error (Bq/Kg)	Unsupported Pb-210 (Bq/Kg)	Unsupported Pb-210 error (Bq/Kg)	Ra-226 (Bq/Kg)	Ra-226 error (Bq/Kg)	Cs-137 (Bq/Kg)	Cs-137 error (Bq/Kg)	Average Date of Section (year A.D.)	95% confidence error (± years)
2013-ON30MC (Composite core)														
2013-O030MC-01	0-1	1	0.5	0.071	1357	28	1278	30	105	15	56	2	2012.2	1.7
2013-O030MC-02	1-2	1	1.5	0.140	1250	21	1171	24	81	11	59	2	2009.4	1.9
2013-O030MC-03	2-3	1	2.5	0.250	1038	12	959	17	88	6	66	1	2005.9	3.2
2013-O030MC-04	3-4	1	3.5	0.394	799	19	720	22	63	11	79	2	2000.9	4.4
2013-O030MC-05	4-5	1	4.5	0.588	547	17	467	20	63	10	107	2	1994.2	6.2
2013-O030MC-06	5-6	1	5.5	0.794	377	13	297	17	65	9	143	2	1986.3	7.2
2013-O030MC-07	6-7	1	6.5	0.998	326	15	247	19	67	12	187	3	1978.3	8.0
2013-O030MC-08	7-8	1	7.5	1.184	304	9	224	15	60	7	232	2	1970.6	8.4
2013-O030MC-09	8-9	1	8.5	1.376	291	15	211	19	55	12	179	3	1963.1	9.3
2013-O030MC-10	9-10	1	9.5	1.585	212	15	133	19	49	11	96	3	1955.2	10.5
2013-O030MC-11	10-12	2	11	2.074	168	10	89	15	63	6	22	1	1941.5	18.0
2013-O030MC-12	12-14	2	13	2.569	152	7	73	14	46	5	2	1	1922.1	20.1
2013-O030MC-13	14-16	2	15	3.092	106	14	27	18	61	9			1902.0	22.7
2013-O030MC-14	16-18	2	17	3.630	102	9	23	15	41	7			1881.1	25.2
2013-O030MC-15	18-20	2	19	4.174	98	6	19	13	57	5			1859.8	27.5
2013-O030MC-16	20-22	2	21	4.713	88	5	9	12	51	4			1838.5	29.6
2013-O030MC-17	22-24	2	23	5.268	78	7			60	5			1816.9	32.1
2013-O030MC-18	24-26	2	25	5.843	73	8			45	7			1794.7	34.8
2013-O030MC-19	26-28	2	27	6.419	78	7			47	6			1772.0	37.1
2013-ON30MC-20	28-30	2	29	6.993	70	6			54	4			1749.3	39.4
2013-ON30MC-21	30-32	2	31	7.585	78	7			60	7			1726.4	42.1
2013-ON30MC-22	32-34	2	33	8.179	72	5			48	4			1703.0	44.6
2013-ON30MC-23	34-36	2	35	8.792	72	6			47	4			1679.2	47.4
2013-ON30MC-24	36-38	2	37	9.405	62	10			38	7			1655.1	49.9
2013-ON30MC-A (Subcore A)														
2013-ON30MC-A-01	0-1	1	0.5	0.102	1315	26	1235	32	114	14	49	2	2011.8	2.0
2013-ON30MC-A-02	1-2	1	1.5	0.225	1178	13	1099	23	73	7	61	1	2008.0	2.6
2013-ON30MC-A-03	2-3	1	2.5	0.369	1091	24	1012	31	68	12	66	3	2003.5	3.4
2013-ON30MC-A-04	3-4	1	3.5	0.551	491	15	411	24	47	12	73	3	1998.0	4.5
2013-ON30MC-A-05	4-5	1	4.5	0.757	491	20	412	28	79	13	81	3	1991.4	5.4
2013-ON30MC-A-06	5-6	1	5.5	0.975	378	18	298	26	67	11	128	3	1984.3	6.2
2013-ON30MC-A-07	6-7	1	6.5	1.187	340	11	261	22	60	7	169	2	1977.0	6.6
2013-ON30MC-A-08	7-8	1	7.5	1.375	324	18	245	26	60	13	249	4	1970.2	6.7
2013-ON30MC-A-09	8-9	1	8.5	1.561	309	18	229	26	43	11	286	4	1963.9	7.1
2013-ON30MC-A-10	9-10	1	9.5	1.741	230	20	150	28	51	13	147	3	1957.7	7.4
2013-ON30MC-A-11	10-12	2	11	2.187	195	17	115	25	63	12	28	2	1947.1	13.1
2013-ON30MC-A-12	12-14	2	13	2.687	166	9	86	21	59	6			1931.1	15.2
2013-ON30MC-A-13	14-16	2	15	3.203	134	16	55	25	47	11			1913.9	16.8
2013-ON30MC-A-14	16-18	2	17	3.737	121	14	42	23	64	11			1896.1	18.4
2013-ON30MC-A-15	18-20	2	19	4.291	111	6	31	20	52	4			1877.7	20.2
2013-ON30MC-A-16	20-22	2	21	4.844	78	15			56	10			1858.9	21.6
2013-ON30MC-A-17	22-24	2	23	5.394	86	9			53	8			1840.2	22.9
2013-ON30MC-A-18	24-26	2	25	5.931	80	8			43	5			1821.9	24.0
2013-ON30MC-A-19	26-28	2	27	6.520	87	9			43	7			1802.8	26.4
2013-ON30MC-A-20	28-30	2	29	7.134	70	9			37	7			1782.4	28.4
2013-ON30MC-A-21	30-32	2	31	7.726	62	8			38	6			1762.0	29.5
2013-ON30MC-A-22	32-34	2	33	8.321	65	4			43	3			1741.9	31.0
2013-ON30MC-A-23	34-36	2	35	8.933	68	10			37.1	7.8			1721.5	32.9
2013-ON30MC-A-24	36-38	2	37	9.546	65	12			65.0	8.7			1700.7	34.4
2013-ON30MC-A-25	38-40	2	39	10.166	57	8			60.3	5.7			1679.9	36.1
2013-ON30MC-B (Subcore B)														
2013-ON30MC-B1	0-1	1	0.5	0.057	1367	29	1293	33	105	18	53	3	2012.6	2.2
2013-ON30MC-B2	1-2	1	1.5	0.135	1349	13	1275	21	96	8	55	1	2010.4	2.2
2013-ON30MC-B3	2-3	1	2.5	0.258	1121	22	1047	27	73	11	60	2	2007.2	3.2
2013-ON30MC-B4	3-4	1	3.5	0.407	902	23	828	28	77	13	68	2	2002.7	4.4
2013-ON30MC-B5	4-5	1	4.5	0.597	627	25	553	30	54	15	77	3	1997.2	5.9
2013-ON30MC-B6	5-6	1	5.5	0.806	368	11	294	19	51	7	84	2	1990.7	7.3
2013-ON30MC-B7	6-7	1	6.5	1.026	343	11	269	19	56	6	149	2	1983.7	8.5
2013-ON30MC-B8	7-8	1	7.5	1.225	338	22	264	27	84	14	183	4	1976.9	9.1
2013-ON30MC-B9	8-9	1	8.5	1.404	322	6	248	17	54	4	263	1	1970.8	9.6
2013-ON30MC-B10	9-10	1	9.5	1.578	309	14	235	21	60	9	288	3	1965.0	10.4
2013-ON30MC-B11	10-12	2	11	1.994	211	11	137	19	57	8	84	2	1955.4	16.3
2013-ON30MC-B12	12-14	2	13	2.475	164	18	90	24	57	12	5	2	1940.8	19.7
2013-ON30MC-B13	14-16	2	15	2.987	165	15	91	22	61	11	3	1	1924.7	22.7
2013-ON30MC-B14	16-18	2	17	3.522	135	15	61	22	56	13			1907.6	25.6
2013-ON30MC-B15	18-20	2	19	4.049	98	17	24	23	52	11			1890.3	28.0
2013-ON30MC-B16	20-22	2	21	4.580	87	10	13	19	47	8			1873.1	30.6
2013-ON30MC-B17	22-24	2	23	5.138	88	7	13	17	56	5			1855.4	33.7
2013-ON30MC-B18	24-26	2	25	5.674	96	9	22	18	56	7			1837.6	35.9
2013-ON30MC-B19	26-28	2	27	6.240	96	10	22	19	52	7			1819.6	39.1
2013-ON30MC-B20	28-30	2	29	6.841	60	11			67	9			1800.6	42.6
2013-ON30MC-B21	30-32	2	31	7.434	73	8			45	6			1781.2	45.3
2013-ON30MC-B22	32-34	2	33	8.028	71	5			54	4			1761.9	48.2
2013-ON30MC-B23	34-36	2	35	8.640	64	5			55	4			1742.3	51.4
2013-ON30MC-B24	36-38	2	37	9.253	73	6			56	5			1722.3	54.3
2013-ON30MC-B25	38-40	2	39	9.874	47	10			55	7			1702.2	57.4
2013-ON30MC-C (Subcore C)														
2013-ON30MC-C1	0-1	1	0.5	0.093	1271	28	1192	34	94	15	47	2	2011.9	6.0
2013-ON30MC-C2	1-2	1	1.5	0.200	1256	52	1177	56	93	24	56	4	2008.4	6.0
2013-ON30MC-C3	2-3	1	2.5	0.337	1032	24	953	31	87	12	53	2	2004.1	6.0
2013-ON30MC-C4	3-4	1	3.5	0.506	757	12	679	23	57	6	61	1	1998.6	6.0
2013-ON30MC-C5	4-5	1	4.5	0.710	530	20	451	28	62	10	67	2	1992.0	6.5
2013-ON30MC-C6	5-6	1	5.5	0.927	414	19	336	27	45	11	92	3	1984.6	7.6
2013-ON30MC-C7	6-7	1	6.5	1.153	318	16	240	25	65	10	137	3	1976.7	8.6
2013-ON30MC-C8	7-8	1	7.5	1.353	315	17	237	26	54	12	168	3	1969.2	9.0
2013-ON30MC-C9	8-9	1	8.5	1.541	306	10	228	22	57	7	246	2	1962.3	9.5
2013-ON30MC-C10	9-10	1	9.5	1.725	282	19	203	27	52	11	236	4	1955.7	10.2
2013-ON30MC-C11	10-12	2	11	2.177	220	15	141	24	57	10	78	2	1944.5	16.7
2013-ON30MC-C12	12-14	2	13	2.667	168	7	90	21	44	5	15	1	1927.8	19.4
2013-ON30MC-C13	14-16	2	15	3.225	123	12	44	23	36	8			1909.2	22.8
2013-ON30MC-C14	16-18	2	17	3.774	119	9	40	21	52	7			1889.6	24.9
2013-ON30MC-C15	18-20	2	19	4.342	112	11	33	22	60	7			1869.8	27.5
2013-ON30MC-C16	20-22	2	21	4.895	93	8	15	21	39	5			1850.0	29.5
2013-ON30MC-C17	22-24	2	23	5.470	67	8			51	6			1830.0	32.2
2013-ON30MC-C18	24-26	2	25	6.015	90	11			39	7			1810.1	33.8
2013-ON30MC-C19	26-28	2	27	6.619	71	8			42	5			1789.8	37.3
2013-ON30MC-C20	28-30	2	29	7.247	61	9			58	8			1768.0	40.3
2013-ON30MC-C21	30-32	2	31	7.840	70	12			51	9			1746.3	42.0
2013-ON30MC-C22	32-34	2	33	8.434	60	4			51	3			1725.3	44.4
2013-ON30MC-C23	34-36	2	35	9.046	70	7			49	5			1704.0	47.2
2013-ON30MC-C24	36-38	2	37	9.659	69	7			46	5			1682.2	49.7
2013-ON30MC-C25	38-40	2	39	10.280	60	9			47	6			1660.4	52.3
2013-ON30MC-D (Subcore D)														
2013-ON30MC-D1	0-1	1	0.5	0.058	1337	25	1251	43	135	14	49	2	2012.5	2.7
2013-ON30MC-D2	1-2	1	1.5	0.149	1317	24	1231	43	92	11	53	2	2009.8	2.7
2013-ON30MC-D3	2-3	1	2.5	0.279	1156	11	1070	37	84	6	64	1	2005.8	3.0
2013-ON30MC-D4	3-4	1	3.5	0.440	795	17	708	39	74	10	71	2	2000.6	3.9
2013-ON30MC-D5	4-5	1	4.5	0.631	574	24	488	42	74	12	71	3	1994.2	4.9
2013-ON30MC-D6	5-6	1	5.5	0.840	398	12	312	37	67	8	99	2	1987.0	5.7
2013-ON30MC-D7	6-7	1	6.5	1.054	314	10	228	36	53	6	148	2	1979.4	6.2
2013-ON30MC-D8	7-8	1	7.5	1.248	349	16	263	38	49	11	218	3	1972.0	6.3
2013-ON30MC-D9	8-9	1	8.5	1.427	323	19	236	40	48	13	295	4	1965.3	6.4
2013-ON30MC-D10	9-10	1	9.5	1.600	270	17	183	39	59	14	239	4	1958.9	6.7
2013-ON30MC-D11	10-12	2	11	2.031	209	11	123	36	56	8	51	1	1948.0	12.3
2013-ON30MC-D12	12-14	2	13	2.531	189	14	103	37	53	9	4	1	1931.2	14.7
2013-ON30MC-D13	14-16	2	15	3.042	162	14	76	38	55	11			1913.0	16.1
2013-ON30MC-D14	16-18	2	17	3.575	127	6	41	35	50	5			1894.1	17.6
2013-ON30MC-D15	18-20	2	19	4.129	119	12	33	37	55	10			1874.5	19.3
2013-ON30MC-D16	20-22	2	21	4.661	100	7	14	36	57	5			1854.9	20.1
2013-ON30MC-D17	22-24	2	23	5.228	92	9	6	36	41	7			1835.1	22.0
2013-ON30MC-D18	24-26	2	25	5.766	107	17	21	39	34	11			1815.1	22.7
2013-ON30MC-D19	26-28	2	27	6.338	74	10			55	7			1795.0	24.5
2013-ON30MC-D20	28-30	2	29	6.937	72	10			51	8			1773.9	26.4
2013-ON30MC-D21	30-32	2	31	7.529	56	10			52	8			1752.4	27.6
2013-ON30MC-D22	32-34	2	33	8.124	65	10			52	8			1731.0	29.0
2013-ON30MC-D23	34-36	2	35	8.736	33	10			30	7			1709.2	30.7
2013-ON30MC-D24	36-38	2	37	9.349	69	10			37	7			1687.1	32.0
2013-ON30MC-D25	38-40	2	39	9.969	44	9			29	7			1664.8	33.6

Figure S1. Comparison of composite core results for ER15 with individual cores from a separate multi-corer cast at the same location.

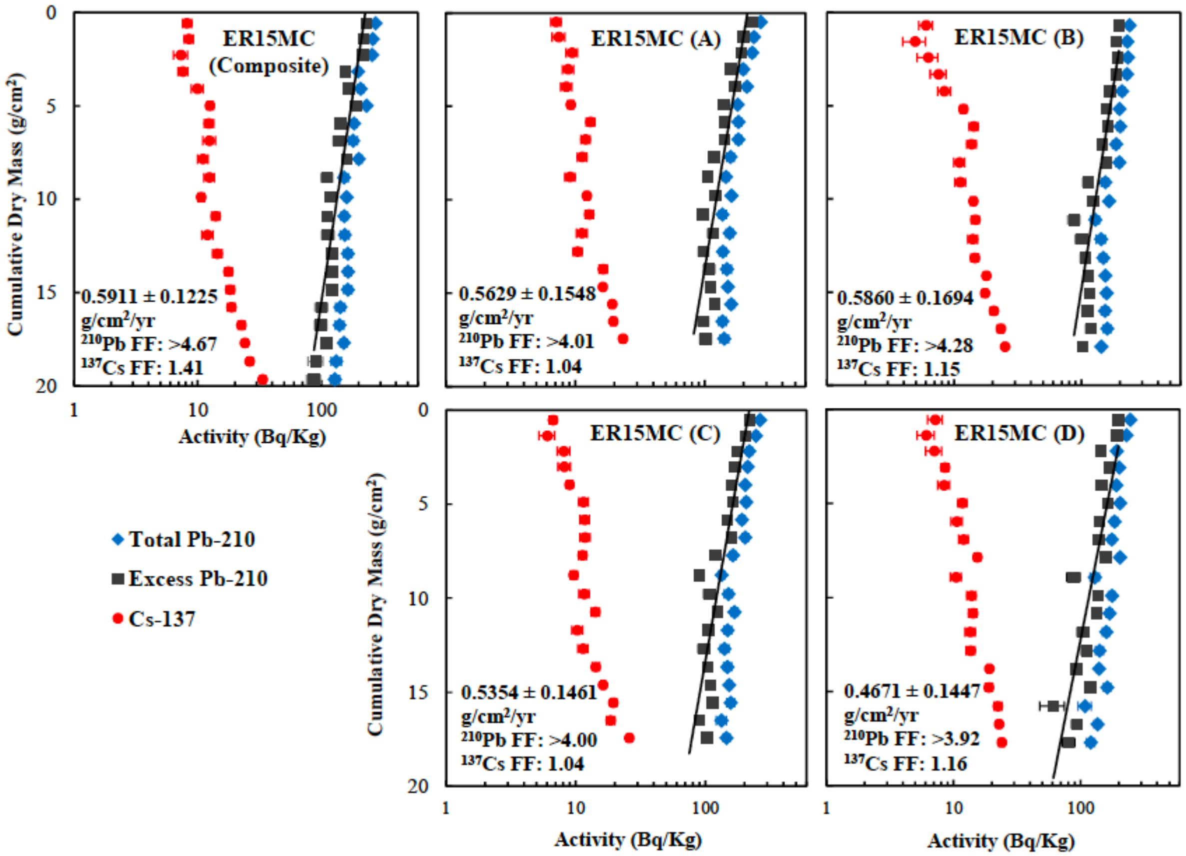

Figure S2. Comparison of composite core results for ON30 with individual cores from a separate multi-corer cast at the same location.

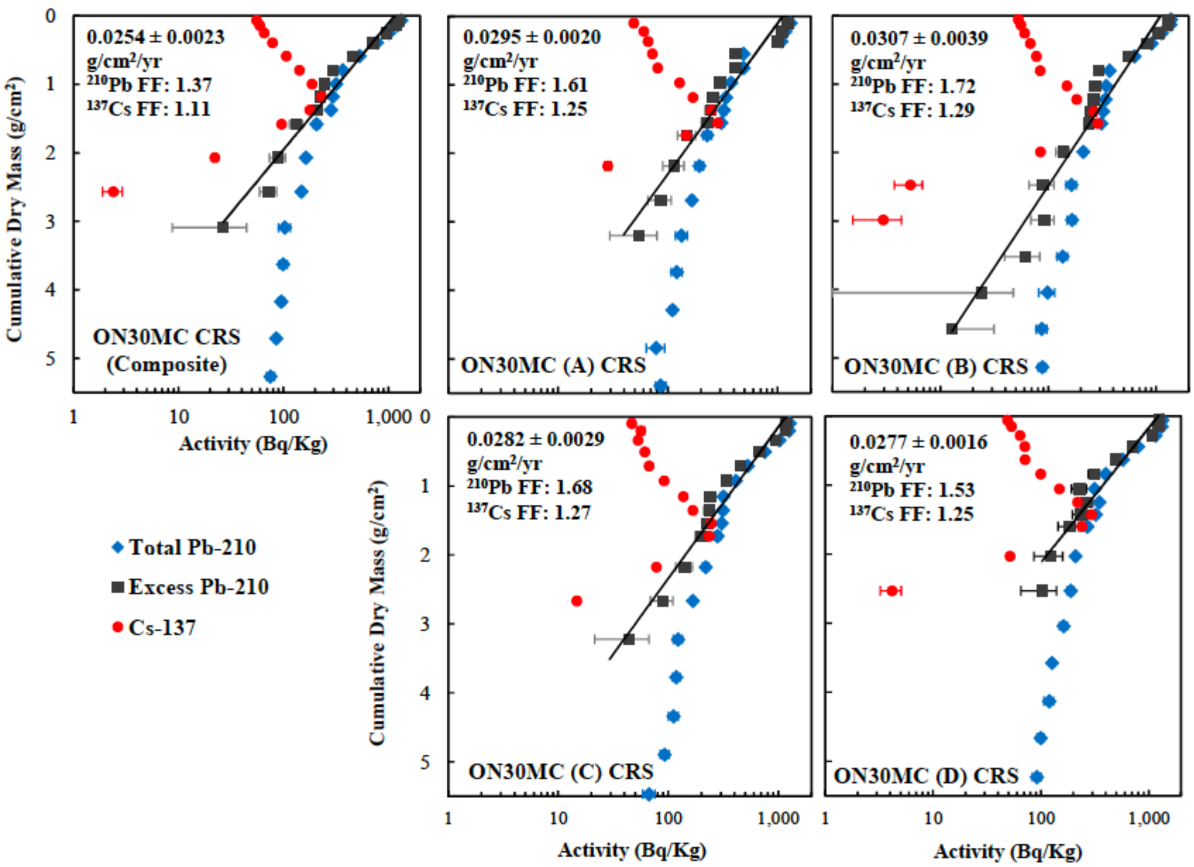

Figure S3. CRC and CIC model plots for data from Lake Superior.

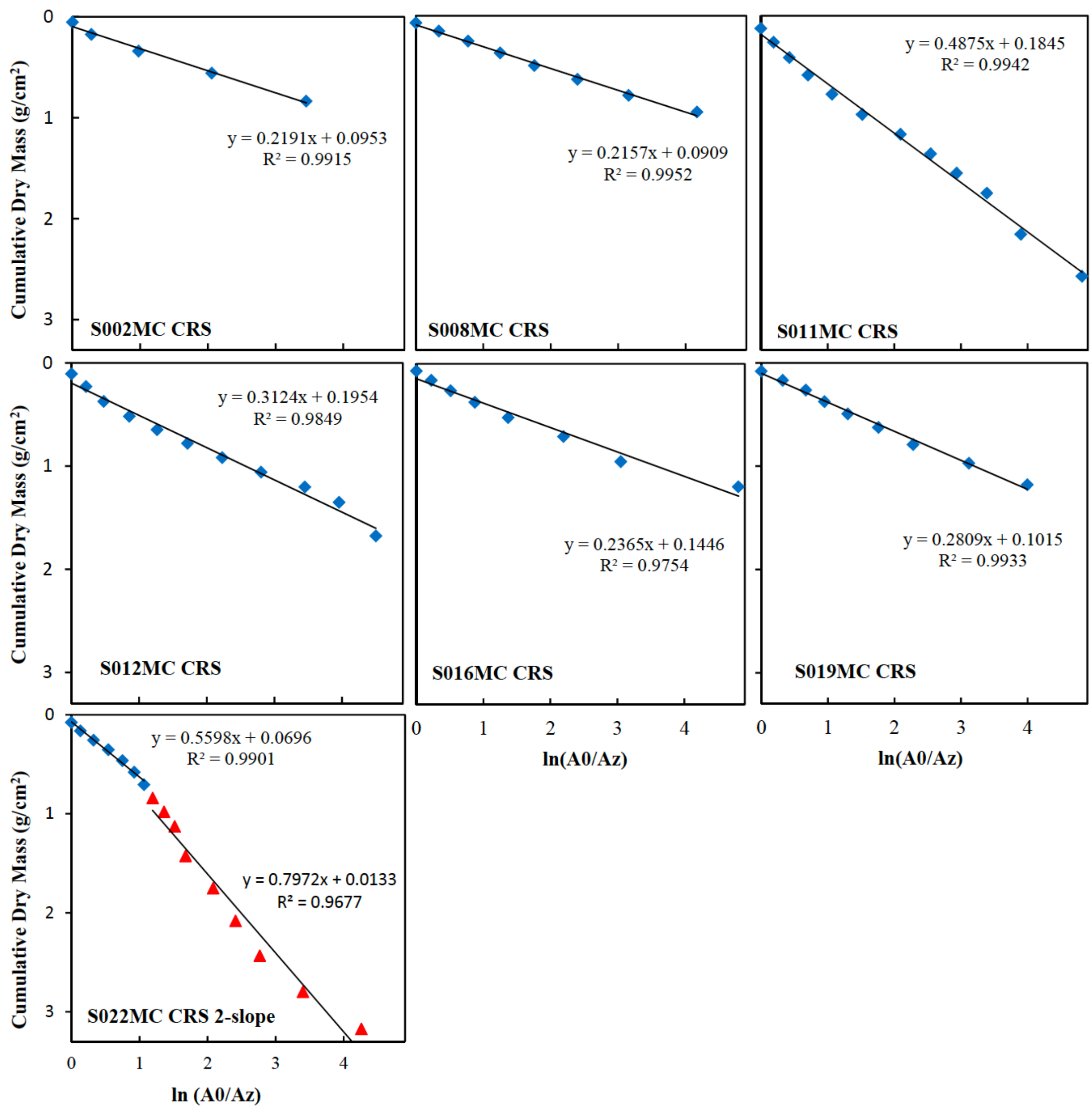

Figure S4. CRC and CIC model plots for data from Lake Michigan.

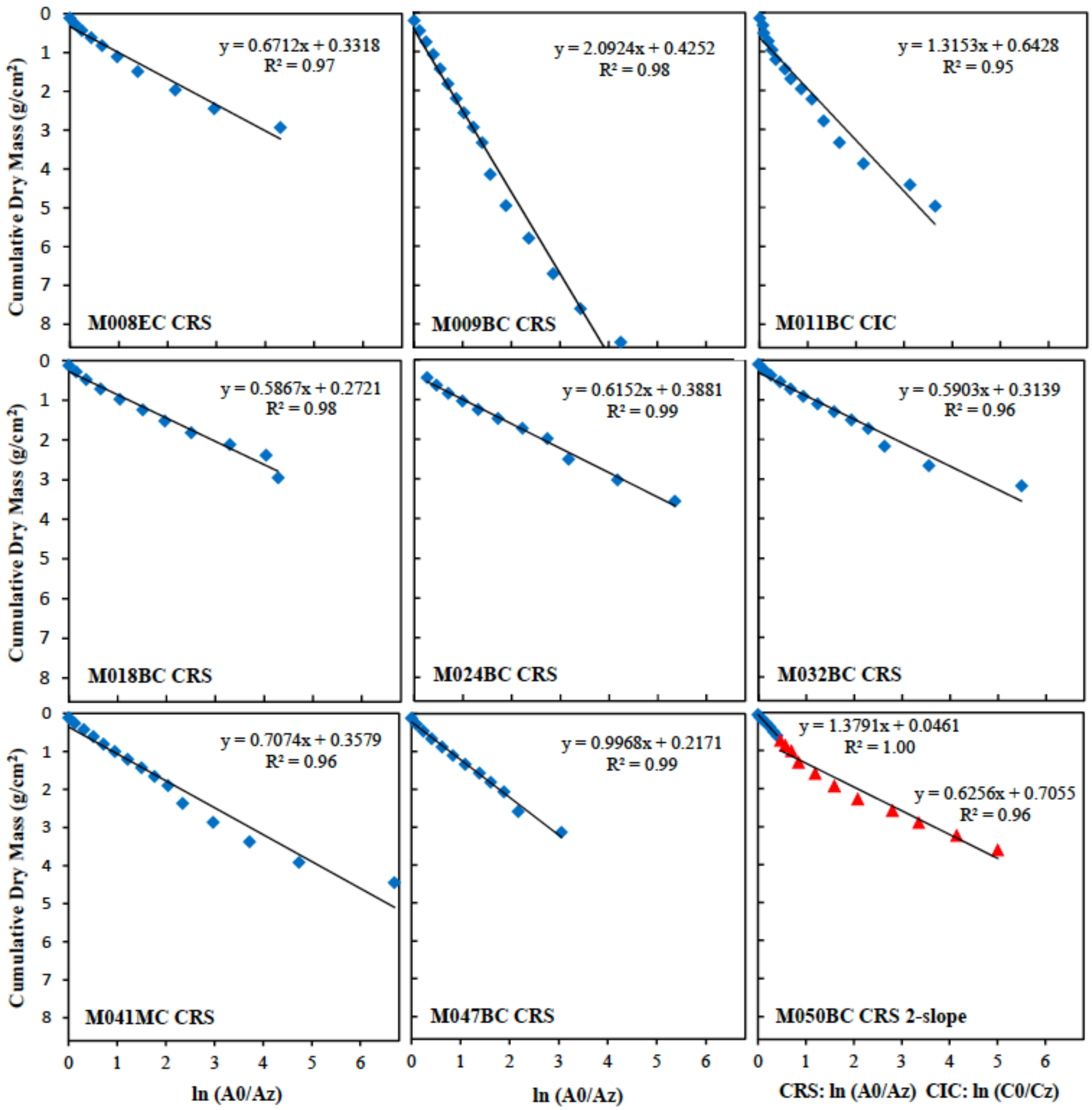

Figure S5. CRC and CIC model plots for data from Lake Huron.

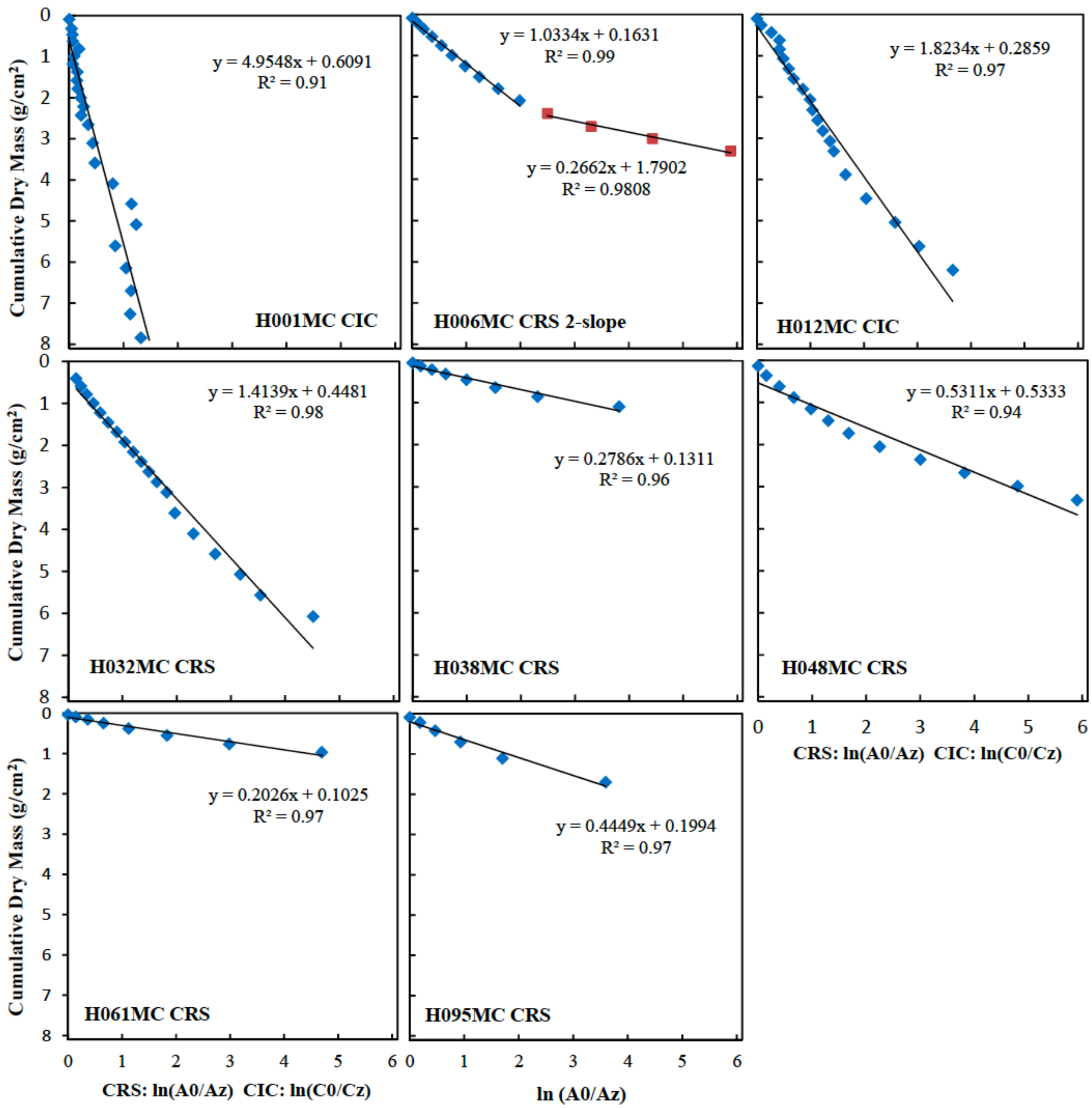

Figure S6. CRC and CIC model plots for data from Lake Erie.

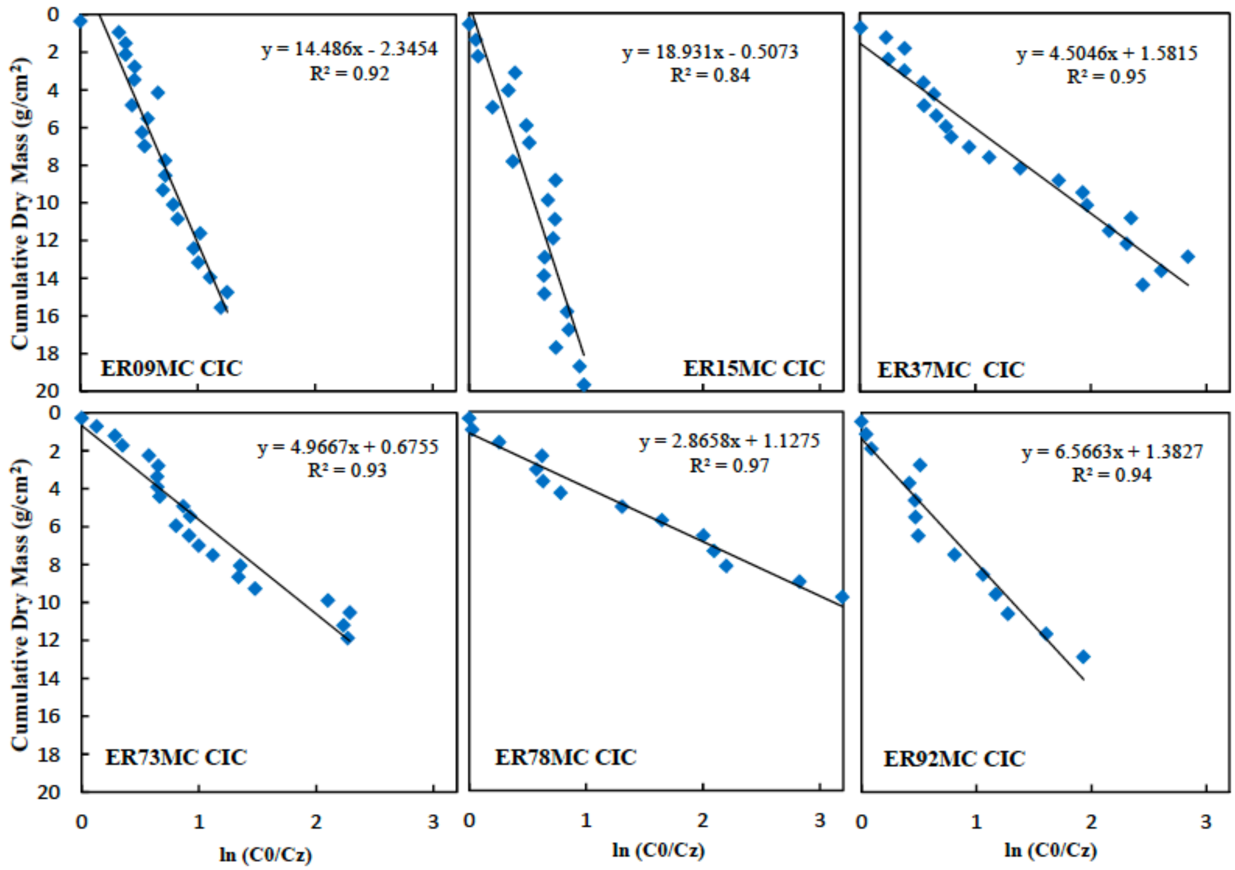

Figure S7. CRC and CIC model plots for data from Lake Ontario.

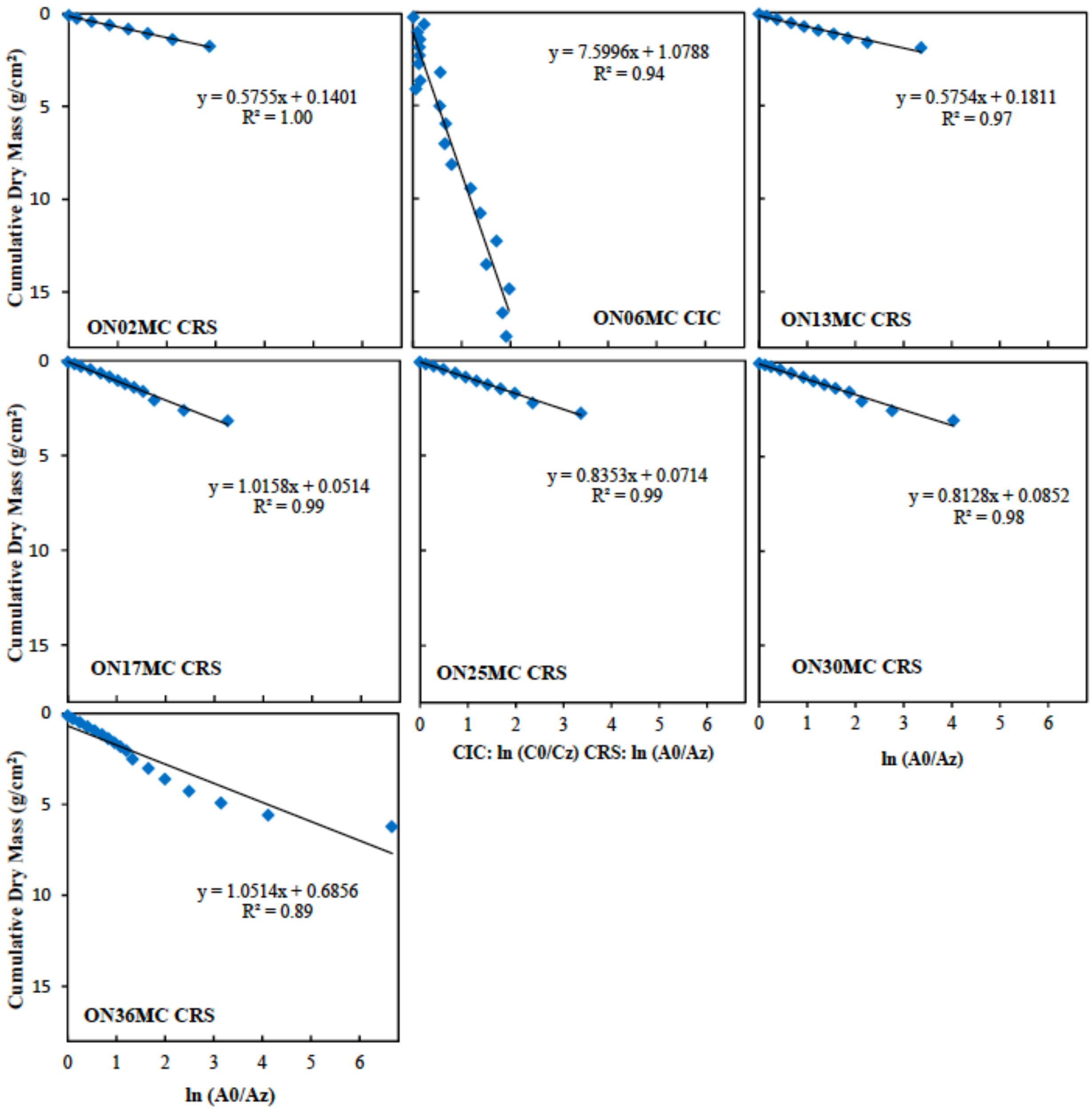

Figure S8. Calendar date profiles for cores from Lake Superior.

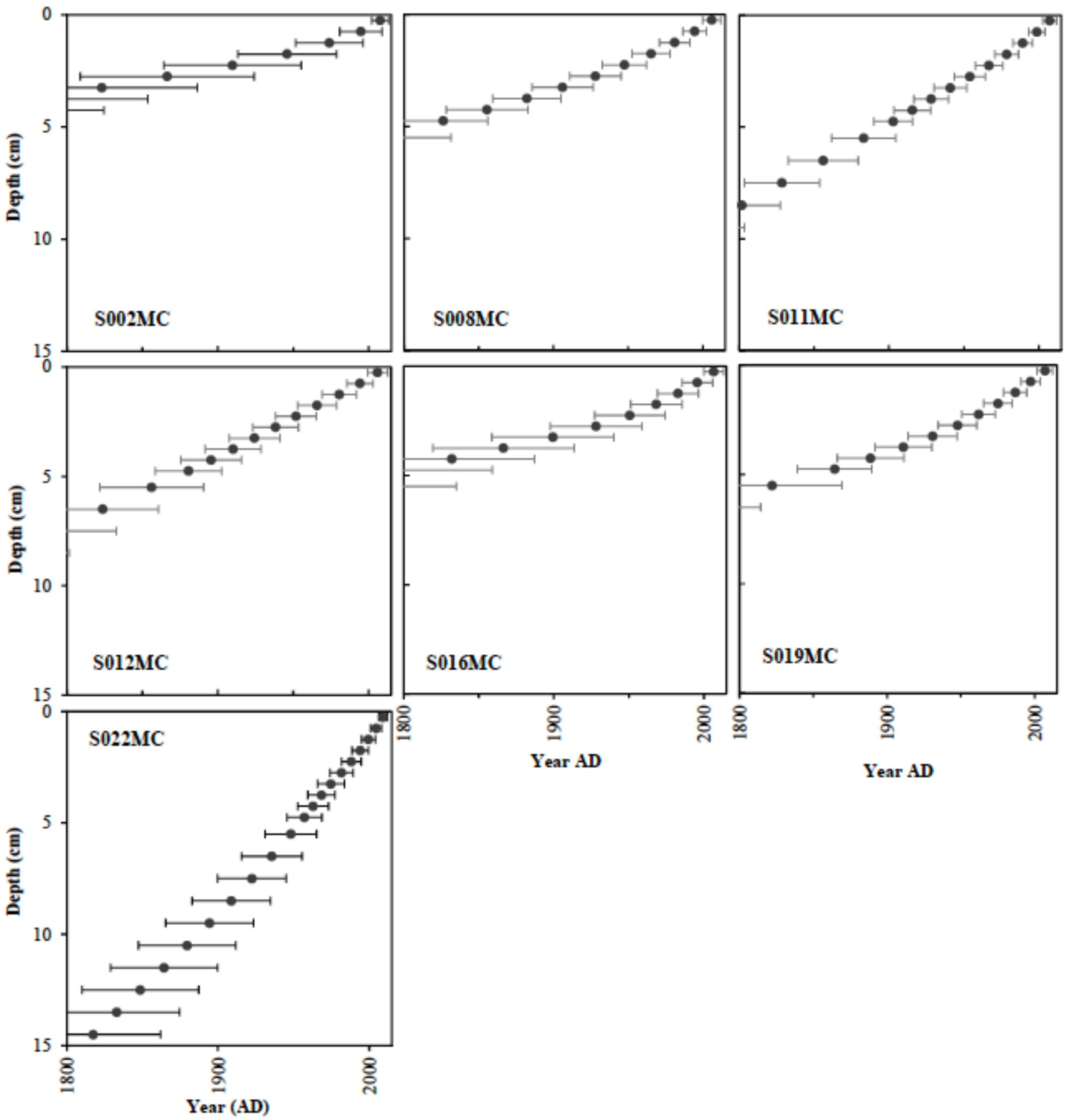

Figure S9. Calendar date profiles for cores from Lake Michigan.

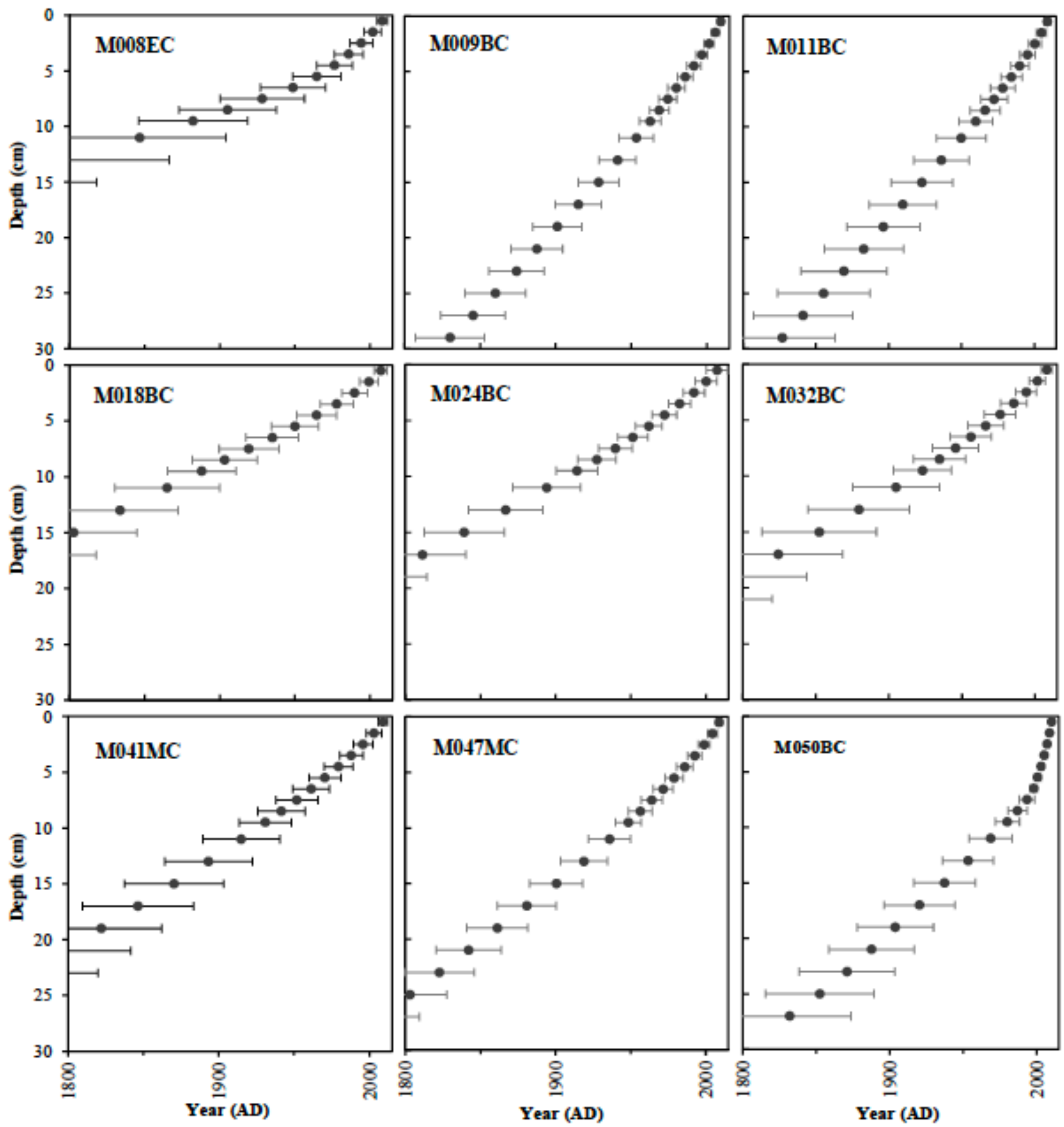

Figure S10. Calendar date profiles for cores from Lake Huron.

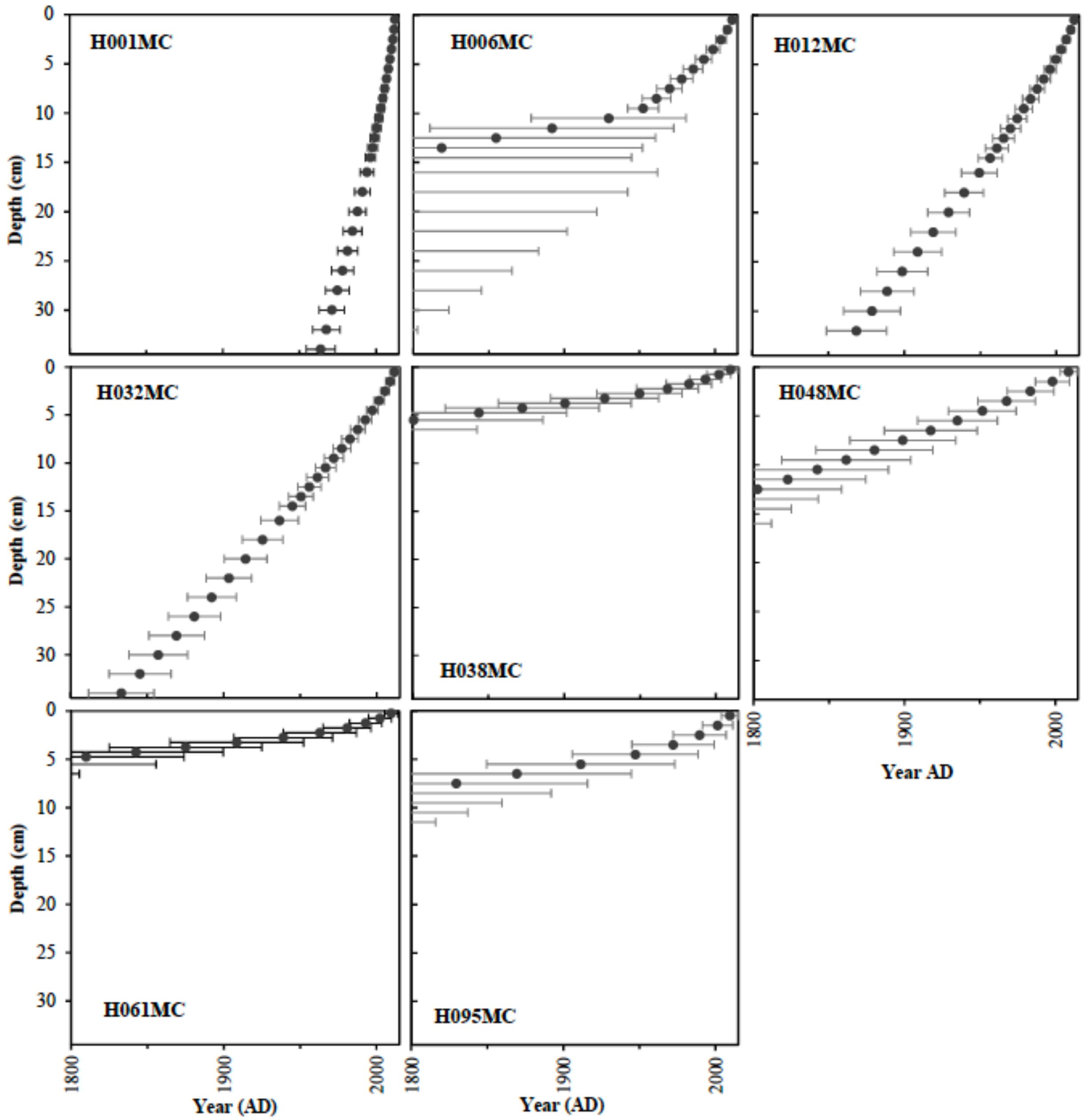

Figure S11. Calendar date profiles for cores from Lake Erie.

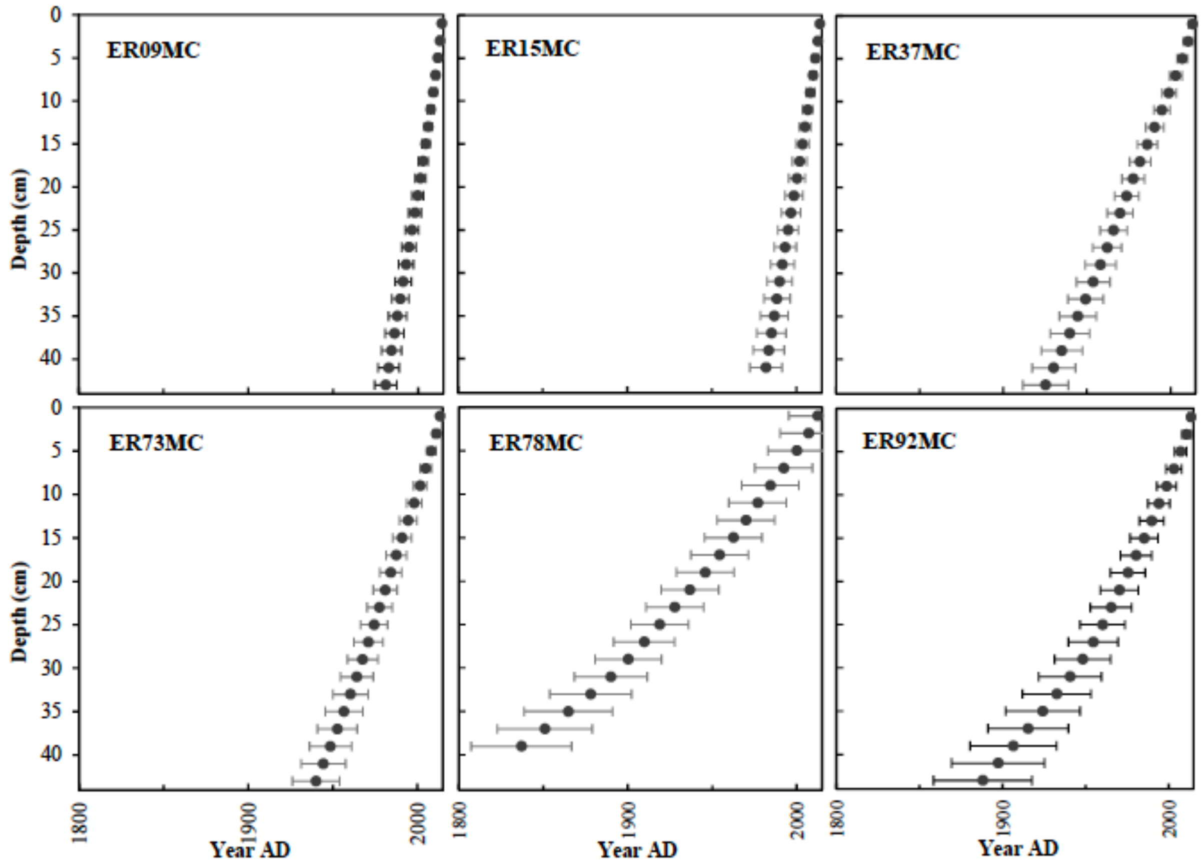

Figure S12. Calendar date profiles for cores from Lake Ontario.